INHARMONICITY IN THE NATURAL MODE FREQUENCIES OF OVERWOUND STRINGS

Pochaman Chumnantas

PhD

University of Edinburgh

1995

DECLARATION

I declare that this thesis has been composed by me and that the work is my own.

Pochaman Chumnantas

ACKNOWLEDGEMENTS

I would like to express my thanks to Dr. Murray Campbell for his teaching, support, encouragement and patience. He gave me both freedom and direction. I would also like to thank to Professor Clive Greated and Dr. Raymond Parks for the guidance and facilities afforded.

I acknowledge the scholarship received from the Thai Government for the whole period of this work.

ABSTRACT

The natural frequencies of piano strings depart somewhat from the harmonic series and the degree of inharmonicity has important implications for tone quality, tuning and the electronic synthesis of piano sounds. Apart from effects due to the finite compliance of the supports, the stiffness of the steel wire from which piano strings are made accounts almost entirely for the inharmonicity of the plain wire strings. It has been shown, however that the string stiffness is not the only source of inharmonicity of the overwound piano strings. Not only the effects of wave-reflection at the terminations of the various copper covering layers of overwound strings, but also the effects of nonuniformity may contribute weak partials that cannot be explained by string stiffness alone.

Some discussions on the stepped string have appeared over the last few years by Levinson, Sakata and Sakata, and Gottlieb, but their analyses have not incorporated the stiffness of the stepped string. In this thesis, an expression for the frequencies of vibration of a stepped overwound string was described, and numerical calculations have been undertaken to compute theoretical mode frequencies for strings with varying degrees of overwinding. The numerical results of the frequency equation were compared with data from experimental measurements of the inharmonicities of overwound strings on a rigid monochord. The rigid monochord has been designed in order to control the parameters and to reduce external effects disturbing the vibration of the strings. It is evident from the comparison that the theory presented here gives a better fit to measured inharmonicities than Fletcher's analysis for a uniform string.

The original motivation for this study was to determine the extent to which the non-uniformity of the overwinding on a bass piano string affected the inharmonicity of its mode frequencies. To examine the extent to which this work was relevant to the behaviour of overwound piano strings with the end support conditions typical of normal use, a series of measurements was performed on the bass strings of a Broadwood grand piano. It is evident from the results that the major cause of the discrepancy between the Fletcher prediction and the measurement is indeed the non-uniformity of the winding.

CONTENTS

DECLARATION

ACKNOWLEDGEMENTS

ABSTRACT

CONTENTS

CHAPTER 1 INTRODUCTION 1

1.1 Outline of research programme. 1

1.2 The history and physics of the piano. 5

1.3 The Theory of Inharmonicity. 13

CHAPTER 2 THEORETICAL CONSIDERATIONS. 28

2.1 Transverse wave equation for a string. 28

2.2 Bending waves in a bar. 31

2.3 Vibrations of a stiff string. 35

2.4 Vibrations of a nonuniform stiff string. 38

CHAPTER 3 NUMERICAL ANALYSIS. 42

3.1 Numerical Root Finding. 42

3.2 Numerical parameters. 45

3.4 Numerical results. 50

CHAPTER 4 EXPERIMENTAL TECHNIQUES AND RESULTS. 59

4.1 Experimental apparatus. 59

4.2 Analogue to digital converter and sampling process. 62
4.3 Fourier Analysis. 67
4.4 Spectrum analysis. 68
4.5 The experimental uncertainty. 72
4.6 Experimental results. 84

CHAPTER 5 COMPARISON. 92
5.1 Comparison between the theoretical and experimental Inharmonicity. 92
5.2 Comparison of the B-coefficients from the theoretical results, experimental results and Fletcher's results. 97
5.3 Uncertainty of experimental fundamental frequencies. 98

CHAPTER 6 MEASUREMENT ON GRAND PIANO STRINGS. 106
6.1 Experimental technique on the grand piano. 106
6.2 The experimental and theoretical results for the grand piano strings. 108

CHAPTER 7 SUMMARY AND CONCLUSION. 118
7.1 Conclusion. 118

APPENDIX A EXAMPLES OF NUMERICAL METHOD. 122

APPENDIX B THEORETICAL MODE FREQUENCIES. **131**

APPENDIX C THEORETICAL INHARMONICITY IN CENTS. **138**

APPENDIX D EXPERIMENTAL MODE FREQUENCIES. **145**

APPENDIX E EXPERIMENTAL INHARMONICITY IN CENTS. **152**

APPENDIX F THE PIANO STRINGS' THEORETICAL AND EXPERIMENTAL MODE FREQUENCIES. **159**

APPENDIX G THE PIANO STRINGS' THEORETICAL AND EXPERIMENTAL INHARMONICITY IN CENTS. **164**

BIBLIOGRAPHY **169**

PUBLICATIONS

CHAPTER 1

INTRODUCTION

1.1 Outline of research programme.

The problem of the vibration of flexible strings with uniform characteristics has been treated by many investigators and the results are well established. The natural frequencies of piano strings depart somewhat from the harmonic series and the degree of inharmonicity has important implications for tone quality, tuning and the electronic synthesis of piano sounds. Apart from effects due to the finite compliance of the supports, the stiffness of the steel wire from which piano strings are made accounts almost entirely for the inharmonicity of the plain wire string. Vibration characteristics of uniform stiff strings are also quite well understood and the predicted mode frequencies are in close agreement with observation [22].

For bass piano strings, the observed inharmonicity is higher than that predicted by considering them as uniform stiff strings, up to some 20% for the most heavily overwound A0 of a Broadwood grand piano in the Acoustics Laboratory of the Department of Physics at the University of Edinburgh. Actually all piano bass strings are characterised by a steel wire core wrapped with copper, or sometimes iron, to increase the string's linear mass density. While the tight coiling of the copper wire ensures close coupling to the core, the windings contribute considerably more to the increase in the string's linear mass density than to its bending stiffness. Most bass strings have a single

winding of copper wire, and it is usually only within the lowest octave that the double winding is used. A double-wound string consists of a bare steel core wrapped with a small diameter copper wire, which is then overspun with a second winding of larger diameter. A small part of the steel core is left exposed near the end of the string. Thus only the outer winding is visible and the existence of the inner winding is evident only from the small change in the diameter of the overall covering near the ends.

Some discussions on the stepped string have appeared over the last few years [71,77,40], but their analyses have not incorporated the stiffness of the stepped string. In this thesis, an expression for the frequencies of vibration of a stepped overwound string is described, and numerical calculations have been undertaken to compute theoretical mode frequencies for strings with varying degrees of overwinding. The experimental inharmonicities of overwound strings on a rigid monochord have been measured, and compared with theoretical results. The rigid monochord has been designed in order to control the parameters and to reduce external effects disturbing the vibration of the strings.

The original motivation for this study was to determine the extent to which the nonuniformity of the overwinding on a bass piano string affected the inharmonicity of its mode frequencies. To examine the extent to which this work was relevant to the behaviour of overwound piano strings with the end support conditions typical of normal use, a series of measurements was performed on the bass strings of a Broadwood grand piano.

We begin the next section with the history of the piano, since the physics of the piano can best be understood by first reviewing the evolution of the modern piano and its principal components. Section 1.3 is a survey of the literature pertaining to the theory of inharmonicity and experimental methods of inharmonicity measurement.

In Chapter 2, the theory of strings in the case of a flexible string, a

uniform stiff string, and a nonuniform stiff string are described. In the first place, it is assumed that the string is perfectly flexible, the only restoring force being due to the tension. Secondly, it is necessary to study the effect of stiffness on the string's motion. A discussion of the transverse vibration of a rigid bar leads to a study of the vibration of a uniform stiff string. Finally, the vibration of a nonuniform stiff string is considered. A derivation of the mode frequencies of a stepped string is presented, taking into account the stiffness of the stepped string.

In Chapter 3, numerical calculations have been undertaken to compute theoretical mode frequencies from the frequency equation in the Chapter 2 for strings with varying degrees of overwinding. Strings with three different core and overwinding dimensions were calculated. Each string with the same core and overwinding dimensions is considered for six uniformly overwound strings and six stepped overwound strings. The Inharmonicity of the departure of the allowed frequencies from the harmonic series are considered.

In order to validate the theory developed in Chapter 2, experiments were carried out to measure the inharmonicity of the overwound strings on a purposed-designed monochord; these are described in Chapter 4. The strings were plucked and the sound was recorded using a microphone mounted a short distance above. The acoustic signal was captured digitally using an A/D converter and was analysed using a Fast Fourier Transform. A program developed in Edinburgh [84] locates the peaks in the spectrum with high accuracy. Also in this chapter, the experimental results of inharmonicity for the uniformly overwound strings on the monochord are first presented. These are followed by the results of inharmonicity for the stepped overwound strings on the monochord.

In Chapter 5 the experimental inharmonicity for the uniformly overwound strings and for stepped overwound strings as shown in Chapter 4 are compared

with the theoretical inharmonicity as shown in Chapter 3. In order to probe in more detail the correspondence between calculated and measured frequencies, and to obtain a direct comparison with the predictions of the theory of Fletcher [40] it is useful to plot the parameter $B=(1/n^2)[(f_n/nf_0)^2-1]$ as a function of mode number.

The original motivation for this study was to determine the extent to which the non-uniformity of the overwinding on a bass piano string affected the inharmonicity of its mode frequencies. The theoretical treatment described in Chapter 2 and 3 assumed that the end supports of the string were completely rigid, and the experimental results given in Chapter 4 and 5 were obtained on a monochord which attempted to reproduce this ideal case. To examine the extent to which this work was relevant to the behaviour of overwound piano strings with the end support conditions typical of normal use, a series of measurements was performed on the bass strings of a Broadwood grand piano in the Acoustics Laboratory of the Department of Physics at the University of Edinburgh. This piano was built in 1871, and was renovated and restrung in 1992. These will be described in Chapter 6.

Finally, the work is summarised in Chapter 7, the important findings are restated and future work is discussed.

Appendix A shows two examples of numerical solutions of the frequency equation. Appendix B tabulates the results for the theoretical mode frequencies of the 36 different strings studied, and Appendix C gives the corresponding inharmonicities. The results for the experimental mode frequencies of the uniformly and stepped overwound strings and the corresponding experimental inharmonicities comprise Appendices D and E. Appendix F tabulates theoretical and experimental mode frequencies for 8 strings on the Broadwood grand piano; Appendix G shows the results for the piano strings' theoretical and experimental inharmonicities.

1.2 The history and physics of the piano.

Almost every musical tone, whether it is produced by a vibrating string, a vibrating column of air or any other vibrating system, consists of a fundamental tone and a number of the partial tones or overtones. The complex sound produced by this combination of separate tones has a timbre, or characteristic quality, that is determined mainly by the number of partial tones and their relative loudness. It is timbre that enables one to distinguish between two musical tones that have the same pitch and the same loudness but produced by two different musical instruments. A pure tone - one that consists solely of the fundamental tone - is rarely heard in music.

It is commonly believed that the partial tones produced by all musical instrument are harmonic - that their frequencies are exact whole - number multiples of the frequency of a fundamental tone. This is true for all the woodwinds and under certain conditions for many of the stringed instruments, including the violin. It is only approximately true in the piano. The higher the frequency of the partial tones of any note on the piano, the more they depart from a simple harmonic series.

The physics of the piano can best be understood by first reviewing the evolution of the modern piano and its principal components. Archaeological evidence shows that primitive stringed instruments existed before the beginning of recorded history. An instrument called the psaltery that was played by plucking strings stretched across a box or gourd is referred to several times in the Bible. A similar instrument existed in China some thousand years before the Christian era. In the sixth century B.C. Pythagoras used a simple stringed instrument called the monochord in his investigation of the mathematical relations of musical tones. His monochord consisted of a single string stretched

tightly across a wooden box. It was fitted with a movable bridge that could divide the string into various lengths, each of which could vibrate freely at a different fundamental frequency.

The keyboard is another important component of the modern piano. It did not originate in conjunction with a stringed instrument but with a pipe organ. The organ of Ctesibus, perfected at Alexandria in the second century B.C., had some kind of keyboard. The Roman architect Vitruvius, writing during the reign of Augustus Caesar, describes pivoted keys used in the organs of his day. In the second century A.D. Hero of Alexandria built an organ in which the valves admitting air to the pipes were controlled by pivoted keys that were returned to their original position by springs.

As early as the tenth century the application of a keyboard to a stringed instrument was described by St Odo who wrote of the organistrum, a remarkably ingenious instrument in which several strings rest against a resined wheel. The wheel is turned by a crank setting the strings in vibration, much as does the bow on the strings of a violin. Some of the organistrum's strings are unstopped, providing a drone accompaniment to press against other strings. The tangent mechanism is similar to the simple mechanism of the clavichord.

In the 15th century, on the early clavichords, a piece of metal mounted vertically at the end of the key acted both as a bridge for determining the pitch of the string and as a percussive device for producing the tone. Since one string could be used to produce more than one tone, then were usually more keys than strings. In order to damp the unwanted tone from the shorter part of the string, a strip of cloth was interlaced among the strings at one end.

Several essential characteristics of the modern piano are obtained from the clavichord. The clavichord had metal strings, a percussive device for setting the strings in vibration, a damping mechanism and also an independent soundboard: the board at the bottom of the case did not also serve as the

frame for mounting the strings. Moreover, although the tone of the clavichord was weak, the instrument allowed for the execution of dynamics, that is, for playing either loudly or softly.

At about the same time another forerunner of the modern piano was in process of development. Longer strings were introduced to produce a louder tone in the spinet, or virginal. Now the metal percussive device of the clavichord was no longer adequate to produce vibration in the strings. Instead the strings were set in motion by the plucking action of a quill mounted at right angles on a "jack" at the end of the key. When the key was depressed, the jack moved upward and the quill plucked the string. When the jack dropped back, a piece of cloth attached to it damped the vibration of the string.

Around the beginning of the 16th century experiments with still longer strings and larger soundboards led to the development of the harpsichord. It incorporated several important innovations that have carried over to the modern piano although this instrument was essentially nothing more than an enlarged spinet. The wing-shaped case of the harpsichord is imitated by that of the grand piano. The stratagem of using more than one string per note was adopted for the harpsichord by the middle of the 17th century. The harpsichord also had a "forte stop," which lifted the dampers from the strings to permit sustained tones, and a device for shifting the keyboard, both of which are preserved in the modern piano.

The invention of the piano was forecast by inherent defects in both the clavichord and the harpsichord. The clavichord, on the other hand, allowed a modest range of dynamics but could not generate a tone nearly as loud as that of the harpsichord. Attempts to install heavier strings in order to increase the volume of either instrument were futile; neither the metal percussive device of the clavichord nor the quill of the harpsichord could excite a heavy string.

Moreover, the cases of these early instruments were not strong enough to sustain the increased tension of heavier strings.

A remedy for these defects was provided by the Italian harpsichord-maker Bartolommeo Christofori, who built the first hammer-action keyboard instrument in 1709. Christofori called his original instrument the "piano-forte," meaning that it could be played both loudly and softly. The idea of having the string struck by hammers was probably suggested to him by the dulcimer, a stringed instrument played by hammers held in the hands of the performer. Christofori recognised that his new instrument would need a stronger case to withstand the increased tension of the heavier strings. By 1720 an improved model of the pianoforte included an escapement device that "threw" the freeswinging hammer upward at the string and also a back-check that regulated the hammer's downward return. An individual damper connected to the action of the hammer was provided for each note.

For a century and a half after Christofori's first piano appeared inventors worked to improve the new instrument, particularly its novel hammer action. Several other types of action were developed, some new and others modelled closely on Christofori's original. Pianos were built in a variety of forms: traditional wing-shaped pianos, square pianos, upright pianos and even a piano-organ combination.

Among the major innovations toward the end of this period was the full cast-iron frame. Constant striving for greater sonority had led to the use of very heavy strings, and the point was reached where the wooden frames of the earlier pianos could no longer withstand the tension. A grand piano with a cast-iron frame that has served as a model for all subsequent piano frames was brought out by the German-born American piano manufacturer Henry Steinway in 1855. Although minor refinements are constantly being introduced, there have been no fundamental changes in the design or construction of pianos

since 1855.

A part of the piano that has received a great deal of attention from acoustical physicists is the soundboard. Some early investigators believed the sound of the piano originated entirely in the soundboard and not in the strings. We now know that the sound originates in the strings; after the very short interval, called the attack time, it is translated by means of a wooden bridge to the soundboard, from which it is radiated into the air. During the attack time sound is also radiated to a lesser degree from both the strings and the bridge.

The development of the full cast-iron frame gave the sound of the piano much greater brilliance and power. The modern frame is cast in one piece and carries the entire tension of the strings; in a large concert-grand piano the frame mass is 180 kilogram and is subjected to an average tension of 270,000 newtons. In order to maintain the tension of the strings each string is attached at the keyboard end to a separate tuning pin, which passes down through a hole in the frame and is anchored in a strong wooden pin block. Since the piano would go out of tune immediately if the tuning pins were to yield to the tremendous tension of the strings, the pin block is built up of as many as 41 cross-grained layers of hardwood.

The standard modern keyboard has 88 keys divided into seven and a third octaves, the first note in each octave having twice the frequency of the first note in the octave below it. Each octave has eight white keys for playing the diatonic scale (whole notes) and five raised black keys for playing the chromatic scale (whole notes plus sharps and flats). In all modern pianos the white keys are not tuned exactly to the diatonic scale but rather to the equally tempered scale, in which the octave is simply divided into 12 equal intervals.

The moving parts of the piano that are involved in the actual striking of the string are collectively called the action. Early in the history of piano-building the hammers were small blocks of wood covered with soft leather.

The inability of leather to maintain its resiliency after many successive strikings led eventually to the use of felt-covered hammers. It can be pricked with a needle to loosen its fibers, and will then produce a mellower tone; if the felt is too hard it produces a harsh tone. The felt can be filed and made harder if the tone is too mellow and lacks brilliance.

A standard piano has three pedals that serve to control the dampers. The forte, or sustaining, pedal on the right disengages all the dampers so that the strings are free to vibrate until the pedal is released or the tones die away. The sostenuto pedal in the middle sustains only the tones that are played at the time the pedal is depressed; all the other tones are damped normally when their respective keys are released. The "soft" pedal on the left shifts the entire action so that the hammers strike fewer than the usual number of strings, decreasing the loudness of the instrument.

Physically, the string motion can be described in the following way. As the hammer strikes the string, the string is deformed at the point of collision. The result is two waves on the string, travelling out in both directions from the striking point. The wavefronts enclose a pulse, or hump, which gradually gets broader.

However, as the string is struck close to its termination at the agraffe, one of the wavefronts soons reaches this end and is reflected. The reflection at a rigid support makes the wave turn upside down. This inverted wave starts out to the right and restores the string displacement to its equilibrium level.

The situation has developed that the wavefront initially travelling to the left, has turned into the trailing end of a pulse of fixed width, propagating to the right towards the bridge. At the bridge, the entire pulse is reflected, the effect being that the pulse starts out in the opposite direction upside down. A new reflection at the agraffe turns it right side up again, and soon the pulse has completed one round trip and continues out on the next lap.

The propagation velocity of the pulse on the string is determined by the tension and mass per unit length of the string, a higher velocity the tauter and lighter the string. The number of round trips per second, the fundamental frequency (closely related to the perceived pitch), also depends on the distance to be covered - the longer the string the longer the round trip time (fundamental period), and hence, the lower the pitch. The pitch of a string is thus determined by a combination of its length, tension, and mass per unit length. In particular, string length can be traded off against mass per unit length in order to reduce the size of the instrument. This can be seen in the bass section, where the strings are wrapped with one or two layers of copper in order to make them heavy and thus relatively short. The advantage of a wrapped string over a plain string is that the mass can be increased without reducing the flexibility drastically. A piano string need not be perfectly flexible, but a too stiff a string would have a detrimental influence on the tone quality as will explained below.

A piano string, like all other strings, has a set of preferred states of vibration, the resonances, or modes of vibration. When a string is vibrating at one of its resonances, a condition which usually only can be reached in the laboratory, the motion of the string is of a type called sinusoidal. The corresponding sound is a musically uninteresting sine wave. In normal use, however, where the string is either struck, plucked or bowed, all resonances are excited, and the result is a set of simultaneously sounding sine waves, partials, forming a complex tone.

Such a tone is conveniently described by its spectrum, which shows the frequencies and strengths (amplitudes) of the partials. As mentioned, the pitch of the tone is related to the frequency of the lowest member in the spectrum, the fundamental. The relations between the amplitudes of the partials and their evolution in time contribute to our perception of tone quality.

The pulse running back and forth on the piano string has a most surprising connection to the string modes (resonances). It can be shown mathematically that the travelling pulse is made up of a sum of all the string modes. The shuttling pulse and an (infinite) sum of string modes of appropriate amplitudes are equivalent; they are just two ways of representing the same phenomena. So while our eyes will detect the pulse motion (if slowed down enough by the use of a stroboscope) our ears prefer to analyse the string motion in terms of its partial or Fourier components, so named after the French mathematician who first described this equivalence.

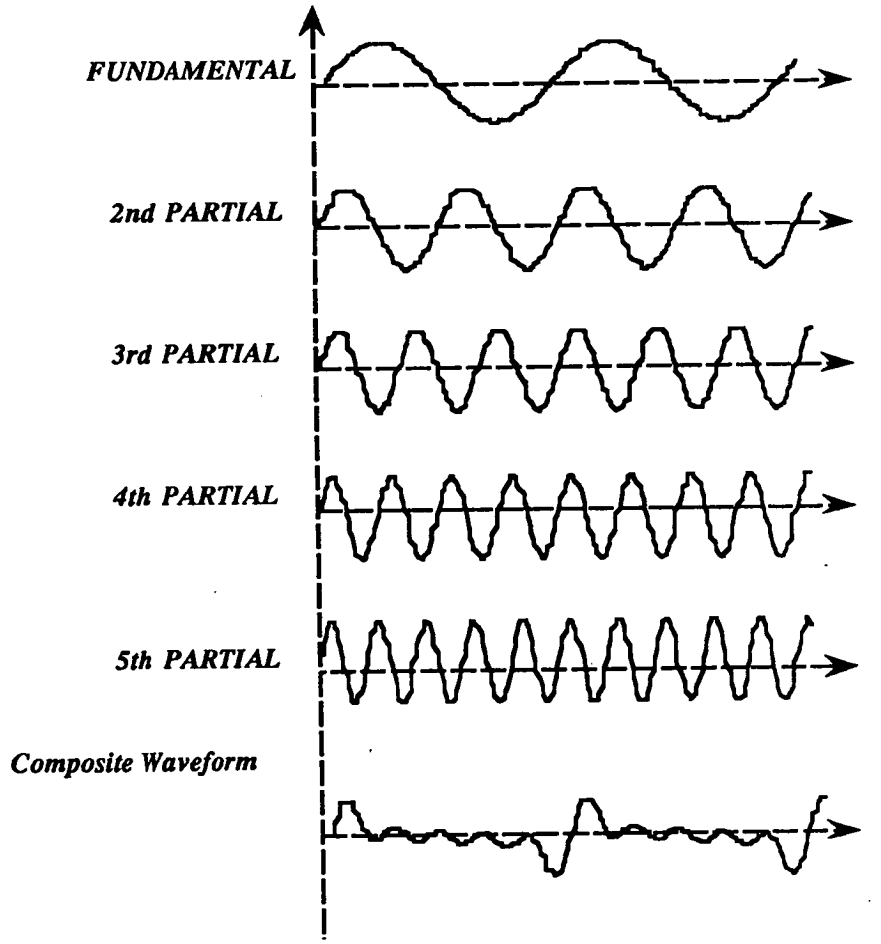

FIGURE 1: Complex periodic waveform and the five harmonic partials of which it is comprised.

Fourier also stated that if the motion is periodic, that is, the same events will repeat indefinitely with regular intervals, the frequencies of the corresponding partials will be harmonic. This means that the frequency ratios between the partials will be exactly 1: 2: 3: 4....., which will be perceived as a sound with a clearly defined pitch and steady tone quality. The statement can also be turned the other way around; if the resonance frequencies of a string are strictly harmonic, the resulting motion of the string will always be periodic. As an example, figure 1 shows a diagram of a complex periodic tone comprised of five harmonic partials. The fundamental frequency is 100 Hz, the second harmonic is at 200 Hz, the third harmonic is at 300 Hz, and so on up to the fifth harmonic at 500 Hz. (For convenience, the fundamental may also be referred to as the first harmonic.) The Figure shows how the harmonics add together to form the complex waveform.

In real pianos, the resonance frequencies of the strings are not exactly harmonic. The frequency ratios are slightly larger than 1: 2: 3: 4..., more like 1: 2.001, 3.005, 4.012..., which is referred to as **"Inharmonicity"**. According to Fourier, the string motion will now not repeat exactly periodically as the note decays, but change slowly which gives a "live" quality to the note.

1.3 Literature Review.

Brook Taylor, an English mathematician, is credited as being the first to develop the correct formula for the frequency of a flexible vibrating string in term of length, tension, and mass. His treatment of the vibratory motion of a stretched string [100] was translated by Lindsay [73].

The problem of the vibrating string was solved analytical by J.L. Lagrange. [69]. He supposed the string made up of a finite number of equally

spaced identical mass particles and studied the motion of this system, establishing the existence of a number of independent frequencies equal to the number of particles. When he passed to the limit and allowed the number of particles to become infinitely great and the mass of each correspondingly small, these frequencies were found to be precisely the harmonic frequencies of the stretched string. The method of Lagrange was adopted by Rayleigh in his "Theory of Sound" [88] and is indeed standard practice to-day, though most elementary books now develop the differential equation of motion of the string treated as a continuous medium by the method by Jean le Rond, called d'Alembert. It is believed that D'Alembert [1], was the first to derive and publish the differential equation of wave propagation called the wave equation.

Kock [68] refers to the work of others who contributed to the understanding of the struck stretched string. Still another prior contributor was R. N. Ghosh [44]. Considering the vibrating string as an electrical transmission line permits the knowledge gained regarding the characteristics of electrical circuits to be used in determining the characteristics of the piano string.

Kock mentions that the partials of piano tones are inharmonic and states that this is undesirable as it impairs the tone quality. "A proposed Loading of Piano Strings for Improved Tone" [79] has been devised by Franklin Miller, Jr. His analysis indicates that by applying a small amount of mechanical loading near one end of a piano string, inharmonicity might possibly be materially reduced, if not completely eliminated, thus improving the tone of the individual strings. Actually, we should keep in mind that the proper amount of inharmonicity in piano tone partials uniformly distributed in the frequency range of the piano enhances the tones and is not undesirable.

Philip M. Morse [81] develops the mathematics related to the vibrations of a stiff string. He also deals with the behaviour of a flexible string. His work serves as a useful background in the theoretical behaviour of the piano string.

Shankland and Coltman [94] presents a study of stretched vibrating strings on a monochord. The experimental apparatus used in their paper takes into account variations in tension produced by the string's vibration. The fundamental frequency of the piano string varies during the decay of the tone and the change contributes to the "life" in the tone. The frequency of vibration decreases slightly immediately after the tone is initiated.

"Observations on the Vibrations of Piano Strings" by Schuck and Young [92], covers a study of the partial frequencies and the decay characteristics of piano tone partials. Careful recording of the variation of amplitudes of partials in tones from single strings as they decayed was done. The decay graphs differ greatly throughout a given piano and from one piano to another. The complex relationship of the relative magnitudes of partials as they decay contributes to the "life" and uniqueness in a piano tone.

Fluctuations in the amplitude of the decay curve of a given partial can be due to one or more of several causes. Schuck and Young mention the rotation of the plane of vibration and the possible transfer of energy from one mode to another. Other possible causes include nonuniformity in stiffness, or mass, of a strings or portion of the piano; conditions at the terminals of the speaking length of the string; inadequate damping, or muting, of other strings in the unison group being checked.

Martin [74] deals with the decay characteristics of tones produced by conventional pianos and introduces some matters to consider when electronic amplification is used with piano tones.

The decay characteristics of piano tones depend upon the energy in the string, how efficiently the energy is utilised to produce sound, and how rapidly the energy is dissipated. In order for a conventional piano to be able to produce the sound power meeting modern requirements in music, the mecahanical impedance of the string must be as large as practicable. Plain strings in the treble portion of the piano

are stiff and rod-like. This results in large inharmonicity values in the strings for the top treble tones. Space limits the string length in the bass portion of the piano and wound string are used to obtain string mass and keep stiffness as low as practicable. The piano is an inefficient radiator of low frequencies and this adds to the problem of low-sound power at the lower frequencies. If required sound power can be obtained by electronic amplification, that burden on the string can be relieved.

Maximum transfer of string energy to radiated sound will occur when the impedance match between string and air is maximum. If a perfect match could be attained, the piano would not produce a musical sound; the energy would be radiated as a step function of short duration.

Martin points out cases in which two different decay times exist in a sustained tone. In these cases, the initial part of the decay characteristic decays at a faster rate than that of the latter part. It appears, however, that Martin did not at that time suggest any mechanism for the double decay, but in later work found that the phenomenon is connected with the presence of more than one string per note, and that the amount of aftersound is affected by the exact manner in which the unisons are tuned [67].

The suggestion that the phase relations among the strings play an important role appears to have been made by Hundley, Martin, and Benioff [58] and in more explicit form by Benade [13]. Benade points out that when three strings vibrate in phase, the motion of the bridge is three times what it would be if one string were vibrating alone; hence, the rate of energy loss of each string is triple. He suggests that, after some time, the strings lose their phase relationship, so that the decay rate becomes equal to that of a single string - hence the break in the decay curve. In fact, these relationships can have effects even more drastic than that: Not only can the decay rate be increased, but it can be decreased if the strings vibrate in exactly opposing phases.

Weinreich [108] showed that the admittance of the piano bridge has a crucial effect on piano tone, and that in the range of ordinary "good" tuning the individual strings cannot be viewed as independent dynamical systems. He developed theoretical expressions that showed how the rate of energy transmission to the bridge as a function of time (including the phenomena of beats and "aftersound") depends on bridge admittance, hammer irregularities, and the exact state in which the piano is tuned. He presented experimental data showing the effects of mutual string coupling on beats and aftersound, as well as the great importance of the two possible directions of the string motion (polarisation); "vertical" and "horizontal".

He concluded that the behaviour of the decaying curve was explained by noting that even a single string vibrating at its fundamental frequency has two distinct modes of vibration corresponding to the two polarisation. The vertical polarisation is the primary one excited by the hammer, and so begins its life at a much higher amplitude than the horizontal one. However, since the bridge, which is attached to the soundboard, "gives" much more easily in the vertical than in the horizontal direction, the decay of the vertical mode is also much more rapid. The relatively slight amount of horizontal vibration becomes, after a while, dominant. He also informed that the fine tuning of the unisons is not so much a matter of regulating the beat rate as of regulating the amount of aftersound. The aftersound is also be affected by irregularities of the hammer, which cause one string to be hit harder than another, and which may cause a greater or lesser excitation of the horizontal vibration.

A computer program that implements a discrete model of a plucked string was extensively modified to allow the modelling of a struck string by R. A. Bacon and J. M. Bowsher [8]. Their model allowed the hammer to strike the string at any one of ninety nine possible positions along the string with a given initial velocity and mass. They showed that output information included

the displacement against time waveforms for the hammer and the string at the struck point, and the times at which the hammer and string made and broke contact. Agreement of their model output with experimental results appeared to vary with the method of the experimenter.

The process of string excitation by striking with hammer lies at the heart of the more general problem of determining the sound produced by a piano. Prediction of the piano string motion presented a challenging problem to the theorist because of the finite time interval during which the string and hammer interact. Even in the limiting case of very small hammer mass, the approximation of a single delta-function impulse is inadequate, as discussed by Hall in Part I [50] of his series work on "Piano string excitation". His Part II [51] and Part III [52] in this series have shown how the spectrum of the piano string motion might be predicted with models that treat the hammer and string as a linear system. A combination of analytic and computer techniques to solve the general case of a hard point hammer with any finite mass was presented in Part II. It was argued that there is no good way to predicted any details of the string energy spectrum without allowing for additional physical processes such as damping. The combined analytic and computer techniques of Part II is extended to solve the general case of a soft point hammer with finite mass in Part III. In Part IV, "Piano string excitation IV: The question of missing modes" [53], it was showed that the piano hammers positioned to strike the strings at certain fractions of their length should produce spectra with "missing modes". The comparisons of the theory on string-hammer interaction with laboratory measurements in Part V [54] showed definite limitations due to: nonlinear mode coupling for finite amplitude, string stiffness and the resulting dispersion, soundboard admittance, finite hammer width, and nonlinearity in the hammer. With these limitations, an examination is made of how well the theory can explain the measured string vibration spectra. He showed that the agreement is

moderately good in the bass and midrange while, at the treble end, the measured spectra fall off significantly faster than the predictions. Accurate modelling of the piano string-hammer interaction requires that the nonlinearity of the force-displacement relation for the hammer be recognised and included, as is shown in "Piano string excitation. VI: Nonlinear modelling" [55]. He found that predictions with these models give significantly better agreement with data than did calculation in his previous part in this series with completely linear models.

Actually, before Hall published "Piano string excitation V: Spectra for real hammers and strings" and "Piano string excitation. VI: Nonlinear modelling", the nonlinear compliance properties of real hammers have been measured and discussed by Suzuki [99] and Boutillon [18]. Suzuki worked on a simulation of the nonlinearity of hammer-string interaction, but he did not compare that with experimental results. Boutillon treated the problem of the nonlinear character of the interaction between the hammer and string based on experimental work in his paper, "Model for piano hammers: Experimental determination and digital simulation" [18]. The hammer was considered as a point mass. He found that numerical simulations of the hammer and string motions based on a two-element model for the hammer were in good agreement with experimental measurements.

In the series of three articles by Askenfelt and Jansson they described an experimental investigation of the tone production in the grand piano. The investigation covered the initial stages, starting with the motion of the key and ending with the string vibrations. Their study is divided into three sections, each section described in a separate article: (1) the timing in the grand piano action [3], (2) the motion of the key and hammer [4], and (3) the interaction between hammer-string and the string vibrations [5]. In the first article the timing in the piano action was found to be dependent on both regulation and dynamic level. They also found that changing the hammer-string distance affected mainly

the timing relation between the key bottom contact and the hammer-string contact. Their second article deals with the typical key and hammer motions at different dynamic levels and for different types of "touch". A *legato* touch with the finger initially resting on the key gave a smooth motion with continuously increasing key velocity. In a *staccato* touch with the finger striking the key from above, an oscillating component at a low frequency (approximately 50 Hz) was observed in the key motion. In the last article they measured the string motion and spectra using an electrodynamic method for sample notes in three ranges of the piano keyboard (bass-mid-treble). In the bass, with a short hammer-string contact relative to the fundamental period, the individual waves were clearly separated. In the midrange, with a contact duration of approximately half a fundamental period, the initial outgoing and reflected waves partly merged, while in the treble, where the contact duration lasts a full period or more, a separation of the string motion into travelling waves was no longer possible.

Chaigne and Askenfelt worked on "Numerical simulations of piano strings. I: A physical model for a struck string using finite difference methods" [24] and "Numerical simulations of piano strings. II. Comparisons with measurements and systematic exploration of some hammer-string parameters" [25]. They developed a physical model of the piano string using finite difference methods. They show in their paper how this numerical approach and the underlying physical model can be improved in order to simulate the motion of the piano string with a high degree of realism. Starting from the fundamental equations of a damped, stiff string interacting with a nonlinear hammer, a numerical finite difference scheme is derived, from which the time histories of string displacement and velocity for each point of the string are computed in the time domain. The interacting force between hammer and string, as well as the force acting on the bridge, are given by the same scheme.

R.W. Young [115] studies the inharmonicity measured for both bass and treble strings in three sizes of Steinway piano. It is found that the bass strings of the usually preferred grand piano have less inharmonicity than have the corresponding strings of a small upright piano.

Harvey Fletcher carried on the study with "Normal Vibration Frequencies of a Stiff Piano String" [40] including consideration of the uniform wrapped string presented for the bass strings of a piano. Fletcher's work is going to be considered in detail in Chapter 2.

Blackham, a research assistant to Harvey Fletcher at the time Fletcher's paper was written, presents some historical background of the piano and a general overview of its construction and its functioning [15]. These are brought out more fully in a paper of Harvey Fletcher, E.Donnell Blackham and Richard Stratton [39]. Pianos vary considerably in size from a small spinet to a large concert piano. They also vary in the quality of design and construction. One should use caution in arriving at broad conclusions based upon a study of small samples. Pianos that are well designed, constructed, and maintained can produce tones that vary greatly in maximum intensity, in decay characteristics, and in the relative magnitudes of the partials in tones. Constructional variations within a given piano and in different pianos include: the hardness, speaking length, diameter, and tension of strings; the stiffness, tightness, uniformity, and length of windings on wound strings; the tuning of strings in unison groups; the hardness, shape, and weight of hammers; the strike line of hammers; the dwell time of hammers on strings; the shape and impedance of the boundaries of string speaking lengths; the length and damping of nonspeaking string portions; the effectiveness of the dampers; the acoustic response of the bridge-soundboard combination; and the efficiency and recovery characteristics of the key-action combination. The piano string serves as the primary element in piano tone production.

A few years after Fletcher's paper, Dietrich Wolf and Helmut Müller worked on "Normal Vibration Modes of Stiff Strings" [113]. They compare the theoretical and experimental behaviour of a stiff steel string vibrating under clamped boundary conditions. They developed apparatus to make it experimentally possible, attaining clamped boundary conditions by attaching one end of a string to a rigid support and passing another end over a balanced wheel maintained under constant tension by a weight acting on the free end. The string was set in forced vibration by an electromagnet, which was driven by an amplifier connected to a quartz-controlled standard frequency generator. In order to observe the string vibrations, a magnetic receiver system was placed near the string, transforming by induction the string's motion into an electric signal. The receiver was shielded carefully against interfering voltages. The signal was fed into a voltmeter and an oscilloscope. As this signal is directly proportional to the velocity of the string, resonance occurs exactly at the natural frequencies. They said in their paper that the experimental results observed with this arrangement agree with the calculated data at an accuracy of about 0.1%.

More recently, many other investigators have studied the piano string inharmonicity problem with plain steel strings and overwound bass strings.

Boutillon, Radier, Valette and Castellengo [17] studied three different effects for a vibrating piano stiff string: the eigenfrequencies as a function of time, the evolution of frequency and the longitudinal force. They calculated the natural frequencies and the inharmonicity coefficient of the string using Fletcher's equation. They carried out a comprehensive study of inharmonicity on a piano using analogue and FFT techniques, only one of the two or three strings associated with a note being allowed to vibrate. The results obtained confirmed the calculated results. Differential spectral analysis (ASD) was used to permit the determination of precise frequencies in a brief signal, offering

considerable simplification of the methods used for such calculations both in time and in equipment. They showed the results of the analysis of the G2 string, agreeing with the results obtained previously by the analogue method and by FFT. In earlier mearsurements, the thirteenth partial did not appear to follow the law of inharmonicity; ASD allowed the detection of two components in it. They found that the more intense component was a harmonic of the fundamental; the frequency of the weaker component (impossible to measure by FFT) agreed with the law of inharmonicity. The evolution of the fundamental frequency of the sound emitted by a bench on which was mounted a piano string, not too taut and strongly excited was shown. They found that as the amplitude decayed, the natural frequencies decreased in time. They also found that the measurement of the longitudinal force on the support gives direct evidence of the physical nature of the octave vibration.

Alexander J. Bell and Raymond Parks [12] showed that Fletcher's formula $f_n = nf_0(1+Bn^2)^{1/2}$ is not completely adequate in predicting the modal frequencies of a piano string. Although a complete solution depends on the solution of a transcendental equation, they showed that, by recourse to Rayleigh, a similar equation of the form $f_n = nf_0(1+Bn^2-Cn^4)^{1/2}$ can be derived. They still considered that the bass piano string was uniformly overwound.

Actually all piano bass strings are not uniformly overwound. A small part of the steel core is left exposed near the end of the strings.

Some discussions about this problem have appeared by Levinson [71], Sakata and Sakata [91] and Gottlieb [46]. Levinson studied the free vibration of a string with stepped mass density and derived an exact equation for calculating the natural frequency, but did not obtain any numerical solutions.

Sakata and Sakata derived an exact frequency equation for a string with stepped mass density and proposed an approximate formula for estimating the

fundamental natural frequency of the string.

In Gottlieb's work, the three-part string, with two step discontinuities in density, was investigated in some detail for both fixed and free end conditions. Aspects of the "four-part" and "m-part" string problems were also discussed. However, these derivations have not taken into account the stiffness of the stepped string.

Michael Podlesak and Anthony R. Lee worked on "Dispersion of waves in piano strings" [85]. It was shown how the group velocity of transverse waves in piano strings can be measured as a function of frequency with the aid of a short-time spectral analysis method. Examples of group velocity measurements appeared. The relationship between the group and phase velocity, as a function of frequency, was also illustrated in their work. "Effect of Inharmonicity on the Aural Perception of initial Transients in Low Bass Tones" [86] showed numerical modelling of low bass tones based on the string displacement waveform of a piano, revealing a marked correlation between a perceived pitch glide in the initial transient of the tone and the inharmonic relationship between the tone's partials.

Musical timbre is the characteristic tone quality of a particular class of sounds. Musical timbre is much more difficult to characterise than either loudness or pitch because it is such a diverse phenomenon. No one-dimensional scale - such as the loud/soft of intensity or the high/low of pitch - has been postulated for timbre, because there exists no simple pair of opposites between which a scale can be made. Because timbre has so many facets, computer techniques for multidimensional scaling have constituted the first major progress in quantitative description of timbre since the work of Hermann von Helmholtz in the nineteenth century.

Fourier transform spectroscopy enables researchers to obtain the spectrum of a sound from its waveform. A computer technique which performs a

Fourier transform on a digital signal is the Discrete Fourier Transform (DFT). The DFT is computationally intensive, but through a clever ordering of the computer operations involved in performing a DFT, Cooley and Tukey were able to reduce the number of computer operations significantly. Their algorithm is known as the Fast Fourier Transform (FFT) [28].

The techniques that have been exploited to describe transient musical signals have relied on the determination of the amplitude of the various Fourier Coefficients as a function of time. Thus the transient signal has been regarded as piecewise continuous and both analogue and digital methods have been applied to obtain the coefficients [10]. Analogue methods are satisfactory for slowly varying signals but digital methods generally appear more appropriate for rapidly varying sounds.

An alternative approach was that of using the Fourier Transform of the complete note. It had been used for a simple decaying sine wave [78], but had been considered as too "obscure" for application to music [65].

Alfredson and Steinke [2] discussed the application of the Fourier Transform to a piano note and compared it with the more familiar Fourier coefficients. It was concluded that the Fourier transform had an advantage in terms of frequency resolution but that the two methods were to some extent complementary.

The Fourier Transform is an alternative method of viewing musical sounds. The time history of the sound is not so obvious as in the method of plotting the Fourier coefficients as a function of time. However, greater detail in resolving the frequency components appeared to be possible. Both methods commenced with the same basic information -the time history of the note. This time history of course could be reconstituted with either approach.

For many applications in musical acoustics, the power spectrum is a most effective way of describing the component frequencies present in a sound,

together with their relative amplitudes.

The Fourier Transform processes a number of samples, n, taken at regular intervals over a total time, T, and determines the amplitude and phase for n/2 calculation frequencies, each being an integral multiple of the frequency interval 1/T. The output from the DFT can be considered as n/2 frequency bins at intervals of 1/T, each containing a calculated sum of the total amplitude of components lying within a band around its centre frequency.

In the ideal case of a periodic signal where the portion of signal analysed spans an exact number of cycles of the fundamental, each component of the signal corresponds to one of the lines of the FFT. If this ideal condition is not present, the signal frequencies lie between the calculation frequencies, causing the analysis to attribute them in a widespread pattern which varies according to the frequency mismatch, an effect termed "leakage". The ideal situation is often unattainable, as the signal frequency may not be known in advance, or the sample rate may not be adjustable to the precise value. More importantly, analysis should cope with several signals combined, at unknown frequencies.

The remedy is to multiply the data time-series by a "window function" [56] which is unity in the middle and tapers towards zero at each end. The effect is to give a rounded peak spanning several frequency intervals, with fairly uniform shape regardless of where the signal frequency lies within the frequency interval, and with a substantial reduction in the leakage to distant bins. Peak shape depends on the window function, but for a given function the peak always spans the same number of frequency bins even when their width is altered by other factors such as transform size.

The result of the DFT performed on windowed data is the convolution of the DFT of the window function and the DFT of the raw data. This mathematical statement unfortunately does not offer a simple way of recovering

the frequency information. In the present work, an empirical approach has been developed from careful study of the characteristics of the output for calibration signals by Raymond Parks [84].

CHAPTER 2

THEORETICAL CONSIDERATION

In this chapter, the theory of strings in the case of a flexible string, a uniform stiff string, and a nonuniform stiff string are described. In the first place, it is assumed that the string is perfectly flexible, the only restoring force being due to the tension. Secondly, it is necessary to study the effect of stiffness on the string's motion. A discussion of the transverse vibration of a rigid bar leads to a study of the vibration of a uniform stiff string. Finally, the vibration of a nonuniform stiff string is considered. A derivation of the mode frequencies of a stepped string is presented, taking in to account the stiffness of the stepped string.

2.1 Transverse wave equation for a string.

The study of vibrating strings has a long history. Pythagoras is said to have observed how the division of a stretched string into two segments gave pleasing sounds when the lengths of these two segments had a simple ratio (2:1, 3:1, 3:2, etc.). These are examples of normal modes of a string fixed at its ends. Closer examination of the motion of a string reveals that the normal modes depend upon the mass of the string, its length, the tension applied, and the end conditions.

Consider a uniform string (Fig. 2.1) with linear density σ (kg/m)

stretched to a tension T (newtons). The net force dF, restoring segment ds to its equilibrium position, is the difference between the y components of T at the two ends of the segment:

$$dF_y = (T\sin\theta)_{x+dx} - (T\sin\theta)_x. \qquad \text{.....(2.1)}$$

Applying the Taylor's series expansion $f(x+dx) = f(x) + \frac{\partial f(x)}{\partial x}dx + \ldots$ to $T\sin\theta$ and keeping first-order terms gives

$$dF_y = [(T\sin\theta)_x + \frac{\partial(T\sin\theta)}{\partial x}dx] - (T\sin\theta)_x = \frac{\partial(T\sin\theta)}{\partial x}dx. \qquad \text{.....(2.2)}$$

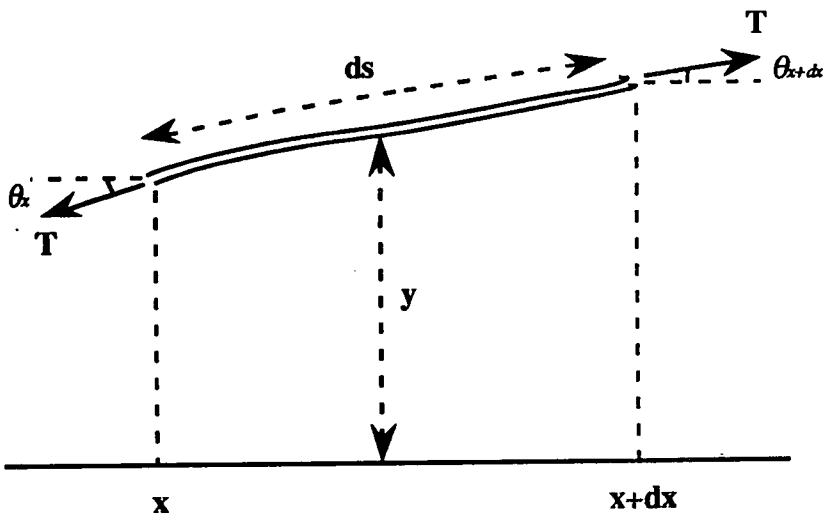

Fig. 2.1 Forces on an elementary length of flexible string.

For small displacement y, $\sin\theta$ can be replaced by $\tan\theta$, which is also $\partial y/\partial x$, and the tension T can be taken as constant (independent of x). The net transverse force on the element becomes

$$dF_y = \frac{\partial(T\,\partial y/\partial x)}{\partial x}dx = T\frac{\partial^2 y}{\partial x^2}dx. \qquad \text{.....(2.3)}$$

The mass of the segment ds is σds, so Newton's second law of motion becomes

$$T\frac{\partial^2 y}{\partial x^2}dx = (\sigma ds)\frac{\partial^2 y}{\partial t^2}. \qquad \text{.....(2.4)}$$

Since dy is small, $ds \cong dx$. Also, we write $c^2 = \frac{T}{\sigma}$ and obtain

$$\frac{\partial^2 y}{\partial t^2} = \frac{T}{\sigma}\frac{\partial^2 y}{\partial x^2} = c^2\frac{\partial^2 y}{\partial x^2}. \qquad \text{.....(2.5)}$$

This is the well-known equation for transverse waves in a vibrating flexible string.

The general solution of Eq.(2.5) can be written

$$y = A\sin(\frac{2\pi f}{c}x)\cos(2\pi ft - \phi) \qquad \text{.....(2.6)}$$

when the boundary condition that $y = 0$ when $x = 0$ is required.

Consider a perfectly flexible round string of length l, which is stretched between rigid supports under a tension T. When the secondary condition $y = 0$ at $x = l$ is added, all the possible standing waves indicated in Eq.(2.6) can be used only if they have nodal points at $x = l$. Since the distance between nodal points depends on the frequency, the string fixed at both ends cannot vibrate with simple harmonic motion of any frequency; only a discrete set of frequencies is allowed, the set that makes $\sin(2\pi fl/c)$ zero. The distance between nodal points must be l, or it must be $(l/2)$, or $(l/3)$ . . . etc. The allowed frequencies are therefore $(c/2l)$, $(2c/2l)$, $(3c/2l)$ . . . etc., and the different allowed simple harmonic motions are all given by the expression

$$f_n\left(\begin{matrix}\text{flexible string}\\ \text{under tension}\end{matrix}\right) = n(\frac{1}{2l})\sqrt{\frac{T}{\sigma}}. \qquad \text{.....(2.7)}$$

For such a string we see that $f_n = nf_1$; i.e., the natural frequencies form an exact harmonic series. Eq.(2.7) states that the frequencies of all the overtones of such a string are integral multiples of fundamental frequency f_1. Overtones bearing this simple relation to the fundamental are called harmonics, the fundamental frequency being called the first harmonic, the first overtone (twice the fundamental) being the second harmonic, and so on.

2.2 Bending waves in a bar.

In the previous section, the motion of a somewhat idealised string was analysed. We assumed that the string was perfectly flexible, and that the only restoring force was due to the tension. However, we cannot put off studying the effect of stiffness on the string's motion, and we shall begin the study by discussing the transverse vibrations of bars.

There is no sharp distinction between what we mean by a bar and what we mean by a string. In general, tension is more important as a restoring force than stiffness for a string, and stiffness is more important for a bar; but there is a complete sequence of intermediate cases from stiff strings to bars under tension. The perfectly flexible string is one limiting case, where the restoring force due to stiffness is negligible compared with that due to the tension. The rod or bar under no tension is the other limiting case, the restoring force being entirely due to stiffness.

The first limiting case was studied in the previous section. The second case, the bar under no tension, will be studied in this section, and the intermediate cases will be dealt with in a later section.

A bar or rod is capable of transverse vibrations in somewhat the same manner as a string. The dependence of the frequency on tension is more complicated than it is in a string, however. In fact, a bar vibrates quite nicely

under zero tension, the elastic forces within the bar supplying the necessary restoring force in this case.

When a bar is bent, the outer part is stretched and the inner part is compressed. Somewhere in between is a neutral axis whose length remains unchanged, as shown in Fig. 2.2. A filament located at a distance z below the neutral axis is compressed by an amount $zd\phi$. The strain is $zd\phi/dx$, and the amount of force required to produce the strain is $QdS(zd\phi/dx)$ where dS is the cross sectional area of the filament and Q is Young's modulus.

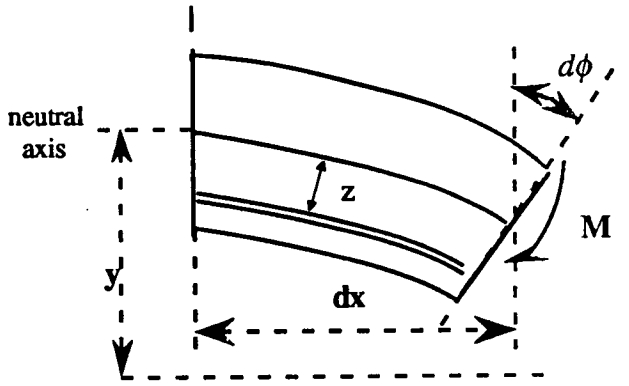

Fig. 2.2 (a) Bending strains in a bars.

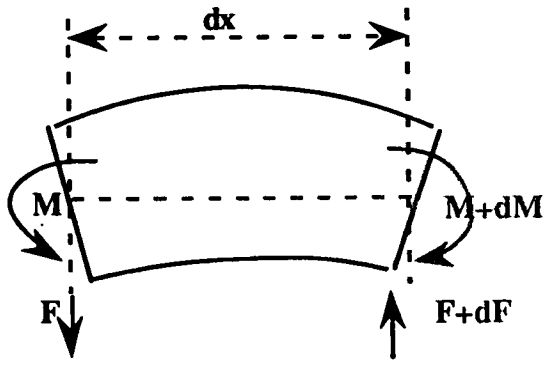

(b) Bending moments and shear forces in a bar.

The moment of this force about the neutral axis is $(Qd\phi/dx)z^2dS$, and so the total moment required to compress all the filaments is

$$M = \left(\frac{Qd\phi}{dx}\right)\int z^2 dS. \qquad \text{.....(2.8)}$$

It is customary to define a constant κ called the radius of gyration of the cross section such that

$$\kappa^2 = \frac{1}{S}\int z^2 dS, \qquad \text{.....(2.9)}$$

where $S = \int dS$ is the total cross section. The bending moment is thus

$$M = \frac{Qd\phi S\kappa^2}{dx} \equiv -QS\kappa^2 \frac{\partial^2 y}{\partial x^2}. \qquad \text{.....(2.10)}$$

since $d\phi \equiv -(\frac{\partial^2 y}{\partial x^2})dx$ for small $d\phi$.

The bending moment is not the same for every part of the bar; it is a function of x, the distance from one end of the bar. In order to keep the element of bar in balance, there must be the difference in the moments acting on the two ends of the element balanced by a shearing force represented by F. The moment of the shearing force is Fdx and this must equal dM for equilibrium, which means that.

$$F = \frac{\partial M}{\partial x} = -QS\kappa^2 \frac{\partial^3 y}{\partial x^3}. \qquad \text{.....(2.11)}$$

The shearing force F is also a function of x and may be different for different ends of the element of bar. This leaves a net force $dF = (\partial F/\partial x)dx$ acting on the element, perpendicular to the bar's axis; and this force must equal the element's acceleration times its mass σdx where σ is the linear mass density of the material of the bar. Therefore the equation of motion of the bar is

$$(\frac{\partial F}{\partial x})dx = (\sigma dx)\frac{\partial^2 y}{\partial t^2} \qquad .....(2.12)$$

$$-QS\kappa^2 \frac{\partial^4 y}{\partial x^4} = \sigma \frac{\partial^2 y}{\partial t^2} \qquad .....(2.13)$$

$$\frac{\partial^2 y}{\partial t^2} = -\frac{QS\kappa^2}{\sigma}\frac{\partial^4 y}{\partial x^4}. \qquad .....(2.14)$$

If $y = Y(x)e^{-2\pi ift}$ is set in Eq.(2.14), Y must satisfy the equation

$$\frac{d^4 Y}{dx^4} = 16\pi^4 \mu^4 Y \qquad .....(2.15)$$

where

$$\mu^4 = \frac{\sigma f^2}{4\pi^2 QS\kappa^2} \qquad .....(2.16)$$

The general solution of this is

$$Y = a\cosh(2\pi\mu x) + b\sinh(2\pi\mu x) + c\cos(2\pi\mu x) + d\sin(2\pi\mu x) \qquad ....(2.17)$$

Consider a bar of length l, fastened by hinges at its two ends to a solid anchorage so that Y and d^2Y/dx^2 are both zero at $x = 0$ and $x = l$; the stiffness properties of the material of this are expressed in terms of its "modulus of elasticity" Q, and σ once more stands for the bar's linear mass density. The nth characteristic frequency of the bar is given by the following formula:

$$f_n(\text{hinged bar}) = (\frac{n^2 r^2}{l^2})\sqrt{\frac{\pi Q}{2\sigma}} \qquad .....(2.18)$$

Here we notice that $f_n = n^2 f_1$, so that a bar whose first mode frequency f_1 is 100 Hz will produce components at $2^2 \times 100 = 400$ Hz, $3^2 \times 100 = 900$ Hz, etc., instead of the 100-, 200-, 300-,... Hz sequence of the flexible string. That is the natural frequencies for a bar are much more widely spaced than they are for a string. We also notice that the frequency varies

inversely as the square of the bar's length, so that doubling the length moves the sound down two octaves in pitch. Observe that the bar's radius appears in the numerator, instead of in the denominator, so that an increase in the thickness of the bar raises its frequency instead of lowering it as is the case for a flexible string under tension.

2.3 Vibrations of a stiff string.

When a string is under a tension of T newton, and also has stiffness, its equation of motion is

$$T\frac{\partial^2 y}{\partial x^2} - QS\kappa^2 \frac{\partial^4 y}{\partial x^4} = \sigma \frac{\partial^2 y}{\partial t^2}. \qquad \text{.....(2.19)}$$

This equation can be obtained by combining the derivations in the two previous sections. The constant S is the area of cross section of the string, κ its radius of gyration, σ its linear mass density and Q the modulus of elasticity of the material.

If $y = Y(x)e^{-2\pi ift}$ is set in Eq.(2.19), Y must satisfy the equation

$$\frac{d^4Y}{dx^4} - 8\pi^2\beta^2\frac{d^2Y}{dx^2} - 16\pi^4\gamma^4 Y = 0, \quad \text{where } \beta^2 = (T/8\pi^2 QS\kappa^2), \quad \gamma^2 = (f/2\pi)\sqrt{\sigma/QS\kappa^2}. \qquad \text{....(2.20)}$$

Setting $Y = Ae^{2\pi\mu x}$, we obtain an equation for the allowed values of μ: $\mu^4 - 2\beta^2\mu^2 - \gamma^4 = 0$. This equation has two roots for μ^2 and therefore four roots for μ:

$$\mu = \pm\mu_1, \qquad \mu_1^2 = \sqrt{\beta^4 + \gamma^4} + \beta^2 \qquad \text{.....(2.21)}$$

$$\mu = \pm i\mu_2, \qquad \mu_2^2 = \sqrt{\beta^4 + \gamma^4} - \beta^2 \qquad \text{.....(2.22)}$$

$$\mu_1^2 = 2\beta^2 + \mu_2^2, \qquad \mu_1\mu_2 = \gamma^2 \qquad \text{.....(2.23)}$$

The general solution of Eq.(2.19) can then be written

$$Y = a\cosh(2\pi\mu_1 x) + b\sinh(2\pi\mu_1 x) + c\cos(2\pi\mu_2 x) + d\sin(2\pi\mu_2 x) \qquad \text{.....(2.24)}$$

The boundary conditions.

Boundary conditions are important in determining the general behaviour of the string, its allowed frequencies, etc. The fact that a string is fastened to supports is an example of a boundary condition. It is a requirement on the string at a given point in space which must be true for all time, as opposed to initial conditions, which fix the dependence of y and v on x at a given time.

If the string is fastened to rigid supports a distance l cm apart, the boundary condition is that y must be zero at each end, for all values of the time. For the case when the two ends of the string are clamped, the boundary condition at these ends are that both y and its slope $(\partial y/\partial x)$ must be zero at each end. The other important case is when the string is hinged at both ends, making $y=0$ and also $(\partial^2 y/\partial x^2)=0$ at each end.

If the boundary conditions are symmetrical, it will be useful to place the point $x = 0$ midway between the supports. The normal functions will then be even functions, $\Psi(-x)=-\Psi(x)$; or they will be odd ones, $\Psi(-x)=-\Psi(x)$. In either case, if the boundary conditions at one end, $x=(l/2)$ are fitted, they will also fit at the other end, $x=-(l/2)$. The even functions from the general equation Eq.(2.24) are built up out of the combination

$$Y = a\cosh(2\pi\mu_1 x) + c\cos(2\pi\mu_2 x) \qquad \text{.....(2.25)}$$

and the odd functions from the combination

$$Y = b\sinh(2\pi\mu_1 x) + d\sin(2\pi\mu_2 x) \qquad \text{.....(2.26)}$$

The hinged boundary conditions $Y=0$ and also $(\partial^2 Y/\partial x^2)=0$ at $x=\pm l/2$ are considered. Then the even functions Eq.(2.25) will fit if $a = 0$ and $\cos(\pi\mu_2 l)=0$; that is,

$$\mu_2 = \frac{n}{2l} \qquad .....(2.27)$$

where n can be 1, 3, 5, 7, or any odd integer.

If the odd functions are used, then b are zero and $\sin(\pi\mu_2 l)=0$, or

$$\mu_2 = \frac{n}{2l} \qquad .....(2.28)$$

where $n = 2, 4, 6, 8$, or any even integer.

For each values of μ_2, there is a corresponding frequency f of the odd and even partials obtained from Eq.(2.22) as

$$f_n = nf_0(1+Bn^2)^{1/2} \qquad .....(2.29)$$

where
$$B = (\pi^2 QS\kappa^2/4l^4\sigma f_0^2) \qquad .....(2.30)$$

Eq.(2.29) and (2.30) are derived in Fletcher's paper [40] "Normal Vibration Frequencies of a Stiff Piano String". The parameter f_0 is the first mode frequency of an ideal flexible string, which has the same length, tension and mass density as the real string, but with no bending stiffness. The parameter B, the inharmonicity coefficient, can be written as $B = (\pi^2 R/4l^4\sigma f_0^2)$, where l is the length and σ the linear mass density of the string; $R = QS\kappa^2$, where Q is the Young's modulus of elasticity, S is the cross-sectional area, and κ is the radius of gyration of the cross-section about an axis through the centre of the string and perpendicular to its length. For a uniform string of circular cross-section and diameter d, $\kappa = d/4$.

Fletcher proposed that a similar treatment could be applied to an overwound string by making the assumption that the overwinding increased the

linear mass density of the string without increasing its bending stiffness. The relationship between mode frequency and mode number has again the form of Eq.(2.29); in the evaluation of the inharmonicity coefficient B, R is calculated using the dimensions and elasticity of the solid core, while the calculation of σ includes the additional mass and volume of the overwinding. For a string consisting of a steel core of density ρ_s and diameter d, with a single overwound layer of copper of density ρ_c and maximum diameter D,

$$\sigma = \rho_c \frac{\pi^2}{16} D^2 + (\rho_s \frac{\pi}{4} - \rho_c \frac{\pi^2}{16}) d^2 . \qquad .....(2.31)$$

A comparable formula gives the linear mass density of a doubly overwound string [40].

2.4 Vibrations of a nonuniform stiff string.

In this section we derive an expression for the frequencies of vibration of a stepped stiff string. Consider the vibration of an M-part string fixed at its ends. The (displacement) finite element formulation of the one-dimensional fourth-order differential equation Eq.(2.19) is

$$T \frac{\partial^2 y_i}{\partial x^2} - R_i \frac{\partial^4 y_i}{\partial x^4} = \sigma_i \frac{\partial^2 y_i}{\partial t^2} \qquad \mathbf{i = 1, 2, 3,....., m} \qquad .....(2.32)$$

where y_i is the (small) transverse displacement of the string originally lying on the x-axis, t is the time, T is the tension, and R and σ are as defined in Section 1.3. The right hand end of the i^{th} segment, of length l_i, is at $x = x_i$; the ends of the complete string, taken to be hinged, are at $x=0$ and $x=l$.

If $y_i = Y_i(x) e^{-2\pi i f t}$ is set in Eq.(2.32), Y_i must satisfy the equation

$$T\frac{d^2Y_i}{dx^2} - R_i\frac{d^4Y_i}{dx^4} = -\sigma_i(4\pi^2 f^2)Y_i \qquad i = 1, 2, 3,...., m \qquad .....(2.33)$$

The boundary conditions are

$$\begin{aligned} Y_1(0) &= Y_m(l) = 0 \\ Y_1''(0) &= Y_m''(l) = 0 \end{aligned} \qquad .....(2.34)$$

and the junction conditions

$$\begin{aligned} Y_i(x_i) &= Y_{i+1}(x_i) \\ Y_i'(x_i) &= Y_{i+1}'(x_i) \\ R_iY_i''(x_i) &= R_{i+1}Y_{i+1}''(x_i) \\ TY_i'(x_i) - R_iY_i'''(x_i) &= TY_{i+1}'(x_i) - R_{i+1}Y_{i+1}'''(x_i). \end{aligned} \qquad .....(2.35)$$

The boundary conditions are those for simple hinged supports and the junction conditions express the continuity of the displacement, slope, moment, and shear at the junctions of the M segments of the stiff string.

A two segment stiff string.

In the case of a two segment stiff string the general solutions of Eq.(2.33) with m=2, can then be written, from Eq.(2.24), as

$$Y_1 = a\cosh(2\pi\mu_{11}x) + b\sinh(2\pi\mu_{11}x) + c\cos(2\pi\mu_{12}x) + d\sin(2\pi\mu_{12}x) \quad ..(2.36)$$

$$\begin{aligned} Y_2 = {} & e\cosh(2\pi\mu_{21}(l-x)) + f\sinh(2\pi\mu_{21}(l-x)) \\ & + g\cos(2\pi\mu_{22}(l-x)) + h\sin(2\pi\mu_{22}(l-x)) \end{aligned} \qquad .....(2.37)$$

The boundary conditions are

$$\begin{aligned} Y_1(0) &= Y_2(l) = 0 \\ Y_1''(0) &= Y_2''(l) = 0 \end{aligned} \qquad .....(2.38)$$

The junction conditions are

$$Y_1(a_1) = Y_2(a_1) \qquad \text{.....(2.39)}$$

$$Y_1'(a_1) = Y_2'(a_1) \qquad \text{.....(2.40)}$$

$$R_1 Y_1''(a_1) = R_2 Y_2''(a_1) \qquad \text{.....(2.41)}$$

$$TY_1'(a_1) - R_1 Y_1'''(a_1) = TY_2'(a_1) - R_2 Y_2'''(a_1) \qquad \text{.....(2.42)}$$

By applying these junction and boundary conditions to the general solution Eq.(2.36) and (2.37), we can then get Eq.(2.43), from which the normal mode frequencies can be found. Afterwards, this equation will be called the frequency equation:

$$\begin{aligned}
&\{\frac{R_1}{R_2}\frac{\mu_{11}^2}{\mu_{22}^2}+1\}\{\mu_{11}\tanh(\mu_{21}a_2)+\mu_{21}\tanh(\mu_{11}a_1)\} \\
&\times\{\frac{R_1}{R_2}\frac{\mu_{12}^2}{\mu_{21}^2}+1\}\{\mu_{12}\tan(\mu_{22}a_2)+\mu_{22}\tan(\mu_{12}a_1)\} \\
&-\{\frac{R_1}{R_2}\frac{\mu_{11}^2}{\mu_{21}^2}-1\}\{\mu_{11}\tan(\mu_{22}a_2)+\mu_{22}\tanh(\mu_{11}a_1)\} \\
&\times\{\frac{R_1}{R_2}\frac{\mu_{12}^2}{\mu_{22}^2}-1\}\{\mu_{12}\tanh(\mu_{21}a_2)+\mu_{21}\tan(\mu_{12}a_1)\}=0 \qquad \text{.....(2.43)}
\end{aligned}$$

Equation (2.43) contains four parameters $\mu_{11},\mu_{12},\mu_{21},\mu_{22}$ which are functions of the frequency, f_n.

$$\mu_{jk} = \sqrt{(\sqrt{(\frac{T}{2R_j})^2 + (2\pi f_n)^2 \frac{\sigma_j}{R_j}} + (-1)^k \frac{T}{2R_j}} \quad : j,k = 1,2. \qquad \text{....(2.44)}$$

In the case of the overwound string, R is constant if it is considered that its stiffness is constant along its length being due only to the core. The frequency

equation then simplifies to

$$\begin{aligned}&(\frac{\mu_{11}^2}{\mu_{22}^2}+1)(\frac{\mu_{12}^2}{\mu_{21}^2}+1)\{\frac{\mu_{11}}{\mu_{21}}\frac{\tanh(\mu_{21}a_2)}{\tanh(\mu_{11}a_1)}+1\}\{\frac{\mu_{12}}{\mu_{22}}\frac{\tan(\mu_{22}a_2)}{\tan(\mu_{12}a_1)}+1\}\\&-(\frac{\mu_{11}^2}{\mu_{21}^2}-1)(\frac{\mu_{12}^2}{\mu_{22}^2}-1)\{\frac{\mu_{11}}{\mu_{22}}\frac{\tan(\mu_{22}a_2)}{\tanh(\mu_{11}a_1)}+1\}\{\frac{\mu_{12}}{\mu_{21}}\frac{\tanh(\mu_{21}a_2)}{\tan(\mu_{12}a_1)}+1\}=0\end{aligned} \qquad \text{...(2.45)}$$

where

$$\mu_{jk}=\sqrt{(\sqrt{(\frac{T}{2R_1})^2+(2\pi f_n)^2\frac{\sigma_j}{R_1}}+(-1)^k\frac{T}{2R_1}} \quad : j,k=1,2. \qquad \text{.....(2.46)}$$

The allowed frequencies, f_n : (n = 1, 2, 3, 4, ...) can be found numerically from equation (2.45) & (2.46) and will be considered in the next Chapter.

CHAPTER 3

NUMERICAL ANALYSIS

In this chapter, numerical calculations have been undertaken to compute theoretical mode frequencies from the frequency equation in the previous chapter for strings with varying degrees of overwinding. Strings with three different core and overwinding dimensions have been calculated. For each set of core and overwinding dimensions, six uniformly overwound strings and six stepped overwound strings of varying length have been studied. The inharmonicity of each string has been evaluated.

3.1 Numerical Root Finding.

Refer to the frequency equation for the overwound string, eq. (2.41) & (2.42), in the previous chapter. The allowed frequencies, f_n: (n=1,2,3,...), can be calculated numerically by applying Newton's method.

The Mathematica package programmed on an Apple Macintosh computer was used for this method of calculation. FindRoot is a command to search for a numerical solution. In trying to find a solution, FindRoot starts at a specific point, and then progressively tries to get closer and closer to a solution. An example of command FindRoot is

$$FindRoot[lhs == rhs, \{x, x_0\}]$$

for searching for a numerical solution to the equation $lhs == rhs$, starting with $x = x_0$.

Picking good starting points is crucial in getting useful answers from FindRoot. To know how to pick good starting points, we need to understand a little about how FindRoot actually works.

In the simplest case, FindRoot uses the Newton-Raphson method, also called Newton's method. Newton's method for finding the zeros of $f(x)$ is the most commonly used of all one-dimensional root-finding routines. This method requires the evaluation of both the function $f(x)$, and the derivative $f'(x)$, at an arbitrary point x. The Newton formula consists geometrically of extending the tangent line at a current point x_i until it crosses zero, then setting the next guess x_{i+1} to the abscissa of that zero-crossing (see Fig.3.1).

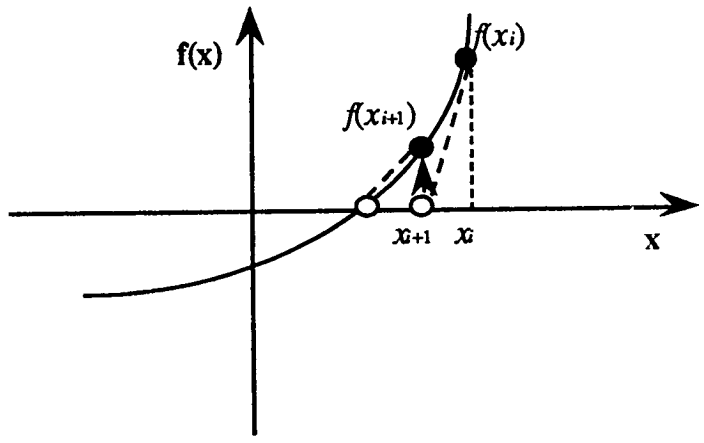

Fig.3.1 Newton's method extrapolates the local derivative to find the next estimate of the root. In this example it works well and converges quadratically.

Algebraically, the method derives from the familiar Taylor series expansion of a function in the neighbourhood of a point,

$$f(x) \approx f(x_0) + f'(x_0)(x - x_0) + \frac{f''(x_0)}{2}(x - x_0)^2 + \ldots . \qquad \ldots .(3.1)$$

For small enough values of $(x-x_0)$, and for well-behaved functions, the terms beyond linear are unimportant, hence $f(x)=0$ implies

$$(x-x_0)=-\frac{f(x)}{f'(x)} \qquad .....(3.2)$$

Within a small distance ε of x the function and its derivative are approximately:

$$f(x+\varepsilon)=f(x)+\varepsilon f'(x)+\varepsilon^2\frac{f''(x)}{2}+...,$$

$$f'(x+\varepsilon)=f'(x)+\varepsilon f''(x)+... \qquad .....(3.3)$$

By the Newton formula,

$$x_{i+1}=x_i-\frac{f(x_i)}{f'(x_i)}, \qquad .....(3.4)$$

so that

$$\varepsilon_{i+1}=\varepsilon_i-\frac{f(x_i)}{f'(x_i)}. \qquad .....(3.5)$$

When a trial solution x_i differs from the true root by ε_i, we can use eq.(3.3) to express $f(x_i)$, $f'(x_i)$ in eq.(3.4) in terms of ε_i and derivatives at the root itself. The result is a recurrence relation for the deviations of the trial solutions

$$\varepsilon_{i+1}=-\varepsilon_i^2\frac{f''(x)}{2f'(x)}. \qquad .....(3.6)$$

Equation (3.6) says that Newton's method converges quadratically. Near a root, the number of significant digits approximately doubles with each step. This very strong convergence property makes Newton the method of choice for

any function whose derivative can be evaluated efficiently, and whose derivative is continuous and nonzero in the neighbourhood of a root.

In general, *Mathematica* distinguishes two kinds of approximate real numbers: *arbitrary-precision* ones, and *machine-precision* ones. The precision of the approximate real number is the number of decimal digits in it which are treated as significant for computation. Arbitrary-precision numbers can contain any number of digits, and their precision is adjusted during computations. Machine-precision numbers, on the other hand, contain a fixed number of digits, and their precision remains unchanged throughout computations. On the computer system used to generate these results, the machine precision is 16 decimal digits.

Examples of FindRoot applied to the frequency equation will be shown in Appendix A , but before we consider an example for finding the numerical mode frequency, parameters in the frequency equation have to be defined.

3.2 Numerical parameters.

Theoretical mode frequencies from the frequency equation for the overwound strings have been computed by using numerical root finding. Fig.3.2 shows the notation used for defining the parameters of the overwound string.

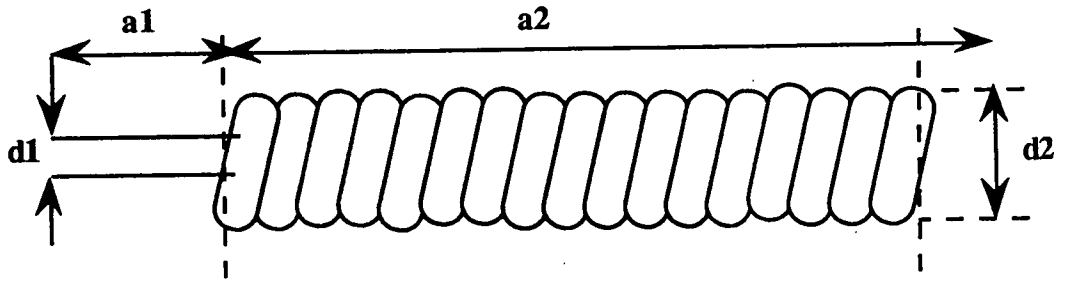

Fig.3.2 The single overwound string.

The 1-st segment of length a1 is the bare string and the 2-nd segment of length a2 has both the steel core and the wrapped copper wire.

Consider again the frequency equation in the case of the overwound string

$$(\frac{\mu_{11}^2}{\mu_{22}^2}+1)(\frac{\mu_{12}^2}{\mu_{21}^2}+1)\{\frac{\mu_{11}}{\mu_{21}}\frac{\tanh(\mu_{21}a_2)}{\tanh(\mu_{11}a_1)}+1\}\{\frac{\mu_{12}}{\mu_{22}}\frac{\tan(\mu_{22}a_2)}{\tan(\mu_{12}a_1)}+1\}$$
$$-(\frac{\mu_{11}^2}{\mu_{21}^2}-1)(\frac{\mu_{12}^2}{\mu_{22}^2}-1)\{\frac{\mu_{11}}{\mu_{22}}\frac{\tan(\mu_{22}a_2)}{\tanh(\mu_{11}a_1)}+1\}\{\frac{\mu_{12}}{\mu_{21}}\frac{\tanh(\mu_{21}a_2)}{\tan(\mu_{12}a_1)}+1\}=0$$

where

$$\mu_{11}=\sqrt{(\sqrt{(\frac{T}{2R_1})^2+(2\pi f_n)^2\frac{\sigma_1}{R_1}}-\frac{T}{2R_1}}$$

$$\mu_{12}=\sqrt{(\sqrt{(\frac{T}{2R_1})^2+(2\pi f_n)^2\frac{\sigma_1}{R_1}}+\frac{T}{2R_1}}$$

$$\mu_{21}=\sqrt{(\sqrt{(\frac{T}{2R_1})^2+(2\pi f_n)^2\frac{\sigma_2}{R_1}}-\frac{T}{2R_1}}$$

$$\mu_{22}=\sqrt{(\sqrt{(\frac{T}{2R_1})^2+(2\pi f_n)^2\frac{\sigma_2}{R_1}}+\frac{T}{2R_1}} \qquad \text{.....(2.48)}$$

Their parameters can then be described

$Q_1=2.000\times10^{11}$: Young's modulus (steel) (N/m^2).

$\rho_1=7.85\times10^3$: Volume mass density (steel: kg/m^3).

a_1 : Steel core length (the 1st segment string).

d_1 : Diameter of the steel core string.

$S_1=\pi d_1^2/4$: Cross section area of the steel core string.

$\rho_2=8.93\times10^3$: Volume mass density (copper: kg/m^3).

a_2 : Length of the overwound string.

d_2 : Diameter of the overwound string.

$S_2 = \pi d_2^2 / 4$: Cross section area of the overwound string.

$\kappa = d_1 / 4$: Radius of gyration of the cross-section of the core about an axis through the centre of the string and perpendicular to its length.

$\sigma_1 = \pi d_1^2 \rho_1 / 4$: Linear mass density of the core string.

$\sigma_2 = \sigma_1 + \frac{\pi^2}{16}(d_2^2 - d_1^2)\rho_2$: Linear mass density of the overwound string.

T : Tension

$f_0 = \frac{1}{2(a_1 + a_2)}\left(\frac{T}{\sigma_2}\right)^{1/2}$: First mode frequency of an ideal flexible string.

$R_1 = Q_1 S_1 \kappa^2$: Core stiffness factor.

As shown above, the tension is related to f_0, the first mode frequency of an ideal flexible string, which is a very important factor in defining the inharmonicity of the strings. For the numerical calculation, the tension has been set to be constant for each of six uniformly overwound strings and six stepped overwound strings with the same core and overwinding dimensions. The constant tension has been derived from an experimental measurement of the first mode frequency for a specific length of the string, supposing that this is the first mode frequency of the ideal flexible string. More details of the experiment to measure the first mode frequency will be given in chapter 5.

The dimensions for the 18 uniform overwound strings and for the 18 2-segment overwound strings are shown in Table 3.1 and 3.2, respectively.

Table 3.1 The dimensions of the uniform overwound strings.

String names	Core diameter d1 (mm.)	Overall diameter d2 (mm.)	Length a (mm.)
U1(1)	1.35	4.20	800
U1(2)			1050
U1(3)			1300
U1(4)			1550
U1(5)			1800
U1(6)			2050
U2(1)	1.40	4.41	800
U2(2)			1050
U2(3)			1300
U2(4)			1550
U2(5)			1800
U2(6)			2050
U3(1)	1.45	4.68	800
U3(2)			1050
U3(3)			1300
U3(4)			1550
U3(5)			1800
U3(6)			2050

Table 3.2 The dimensions of the 2-segment overwound strings.

String names	Core diameter d1 (mm.)	Overall diameter d2 (mm.)	Unwound length a1 (mm.)	Wound length a2 (mm.)	Total length a(mm.)	Unwound fraction a1:a2
S1(1)	1.35	4.20	50	750	800	1:15
S1(2)				1000	1050	1:20
S1(3)				1250	1300	1:25
S1(4)				1500	1550	1:30
S1(5)				1750	1800	1:35
S1(6)				2000	2050	1:40
S2(1)	1.40	4.41	50	750	800	1:15
S2(2)				1000	1050	1:20
S2(3)				1250	1300	1:25
S2(4)				1500	1550	1:30
S2(5)				1750	1800	1:35
S2(6)				2000	2050	1:40
S3(1)	1.45	4.68	50	750	800	1:15
S3(2)				1000	1050	1:20
S3(3)				1250	1300	1:25
S3(4)				1500	1550	1:30
S3(5)				1750	1800	1:35
S3(6)				2000	2050	1:40

3.3 Numerical results.

The mode frequencies that we have obtained by numerically solving the frequency equation are tabulated in Appendix B.

As a basis for discussion of inharmonicity it is sometimes convenient to divide each mode frequency f_n by the corresponding mode frequency of the equivalent ideal (completely flexible) string nf_0, giving a fractional inharmonicity $I_n = f_n/nf_0$. This inharmonicity can also be expressed as a pitch interval:

$$\text{Inharmonicity } (cents) = 3986 \log(I_n)$$

A cent is a unit that divides each of the twelve semitone intervals of the equally tempered scale into 100 equal parts.

The inharmonicity in cents from the numerical results for the 18 uniform overwound strings and the 18 2-segment overwound strings are shown in Appendix C.

The relation between the theoretical inharmonicity and the mode number (n), is presented in Graph 3.1 for the six uniformly overwound strings, U1(1), U1(2), U1(3), U1(4), U1(5) and U1(6). These six uniformly overwound strings are the same in both core and overall diameters (d1=1.35 mm. and d2=4.20 mm.), but they have different lengths. U1(1) is the shortest string, with the length a = 800 mm. and U1(6) is the longest one, with a = 2050 mm. The theoretical results for the inharmonicity in Graph 3.1 show clearly that the shorter the uniformly overwound strings with the same diameter, the higher the inharmonicity. The inharmonicity at the 30th mode of the U1(1) string is 355 cents, but that of the U1(6) string is only 75 cents.

Graph 3.2 presents results for the six uniformly overwound strings, U2(1), U2(2), U2(3), U2(4), U2(5) and U2(6), and Graph 3.3 presents results

for U3(1), U3(2), U3(3), U3(4), U3(5) and U3(6). The results of inharmonicity in Graphs 3.2 and 3.3 confirm that the shorter the strings with the same diameter, the higher the inharmonicity.

The strings of the same length from these three groups, for instance U1(1), U2(1) and U3(1), are different in both core and overall diameters. The theoretical results for the inharmonicity in Graphs 3.1, 3.2 and 3.3 show that the larger the diameter of the strings with the same length, the higher the inharmonicity. The inharmonicity at the 30th mode of the U2(1) string (overall diameter d2=4.41 mm.) is 399 cents, but that of the U3(1) string (overall diameter d2=4.68 mm.) is 446 cents.

Graph 3.4 displays the relation between the theoretical inharmonicity and the mode number (n) for the six 2-segment overwound strings, S1(1), S1(2), S1(3), S1(4), S1(5) and S1(6). The six 2-segment overwound strings, S2(1), S2(2), S2(3), S2(4), S2(5) and S2(6) are displayed in Graph 3.5, and the six 2-segment overwound strings, S3(1), S3(2), S3(3), S3(4), S3(5) and S3(6) are displayed in Graph 3.6.

The theoretical results for the inharmonicity of the stepped overwound strings in Graph 3.4, 3.5 and 3.6 again show that the shorter the strings with the same diameter and the larger the diameter of strings with the same length, the higher the inharmonicity.

The strings in Graph 3.1 and 3.4 are the same in both core and overall diameters. Moreover, U1(1) in Graph 3.1 and S1(1) in Graph 3.4 are the same total length a = 800 mm., but S1(1) is the stepped overwound string with unwound length a1 = 50 mm. and wound length a2 = 750 mm. The inharmonicity at the 30th mode of the S1(1) string is 453 cents, substantially higher than corresponding inharmonicity of 355 cents for the U1(1) string.

The comparisons of the inharmonicity between the uniformly overwound strings and the corresponding stepped overwound strings in Graph 3.1 to 3.6

leads to the conclusion that in the case of the stepped overwound strings, the inharmonicity is indeed significantly higher.

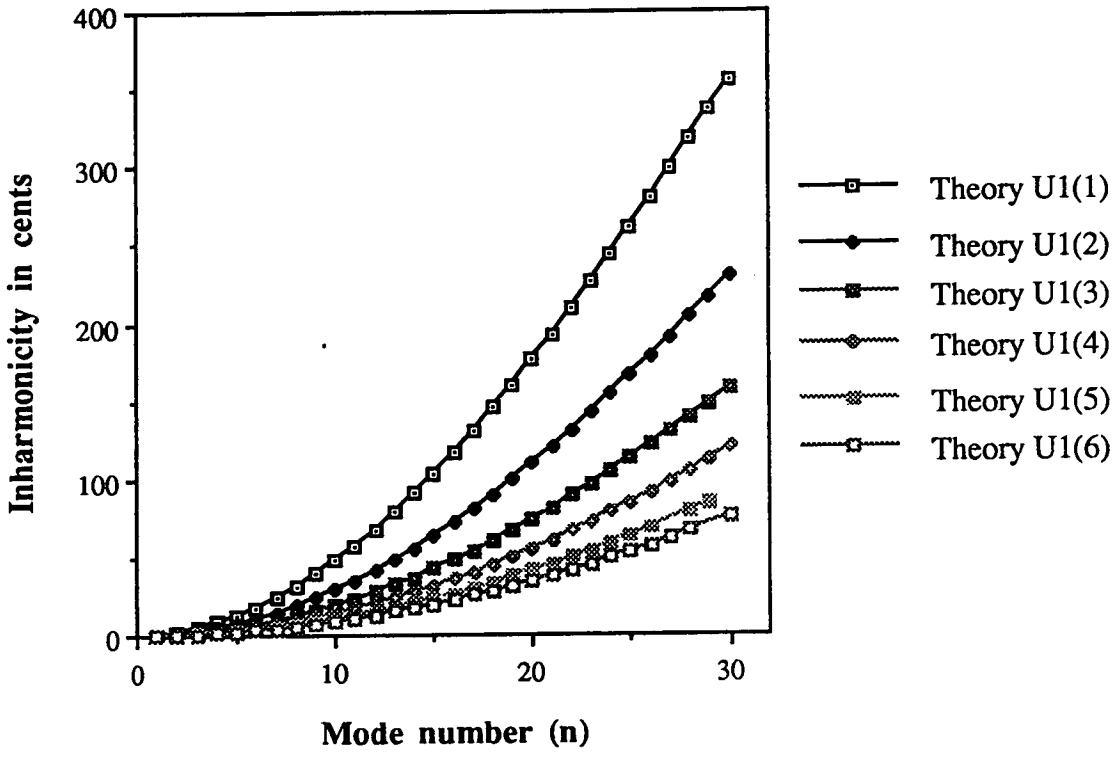

Graph 3.1 The relation between the theoretical inharmonicity and the mode number (n) for the six uniformly overwound strings, U1(1), U1(2), U1(3), U1(4), U1(5) and U1(6).

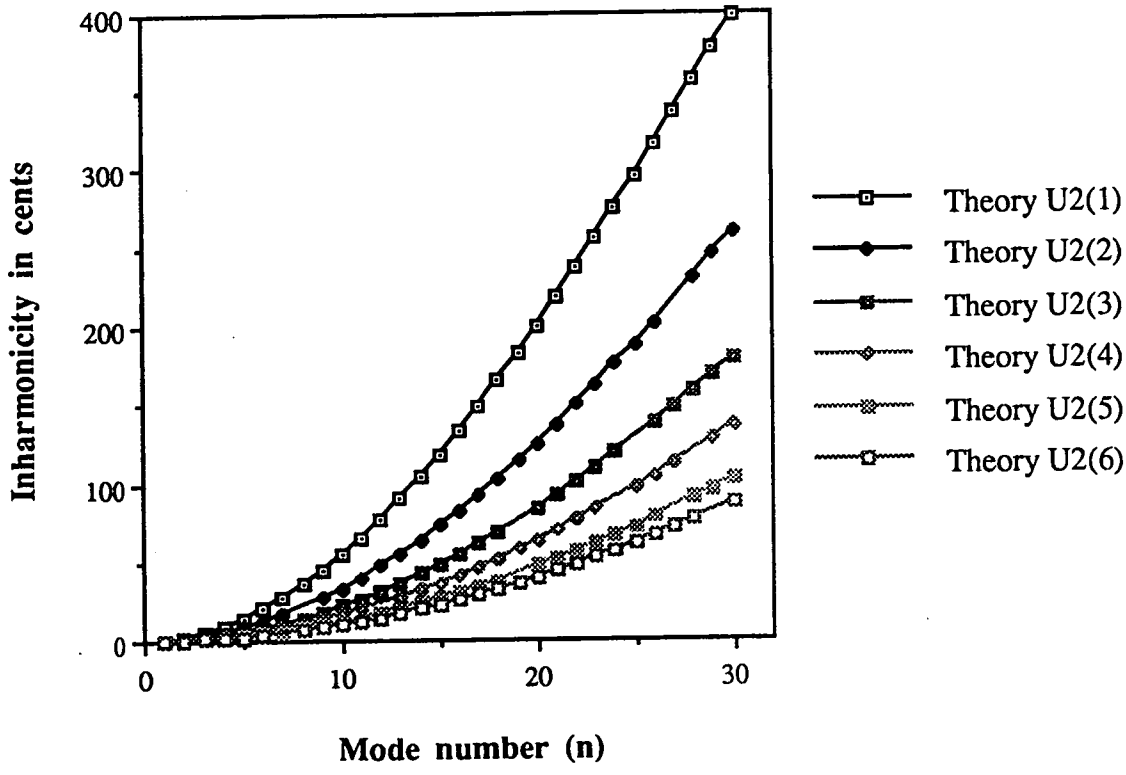

Graph 3.2 The relation between the theoretical inharmonicity and the mode number (*n*) for the six uniformly overwound strings, U2(1), U2(2), U2(3), U2(4), U2(5) and U2(6).

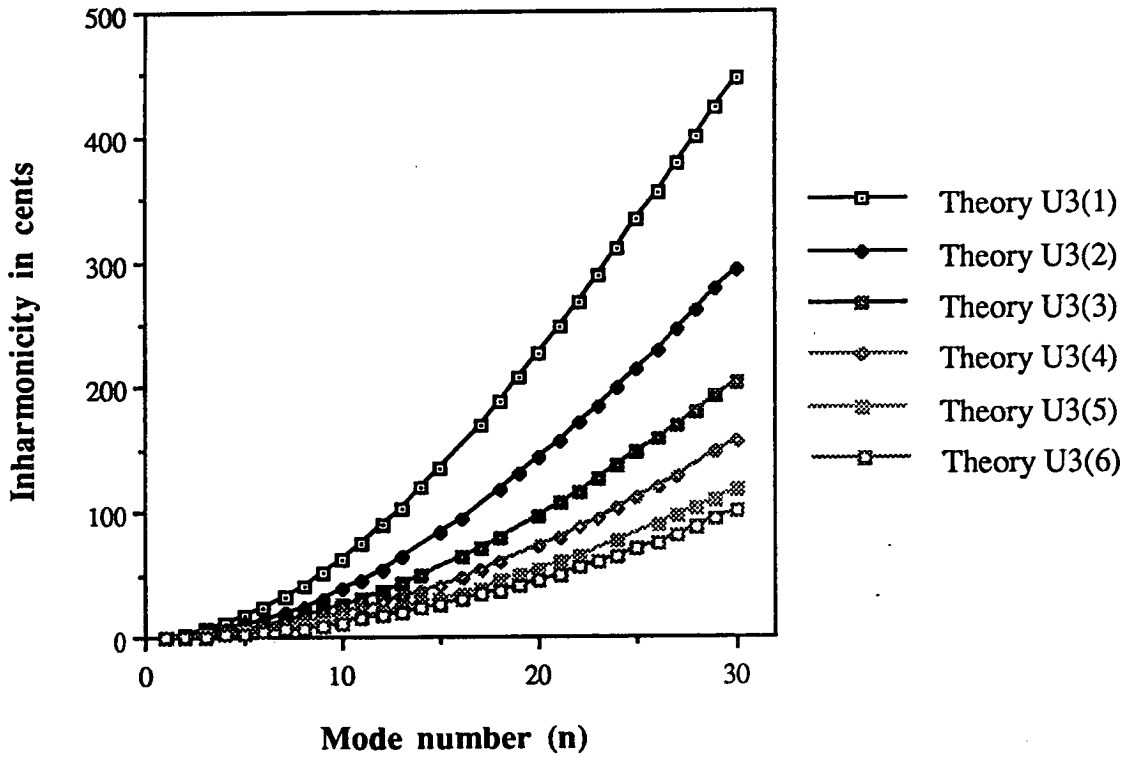

Graph 3.3 The relation between the theoretical inharmonicity and the mode number (n) for the six uniformly overwound strings, U3(1), U3(2), U3(3), U3(4), U3(5) and U3(6).

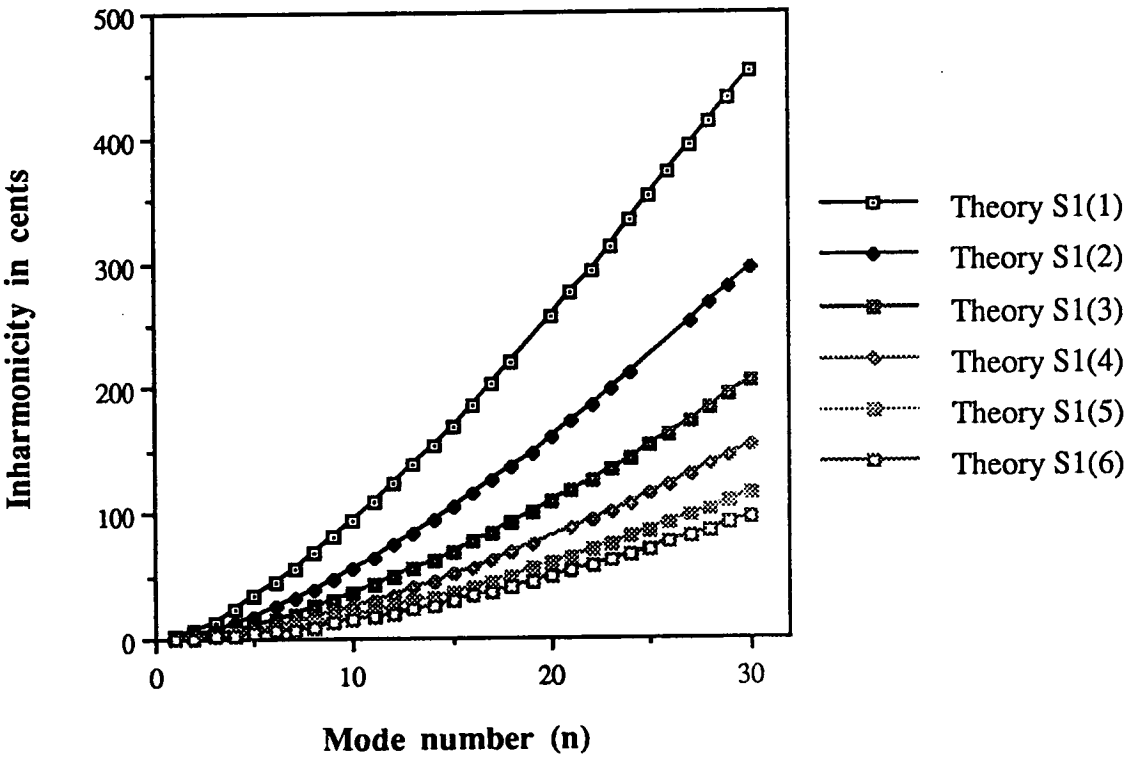

Graph 3.4 The relation between the theoretical inharmonicity and the mode number (*n*) for the six 2-segment overwound strings, S1(1), S1(2), S1(3), S1(4), S1(5) and S1(6).

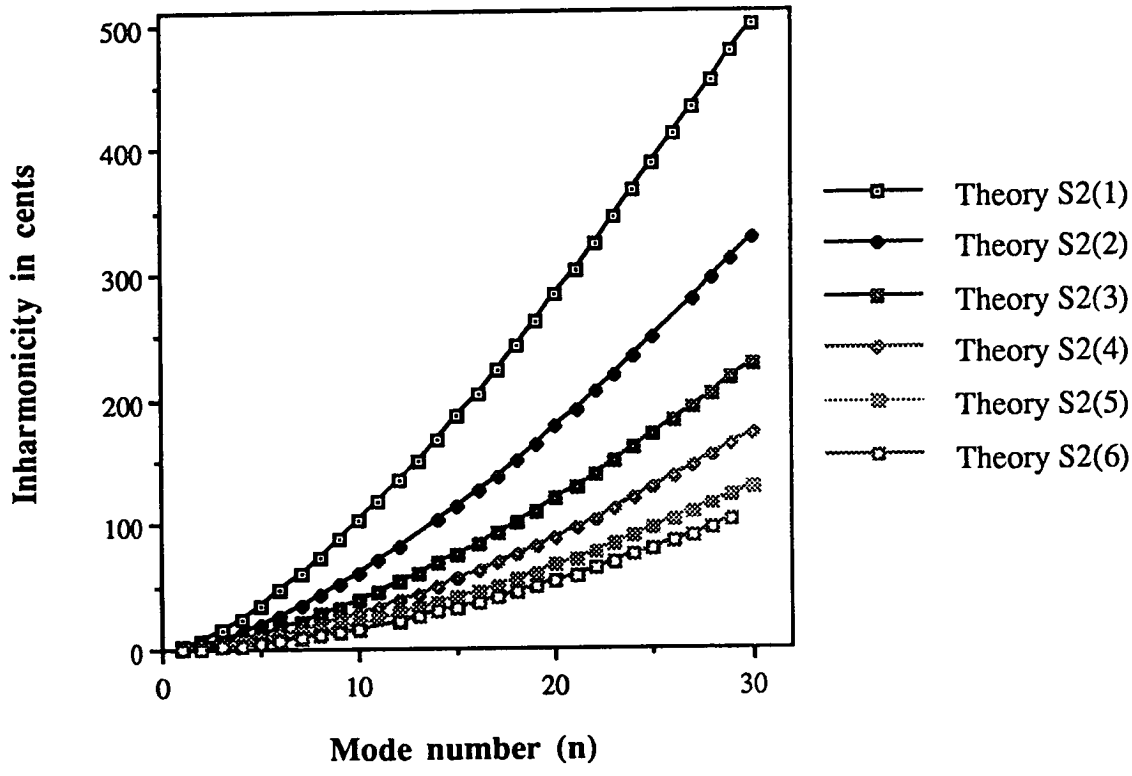

Graph 3.5 The relation between the theoretical inharmonicity and the mode number (n) for the six 2-segment overwound strings, S2(1), S2(2), S2(3), S2(4), S2(5) and S2(6).

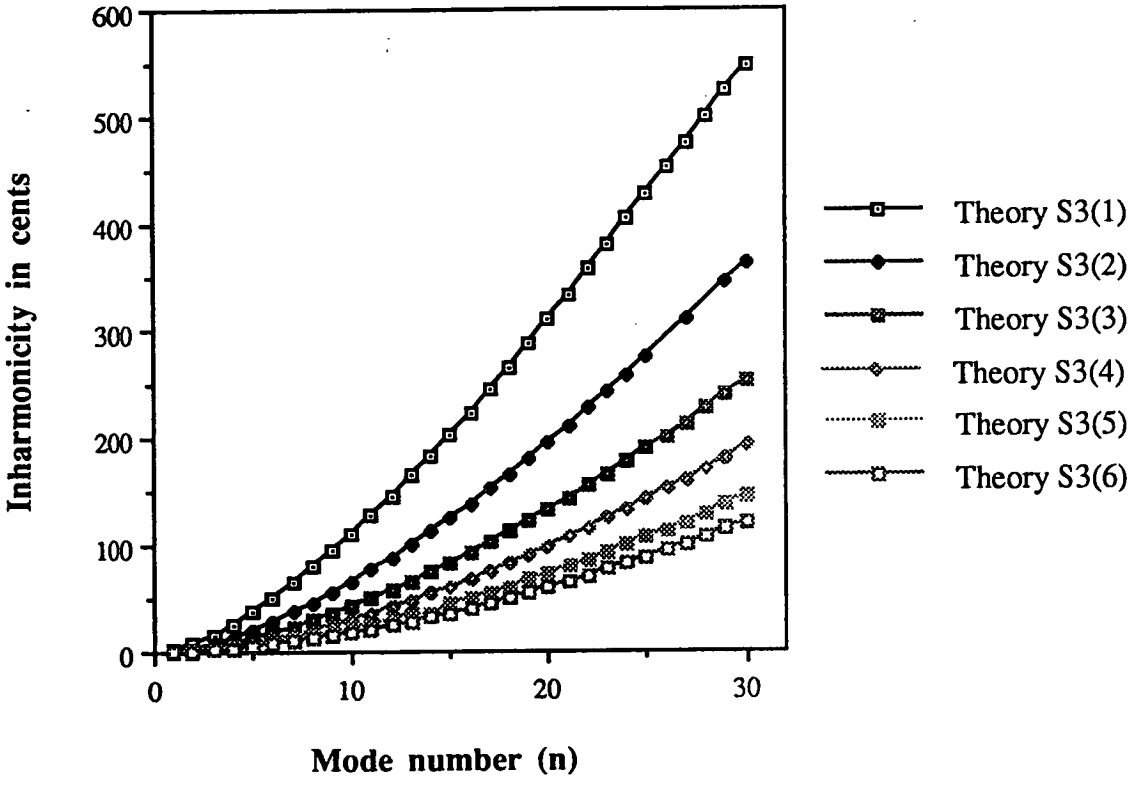

Graph 3.6 The relation between the theoretical inharmonicity and the mode number (n) for the six 2-segment overwound strings, S3(1), S3(2), S3(3), S3(4), S3(5) and S3(6).

CHAPTER 4

EXPERIMENTAL TECHNIQUES AND RESULTS

In order to validate the theory developed in Chapter 2, experiments were conducted to measure the inharmonicity of the overwound strings on a purposed-designed monochord. The strings were plucked and the sound was recorded using a microphone mounted a short distance above. The acoustic signal was captured digitally using an A/D converter and was analysed using an FFT.

The experimental results of inharmonicity for the uniformly overwound strings on the monochord are firstly presented. These are followed by the results of inharmonicity of the stepped overwound strings on the monochord. Data of their experimental mode frequencies and the inharmonicity are shown in Appendix D and E.

4.1 Experimental apparatus.

For the purposes of this experiment the strings were plucked. It was found that plucking the string at a position close to the end with the flesh and nail of the finger or thumb excited the greatest number of modes. It was this method that was mainly used to sound notes from the strings on the monochord.

The monochord as shown in Fig.4.1 is composed of a rigid steel bar, 2 specially designed bridges, a tuner support and a tuner. The rigid steel bar was used to eliminate both the static and acoustic functions performed by a piano soundboard. Statically, it opposes the vertical components of string tension that act on the bridges. Acoustically, the soundboard is the main radiating member in the instrument, transforming some of the mechanical energy of the strings and bridges into acoustic energy.

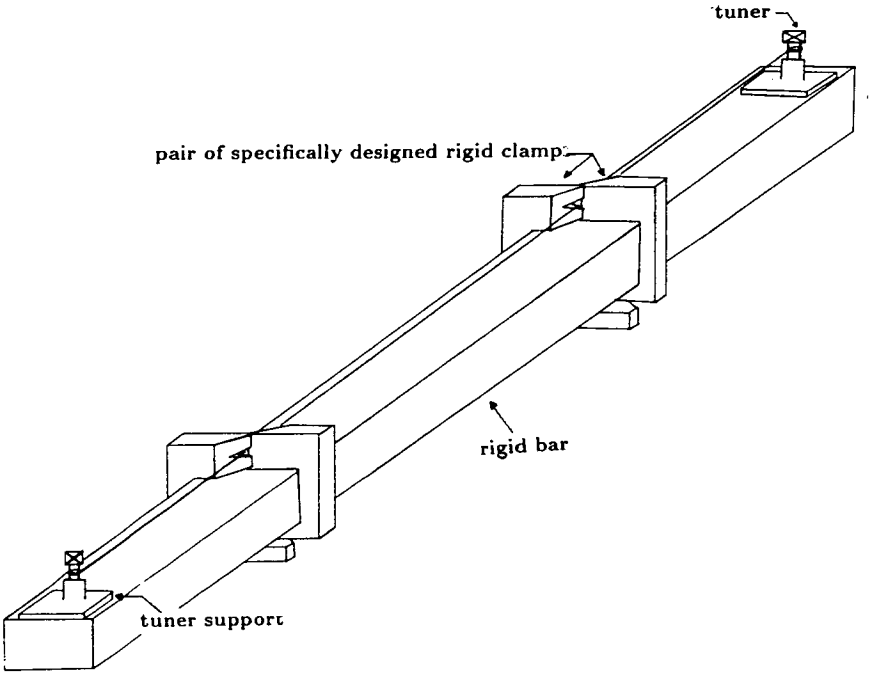

Fig.4.2 The monochord.

The frequency-dependent motion of the bridges and soundboard on a piano is coupled to the string motion, and modifies the natural mode frequencies of the strings. The much greater impedance of the rigid monochord supports is designed to reduce this effect. Each bridge, consisting of a pair of

clamps, stops the end of the string at 3 points in a plane perpendicular to the string length. Initial experiments on a prototype monochord with conventional horizontal bridges showed that the resulting curvature of the string in the vertical plane significantly affected the natural mode frequencies. In fact, two families of modes were identified corresponding to horizontal and vertical motion respectively. To avoid this, the clamps were designed to stop the string without forcing a change of angle.

The sound was recorded using a SHURE SM94 condenser microphone mounted a short distance above the middle point on a string. The acoustic signal was captured digitally using an 8 bit analogue-to-digital converter (ADC) [22] after suitable filtering and amplification. The digital signal was stored on disc for subsequent frequency analysis.

A frequency spectrum for a recorded note was obtained by performing a fourier transform on the recorded digital signal. The fourier transform was performed using the techniques of fast fourier transform (FFT) programmed into a second computer. The frequency interval of the discrete FFT was given by $\Delta f = f_s/n$, where f_s was the sampling rate and n was the corresponding number of points or transform size. In these experiments, the frequency interval was ≈ 4 Hz with $f_s = 8000$ Hz and $n = 2048$.

A programme ("ASFIQR") developed in Edinburgh [84] locates the peaks in the spectrum with high accuracy by an interpolation technique. It has been shown that in the case of a strictly periodic test signal with a signal-to-noise ratio better than 60 dB, it can be estimated to an accuracy better than 1% of a FFT frequency interval.

More details for the analogue-to-digital converter, the fourier analysis, the spectrum analysis and the experimental uncertainty will be shown in the following sections.

4.2 Analogue-to-digital converter and sampling process.

Most of the signals encountered in science and engineering are analogue in nature. That is, the signals are functions of a continuous variable, such as time or space and usually take on values in a continuous range. In this case of study, the signal is musical sound.

Sound is produced by a vibrating source. The vibrations disturb the air molecules that are adjacent to the source by alternately pulling apart and pushing together the molecules in synchronism with the vibrations. Thus, the energy in a sound produces small regions in which the air pressure is lower than average (rarefactions) and small regions in which it is higher (compressions). These regions of alternately rarified and compressed air propagate in the form of a sound wave much in the same manner as the troughs and crests of an ocean wave. When a sound wave impinges on a surface (e.g., an eardrum or a microphone), it causes that surface to vibrate in sympathy with the wave. In this way acoustic energy is transferred from a source to a receptor while retaining the characteristic vibration pattern of the source.

Acoustic energy in the form of pressure waves can be converted into an analogous electrical signal by an appropriate transducer such as a microphone. The transducer produces a voltage that changes constantly in sympathy with the vibrations of the sound wave. To demonstrate that the voltage describes the sound received by the microphone, it can be converted back into sound and compared with the original. Because the change in voltage occurs analogously to the vibrations of the sound, the electrical signal is called an analogue signal.

To change an analogue signal into a suitable form for use by a digital computer, the signal must be converted into numbers. Two types of I/O

devices link the digital computer with the analogue world. These types are distinguished by the direction of transformation. Analogue-to-digital (A/D) converters transform voltages into numbers, and digital-to-analogue (D/A) converters transform numbers into voltages. Data converters are characterised by their precision and speed of conversion. The conversion process relies on the principle that at any point in time, an analogue electrical signal can be assigned an instantaneous value by measuring its voltage. For example, it is possible to state that exactly 2.01 seconds after a certain sound began, the corresponding electrical signal had a value of 0.89 volts.

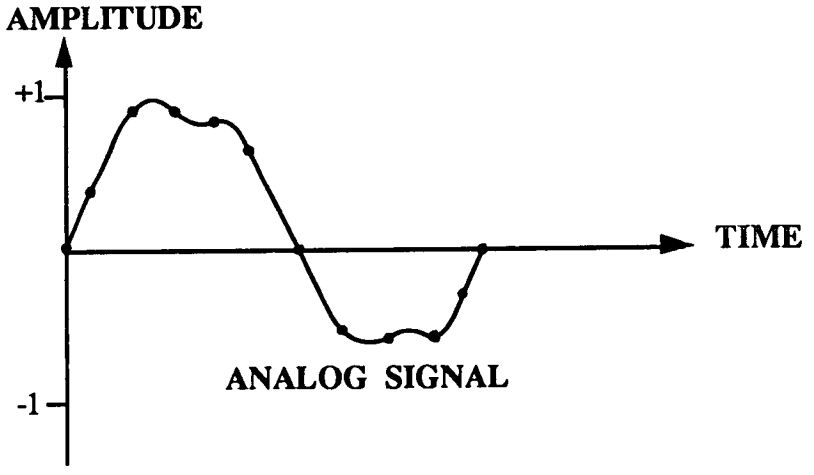

{0, 0.5, 1, 0.77, 0.60, 0.65, 0, -0.59, -0.49, 0.57, -0.67, 0}

DIGITAL SIGNAL

Fig. 4.2 Signal represented in both analogue and digital forms. The dots on the analogue waveform indicate the sampling points.

The analogue voltage that corresponds to an acoustic signal changes continuously, so that at each instant in time it has a different value. It is not possible for the computer to receive the value of the voltage for every instant, because of the physical limitations of both the computer and the data

converters. (And, of course, there are an infinite number of instants in any finite time interval.) Instead, the analogue voltage is measured (sampled) at intervals of equal duration. The output of the sampling process is a discrete or digital signal: a sequence of numbers corresponding to the voltage at each successive sampling time. Fig. 4.2 shows a signal in both digital and analogue form. Observe that the analogue signal is continuous; that is, every point on the waveform is smoothly connected to the rest of the signal. The digital signal is not continuous because it consists of specific samples at discrete times.

The duration of time between samples is known as the sampling interval or sampling period. The inverse, the number of times the signal is sampled in each second, is called the sampling rate or sampling frequency (f_s) and is measured in hertz (samples per second).

One might assume that the more samples taken of a phenomenon, the more accurately it could be represented -which suggests that anything less than an infinite sampling rate would cause some error in the digital signal. Fortunately, a mathematical analysis of the sampling process reveals that no error will be introduced by a finite sampling rate that is more than twice the fastest rate of change of the signal being sampled. That is, the chosen sampling rate must be faster than twice the highest frequency contained in the analogue signal. Conversely, the highest frequency contained in the analogue signal must be less than half the sampling rate. This maximum, $f_s/2$, is called the Nyquist frequency and is the theoretical limit on the highest frequency that can be represented in a digital audio system.

To ensure that the frequencies in the analogue signal are below the Nyquist frequency, an analogue or digital low-pass filter is placed before the A/D converter (so that too high frequencies are filtered out). A filter separates signals on the basis of their frequencies, passing signals of certain frequencies while significantly reducing the amplitudes of other frequencies. An ideal low-

pass filter would permit frequencies below the Nyquist frequency to pass unchanged, but would completely block higher frequencies. Real low-pass filters, however, are not perfect, with the result that, in practice, the usable frequency range is limited to a little more than 40% of the sampling rate instead of the full 50%. Thus, a sampling rate of 40 kHz provides for a maximum audio frequency of slightly above 16 kHz.

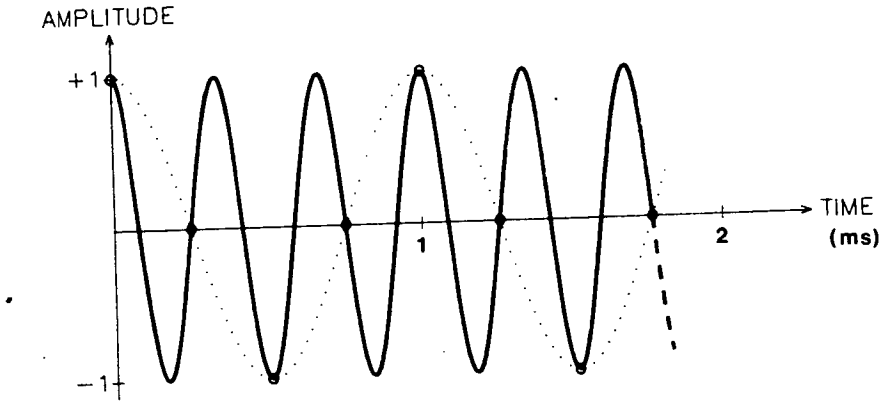

Fig. 4.3 Sampling a 30 kHz sinusoidal tone at a 40 kHz rate. The samples also describe a 10 kHz sinusoidal as shown in the dotted line.

The faster the sampling rate, the higher the frequency that can be represented, but the greater the demands on the speed and the power consumption of the hardware.

What would happen if there were no low-pass filter on the analogue input and a signal were sampled that contained a frequency above the Nyquist frequency? Consider a 30 kHz sinusoidal tone sampled at a 40 kHz rate as in Fig. 4.3.

The resulting digital signal of {1, 0, -1, 0, 1, 0, -1, 0} is the same as the 10 kHz tone. Thus, when the digital signal is converted back to analogue

form, the output of the low-pass filter will be a 10 kHz sinusoidal tone. The 30 kHz tone has the same sample values as a 10 kHz tone, and so it is said to assume an "alias" at 10 kHz. Once a signal appears in a digital system under an alias, there is no way that the computer can determine whether a particular frequency is an alias or not. In a digital system, the alteration caused by the sampling process of frequencies higher than the Nyquist frequency is known as aliasing or foldover.

A low-pass filter at the input to an A/D converter effectively prevents aliasing in a digital signal simply by limiting the range of frequencies going into the converter. Suppose that, on a system with a 40 kHz sampling rate, a user writes a program with the intention of producing a 30 kHz sinusoidal tone. The digital signal that the program would generate is identical to the sequence in the example above, {1, 0, -1, 0, 1, 0, -1, 0,....}, and therefore would be converted into a 10 kHz sinusoidal tone.

Let f_{in} be either a frequency applied to the input of an A/D converter or a frequency intended to be contained in a synthesised sound. For values of f_{in} between $f_s/2$ and f_s, the relationship between f_{in} and the actual frequency output (f_{out}) from the low-pass filter is

$$f_{out} = f_s - f_{in}$$

In this region of f_{in}, observe that f_{out} and f_{in} move in opposite directions. If a system with a 40 kHz sampling rate were programmed with the objective of producing an ascending glissando from 22 kHz to 39 kHz, the sound synthesised would actually descend from 18 kHz to 1 kHz.

Foldover occurs on every multiple of the sampling rate, and so frequencies higher than the sampling frequency will also cause unwanted responses. The general relationship is

$$f_{out} = |nf_s - f_{in}|$$

where n is an integer chosen for each value of f_{in} such that f_{out} is less than the Nyquist frequency. Thus, at a 40-kHz sampling rate, an output of 10 kHz would result from inputs of 10 kHz, 30 kHz, 50 kHz, and so on.

The A/D converter transforms the incoming analogue signal into digital form, and the sound recording computer stores this digital signal on an external memory device such as a disk or tape. Digital recordings have several advantages over analogue ones. The recording medium stores numbers rather than an analogue signal, and so offers superior noise performance and protects the sound more effectively against degradation during long-term storage. In addition, regardless of the number of generations removed, a copy of a digital recording maintains complete fidelity to the original.

4.3 Fourier Analysis.

A Fourier transform enables researchers to obtain the spectrum of a sound from its waveform. A computer technique which performs the Fourier transform on a digital signal is the Discrete Fourier Transform (DFT). The DFT is computationally intensive, but through a clever ordering of the computer operations involved in performing a DFT, Cooley and Tukey [28] were able to reduce the number of computer operations significantly. Their algorithm is known as the Fast Fourier Transform (FFT).

Results of the FFT are a set of discrete lines at frequency intervals of the size of which represent the amount of sound present, at that particular frequency, in the original sound signal.

The frequency interval of the discrete FFT is given by $\Delta f = f_s/n$, where f_s is the sampling rate and n is the corresponding number of points or transform size. In general the FFT size is restricted to be a power of two. For sounds where the frequency is constant as in a sound from a musical

instrument, then the higher the number (n) the more accurate the frequency measurement is. However, for speech where the frequency may change within the measurement, increasing the numbers of points may merely broaden and obscure the peaks.

When recording, the first computer samples the sound at regular intervals and converts each sample to a number in the range 0...255. These numbers are stored in a buffer in RAM . The number of points in the transform is limited by the buffer length - for example if the buffer start is &3800 the buffer end is &5800 then the buffer size is 8K, and so the number of points must be 8192 or less. If the buffer start is set to &3800 and the number of points is 1024 (&400) then only the portion of sound between &3800 and &3C00 (&400 = &3C00 - &3800 = 1024) is analysed. Furthermore, if the sampling rate is 8 kHz, then only the first eighth of a second of the recorded sound has been used for the analysis and thus a linewidth of about 8 Hz should be expected in frequency analysis even for a pure sound. The reasons for this limit have been presented by Brigham [19], but with f_s = 8 kHz and n = 2048 a resolution limit that is twice as sharp (≈ 4 Hz) if the frequency remains constant over the part of the sound being analysed was obtained. However with few detectable harmonics above 2000 Hz the sample rate was increased to 4 kHz for certain recordings. The resolution then obtained was ≈2 Hz and the maximum detectable frequency (the Nyquist limit) was 2000 Hz.

4.4 Spectrum analysis.

For many applications in musical acoustics, the power spectrum is a most effective way of describing the component frequencies present in a sound, together with their relative amplitudes.

In the ideal case of a periodic signal where the portion of signal

analysed spans an exact number of cycles of the fundamental, then the fundamental and its harmonics each correspond to one of the lines of the FFT spectrum ($n\Delta f$). If this ideal condition is not present, the signal frequencies lie between the calculation frequencies, causing the analysis to attribute them in a widespread pattern which varies according to the frequency mismatch, an effect termed "leakage". The ideal situation is often unattainable, as the signal frequency may not be known in advance, or the sample rate may not be adjustable to the precise value. More importantly, analysis should cope with several signals combined, at unknown frequencies.

The remedy is to multiply the data time-series by a "window function" which is unity in the middle and tapers towards zero at each end. The effect is to give a rounded peak spanning several frequency intervals, with fairly uniform shape regardless of where the signal frequency lies within the frequency interval, and with a substantial reduction in the leakage to distant bins. Peak shape depends on the window function, but for a given function the peak always spans the same number of frequency bins even when their width is altered by other factors such as transform size.

Window functions are weighting functions applied to data to reduce the spectral leakage associated with finite observation intervals. From one viewpoint, the window is applied to data (as a multiplicative weighting) to reduce the order of the discontinuity at the boundary of the periodic extension. This is accomplished by matching as many orders of derivative (of the weighted data) as possible at the boundary. The easiest way to achieve this matching is by setting the value of these derivatives to zero at the boundaries so that the periodic extension of the data is continuous in many orders of derivative.

During the course of this experiment a Gaussian windowing function was used.

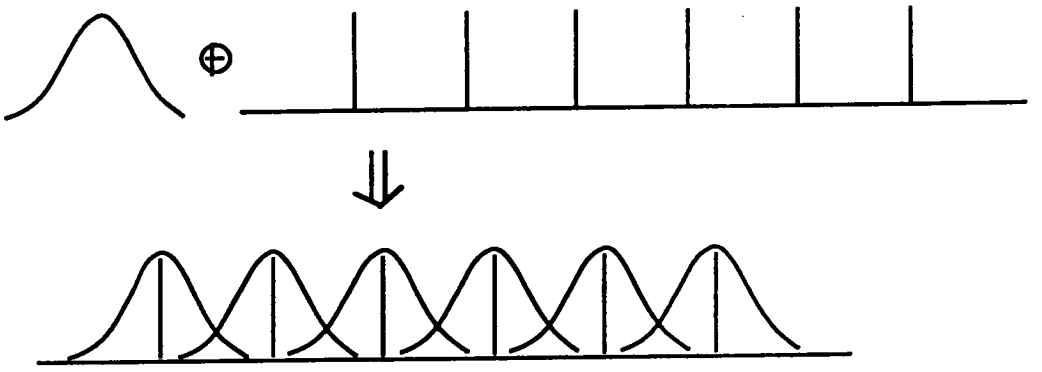

Fig. 4.4 The convolution of these two Fourier transforms with a Gaussian like form at each of the spectral peaks.

When the FFT of the windowed sound signal is performed, one is performing a Fourier transform of a product of two functions equal to $G(t) \times R(t)$, where R(t) is the original recorded sound signal. The Fourier transform of a product is simply the convolution of the separate Fourier transforms of R(t) and G(t). The convolution of these two Fourier transforms then appeared as shown in Fig. 4.4, with a Gaussian like form at each of the spectral peaks.

Windows can be used in estimating power spectra. In the direct method, the power spectrum is estimated by computing the square of the absolute value of the DFT of the windowed sequence. The DFT of the windowed sequence is the convolution of the DFT's of the window and the original sequence. This convolution smoothes the input power spectrum; consequently values of the power spectrum at frequencies separated by less than the width of the main lobe of the spectral window cannot be resolved. In addition to this limit on resolution, the estimate of the power spectrum may contain significant leakage, i.e., erroneous contributions from components of the power spectrum at frequencies possibly distant from the frequency of interest because of the nonzero energy in the spectral window side lobes.

The result of the DFT performed on windowed data is the convolution

of the DFT of the window function and the DFT of the raw data. This mathematical statement unfortunately does not offer a simple way of recovering the frequency information. Instead an empirical approach has been developed from careful study of the characteristics of the output for calibration signals by Raymond Parks [84]. The term "interpolation interval" is convenient to describe the difference between the true signal frequency and the FFT line immediately below it, as a fraction of DFT frequency interval.

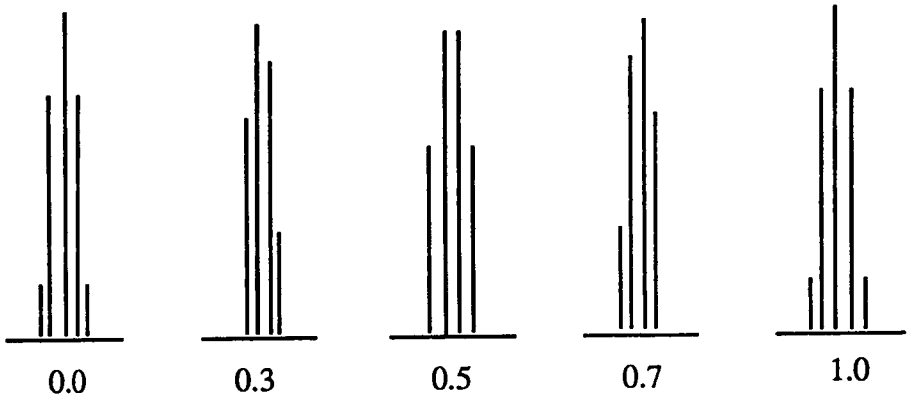

Fig. 4.6 Variation of cluster shape with interpolation interval.

Fig. 4.6 is a montage comparing the DFT line clusters for five interpolation intervals. The pattern for an interpolation interval of 0.0 is identical to that for 1.0. The pattern for 0.0 is symmetrical about a single line, while that for 0.5 is symmetrical about a pair of lines; the skewed patterns for interpolation intervals below 0.5 are mirror images of those above 0.5, with the relative line heights changing smoothly. While an interpolation would be possible using only the relative heights of the two highest lines, the risk of degradation by spurious signals is reduced by using differences between the four highest lines. The three separate estimates are combined with subjectively assigned weights, $w = 10^{h/20}$ where h is the height difference between two lines, to allow for the greater risk of contamination for lower lines. With the preferred window, straight-line interpolation is adequate for differences 1-2 and

2-3, while a second-order polynomial is used for difference 3-4.

The program "ASFIQR" operates on a power spectrum in dB from a disk file in two passes, the first identifying lines which stand out from the background level and the second grouping these lines in clusters and interpolating a centre frequency for each cluster.

Recognition of prominent lines is based on comparison of the running mean of three lines with that of the two before and two after them. If a specified threshold is exceeded, the central line has a flag set for its subsequent treatment.

In the second pass, a cluster is defined as starting where the line flags change from zero to one, and finishing where they return to zero. Within each cluster the highest line is identified, and the lines before and after it compared to establish the polarity of interpolation, i.e. whether the centre frequency is above or below that of the highest line. This result also defines which line is to be used as the fourth highest.

Three separate interpolations are then performed, on the basis of height differences from first-to-second, second-to-third and third-to-fourth lines respectively, and a weighted mean is derived. As a rudimentary indication of the degree of agreement between the three interpolated estimates in each case, an unweighted standard deviation of the three is provided (expressed as a fraction of frequency interval), and the user is left to decide whether to accept or reject the value.

4.5 The experimental uncertainty.

As an indication of the accuracy obtainable, the procedure was applied to a computer-generated complex periodic wave consisting of the first 15 harmonics of fundamental frequency 200 Hz as shown in Fig. 4.7. In this case,

each of the components analysed was represented in the FFT by a cluster of lines whose highest member was at least 50 dB above the noise floor of the spectrum. Graph 4.1 (white blocks) shows the differences between the component frequencies estimated by the ASFIQR program and the true values (200n, n = 1, 2,..., 15). Error frequencies are the order of 0.01 Hz, which is about 0.25% of the FFT frequency interval.

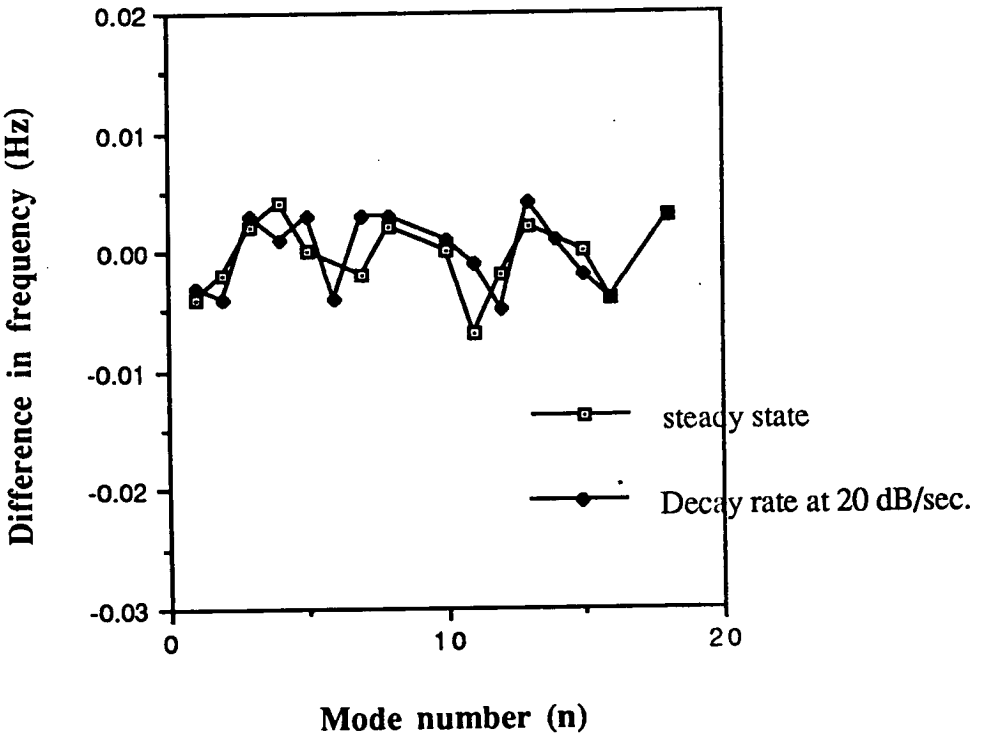

Graph 4.1 shows the difference between the component frequencies estimated by the ASFIQR program and the true values (200n, n = 1, 2, ..., 15). a: Steady state signal (white block). b: Decay rate at 20 dB/sec (diamond).

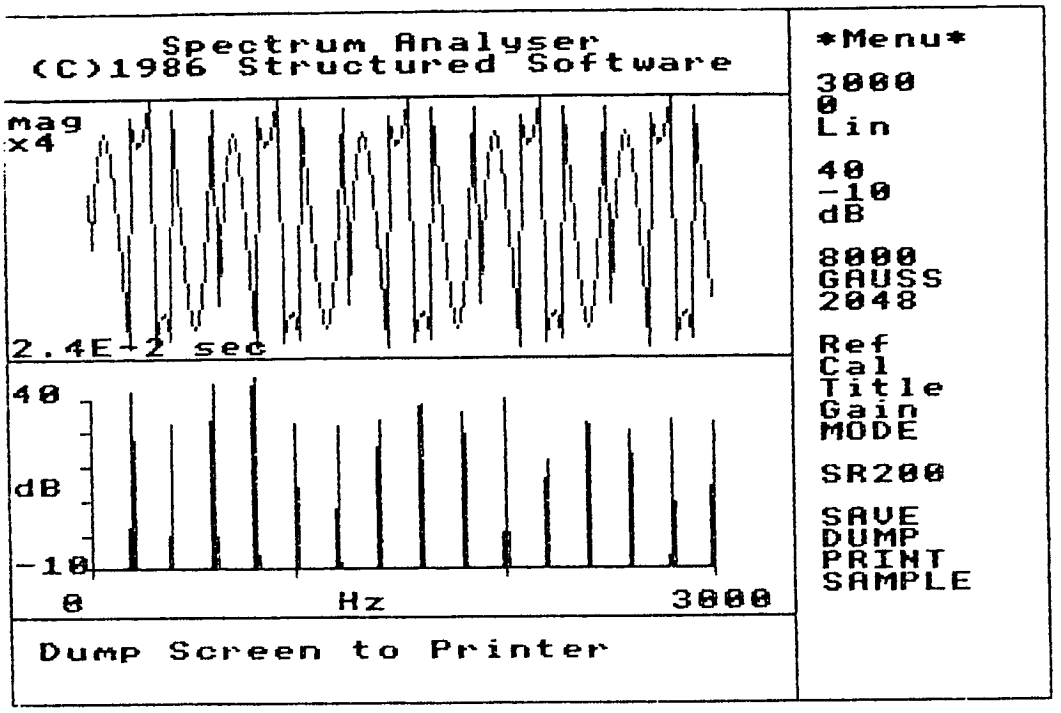

Fig.4.7 an artificial complex sinusoidal wave composed of exact harmonics.

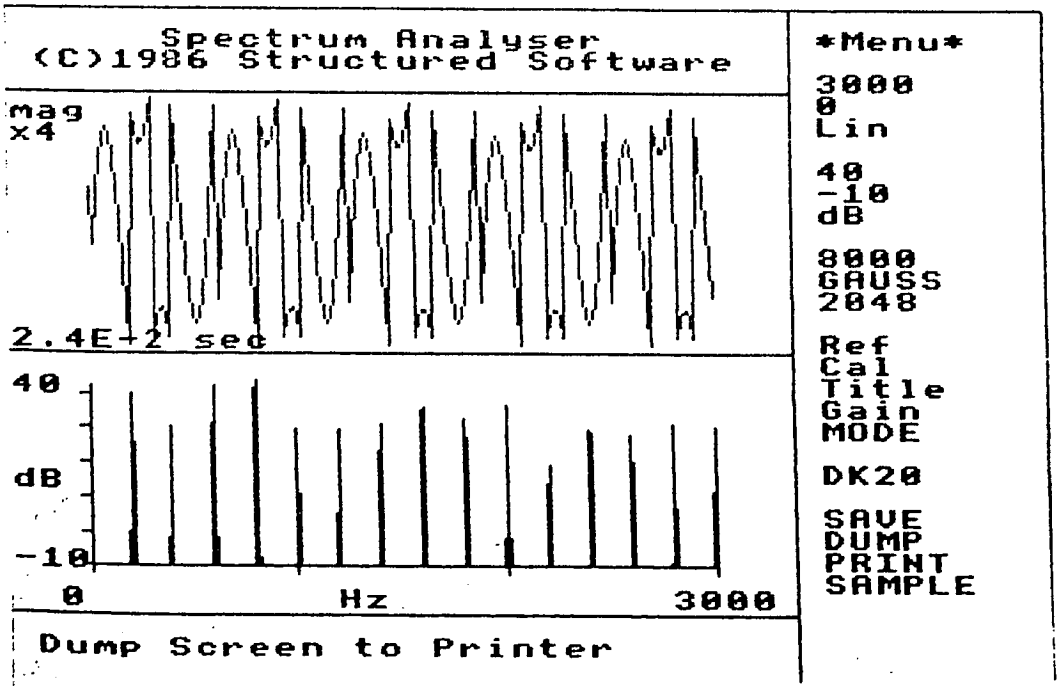

Fig. 4.8 show the artificial complex sinusoidal wave composed of exact harmonics at 20 dB/sec.

In the recorded sound of a plucked string, the decay characteristics of the signal have to be considered. The ability to estimate the frequency of a component to within a small fraction of an FFT interval relies on the assumption that the component is an isolated sinusoidal signal of constant amplitude. This condition is clearly violated by the components of a decaying string. In order to examine the error in frequency estimation caused by the variation in amplitude over the sample time, a program was writen which applied an amplitude envelope with variable decay rate to the signal shown in Figure 4.7. An example is shown in Figure 4.8. The analysis of frequency component error for this signal is shown in Graph 4.1 (diamonds); it is clear that the decay has not significantly increased the error.

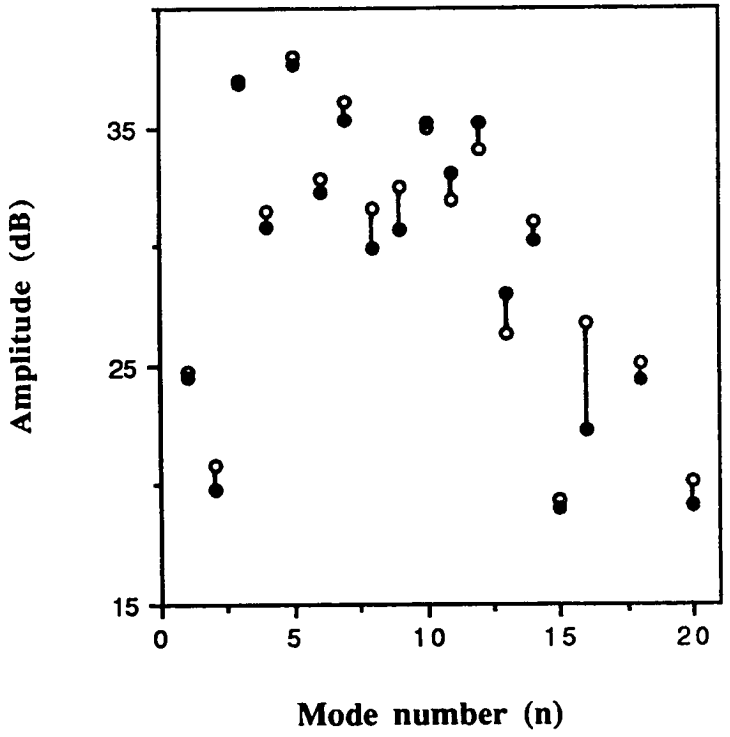

Graph 4.2 Amplitude change in 250 ms time duration of the stepped overwound string, S1(3), on the monochord. a: White circles are the amplitude values at &3800 buffer start (initial time at 0 ms.) b: Black circles are at &4000 buffer start (the initial time at 250 ms.).

Graph 4.2 shows the amplitude change in 250 ms time duration of the stepped overwound string (S1(3) as named in Chapter 3) on the monochord. White circles in Graph 4.2 are the amplitude values of each mode frequency of the recorded signal at &3800 buffer start (initial time at 0 ms.), and black circles are that of the recorded signal at &4000 buffer start (the initial time at 250 ms.). They were analysed with the same sampling rate (8000 Hz) and transform size (2048). Their mode frequencies change at different decay rates but they are not larger than 20 dB/sec: the largest decay rate, that of the 16th mode, is only 16 dB/sec. This behaviour is typical of the strings studied experimentally. It can therefore be concluded that the decay is not likely to have significantly affected the estimates of inharmonicity. With the same method of examining the error in frequency estimation caused by the variation in amplitude, it was found that a decay rate as fast as 40 dB/sec still has not significantly increased the error. This is relevant to the recorded signal of the strings on the piano, whose decay rates are faster than 20 dB/sec because of the effect of the soundboard.

In the recorded digital signal, noise is a very important part to consider. Noise of the same frequency as the signal being measured will obviously affect the result, and there are many possible sources, including analogue noise, the effect of digitisation and the internal rounding noise in the FFT itself. In practice, it is most unlikely that the rounding noise in the FFT will be significant.

To explain how systematic and random errors affect the overall noise level, two closely related concepts, dynamic range and signal-to-noise ratio, will be introduced. A characteristic that is a good indicator of the quality of any system that processes sound is dynamic range: the ratio of the strongest to the weakest signal that can exist in the system. Dynamic range is expressed in dB. The dynamic range of an electronic sound system is limited at the lower end by the

Signal amplitude V_s volts.
Noise amplitude V_n volts.

Signal power $\propto V_s^2$
Noise power $\propto V_n^2$
or
Signal waveform $V_s \sin(2\pi f_1 t + \phi_s)$.
Noise waveform $V_n \sin(2\pi f_1 t + \phi_n)$.

1) **Max signal ($\phi_s = \phi_n$) is $V_s + V_n$.**
2) **Min signal ($\phi_s = \phi_n + \pi$) is $V_s - V_n$.**

The maximum decibel increase is

$$20\log\left(\frac{V_s + V_n}{V_s}\right) = 20\log\left(1 + \frac{V_n}{V_s}\right)$$

$$\left(\frac{V_n}{V_s}\right)^2 = 10^{-\Delta S_n/10}; \left|\frac{V_n}{V_s}\right| = 10^{-\Delta S_n/20}.$$

dB difference in signal is $20\log\left(1+10^{-\Delta S_n/20}\right)$.

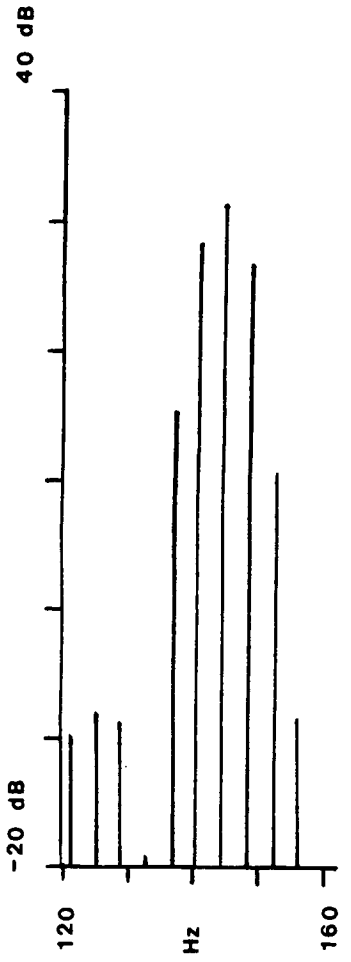

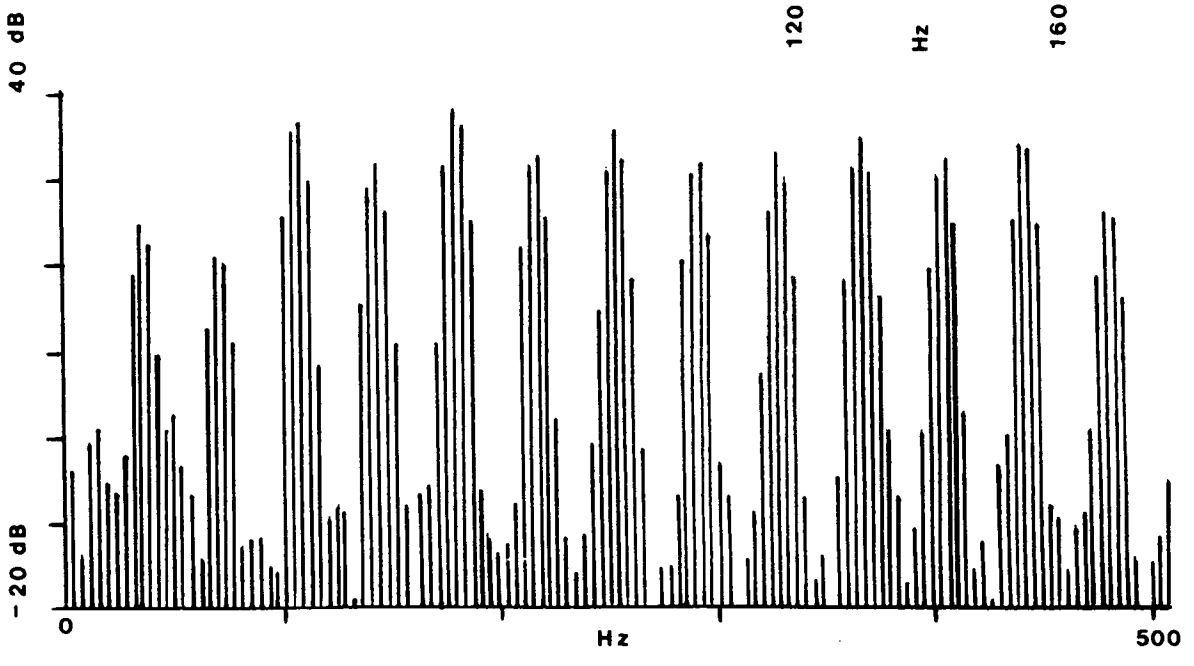

Fig.4.9 shows spectrum analysis of the 2-segment overwound string on the monochord, S1(3), illustrating both signal and noise.

background noise contributed by the electronic components and at the higher end by the level at which the greatest signal can be represented without distortion.

A characteristic associated with dynamic range is signal-to-noise (S/N) ratio which compares the level of a given signal with that of the noise in the system. The term noise can take on a variety of meanings depending on the environment. In electronic sound systems, noise generally takes the form of a hissing sound. A S/N ratio is expressed in dB: $\Delta S_n = 20\log|V_s/V_n|$, where V_s is signal voltage and V_n is the equivalent noise voltage. The dynamic range of an electronic system predicts the maximum S/N ratio possible; that is, under ideal conditions, the signal-to-noise ratio equals the dynamic range when a signal of the greatest possible amplitude is present. The ratio will be somewhat smaller on quiet sounds. As an example, consider a digital sound system with a constant noise level and a dynamic range of 50 dB. The largest signal possible would have an amplitude 50 dB above the noise level, but a signal with a level 10 dB below the maximum would exhibit a S/N ratio of only 40 dB.

The performance of such a system is ordinarily determined by the resolution with which the data converters transform analogue into digital signals and vice versa. When a conversion takes place, the analogue signal is said to be quantized because in digital form it can be represented only to a certain resolution. The net effect of this type of error, called a quantisation error, is the addition of some form of noise to the sound. The amount and audible effect of the quatisation noise depends on the resolution of the converter and the type of signal being converted.

The resolution of converters is measured in bits, corresponding to the size of the datum used to represent each sample of the digital signal. In the case where the audio signal is constantly changing (as in most music), the

dynamic range and hence the best signal-to-noise ratio that can be achieved is approximately 6 dB/bit. For example, a system with 8-bit data converters has a dynamic range of around 50 dB. This means that the noise in the system will be 50 dB below a signal with the largest amplitude possible in the system. The noise level does not change with signal level, so that signals with amplitudes lower than the maximum value will exhibit less than the maximum S/N ratio.

The amplitude of a signal can be either increased or decreased by the addition of noise. Fig.4.9 shows a spectrum analysis of the 2-segment overwound string on the monochord, S1(3), including both signal and noise. If V_s is the amplitude of the component in one bin of the FFT spectrum, and V_n is the amplitude of the noise signal which would be recorded in that bin in the absence of a signal, then the signal amplitude in dB can be changed by $20\log(1+10^{-\Delta S_n/20})$ where $\left|\frac{V_n}{V_s}\right| = 10^{-\Delta S_n/20}$.

Table 4.1 The effect of noise on the estimation of signal frequency.

ΔS_n (dB)	signal changed by noise (dB)	maximum changed frequency (Hz)
20	0.83	0.40
30	0.27	0.20
40	0.086	0.10
50	0.027	0.05

The effect of noise 20 dB below the wanted signal is to give a systematic and random error of 0.83 dB in the amplitude measurement. The effect of this on the estimation of signal frequency was considered by going back to the programme ASFIQR operating on clusters of lines in the power

spectrum. Each line in clusters could be affected by noise of arbitrary phase. By considering the effect of raising or lowering the amplitude of each line by the noise amplitude, it was established that the corresponding variation of estimated frequency was of the order of ±10% of the FFT frequency interval.

In the case of a signal with isolated spectral lines, visual inspection of the plot will allow the noise floor to be estimated. In the experimental work described here only peaks whose largest component was at least 40 dB above the noise were accepted for analysis. In this case the interpolation technique in the ASFIQR programme gives an accuracy of about 2.5% of the FFT frequency interval

By musical sounds we mean signals which are essentially evolutive. They are characterised by a large bandwidth-observation time product. The physical description of such signals needs the simultaneous determination of three parameters: frequency, amplitude and time. The effect of amplitude evolution on the determination of frequency has already been considered. It is possible, however, that the mode frequencies of the measured string are not constant with time. In Bariaux's work [10] on "A Method for Spectral Analysis of Musical Sounds, Description and Performances", he considered the mode frequencies with the time function $f_n(t) = f_n + A\sin(2\pi\nu t + \xi)$ with modulation period $P = 1/(2.5)\Delta f$ where Δf is the frequency interval of FFT. In this work in order to investigate possible time evolution of the frequency of the signal, the recorded signal from a single pluck of the strings was analysed by moving initial time (buffer start) with the same sampling rate (8000 Hz) and transform size (2048). In section 4.3 we described how the sound converts each sample to a number in the range 0...255. These numbers are stored in a buffer in RAM of the first computer. If the buffer start is &3800 and the buffer end is &5800 then the buffer size is 8K. With the transform size at 2048 (&800) then only the portion of sound between &3800 and &4000 (&800 = &4000 -

&3800) is analysed. If we now move the start of the transform sample to &383C, the end of the sampled section is &403C, and the initial time of the analysed signal is delayed by 7.5 ms. For these tests, twenty overlapping slices of the signal were analysed, the start of successive slices being delayed by 7.5 ms. The time evolution of frequency of 4th mode, 12th mode, 26th mode, 30th mode and 33rd mode frequencies of the stepped overwound string (S1(3)) on the monochord are shown in Graph 4.3 to Graph 4.7, respectively. It is evident that some frequency modulation is indeed present in the signals. In Bachmann's work [3] on "High Resolution Frequency Analysis of the Onset of a Piano Sound", he suggested that autoregressive spectrum analysis ("AR") is able to yield high resolution frequency spectra of very short segments of a signal record. On the other hand, the amplitude of frequency modulation of the very short segments of a recorded signal is greater than that shown in Graph 4.3 to 4.7 because of the averaging over a 250 ms sample. However, the magnitude of the variations in measured frequency due to this effect are small in comparison to these introduced by noise fluctuation.

Fortunately, the random error can be reduced by the (time consuming) method of averaging successive readings. In these experiments, each measurement was repeated 25 times by plucking the same string at the same position. To ensure that ambient temperature changes did not influence the results, each set of 25 measurements was completed within an hour. Each experimental point plotted in next section, Chapter 5 and Chapter 6 carries an error bar representing the standard error in the mean of 25 measurements, which was consistent with the calculated uncertainty due to noise corruption of the signal.

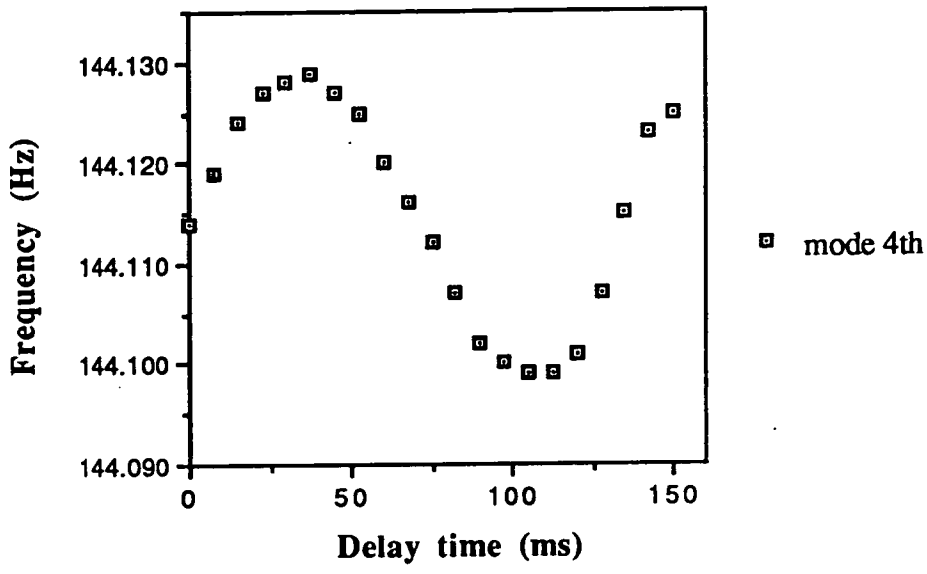

Graph 4.3 shows the time evolution of frequency of the 4th mode of the stepped overwound string on the monochord, S1(3).

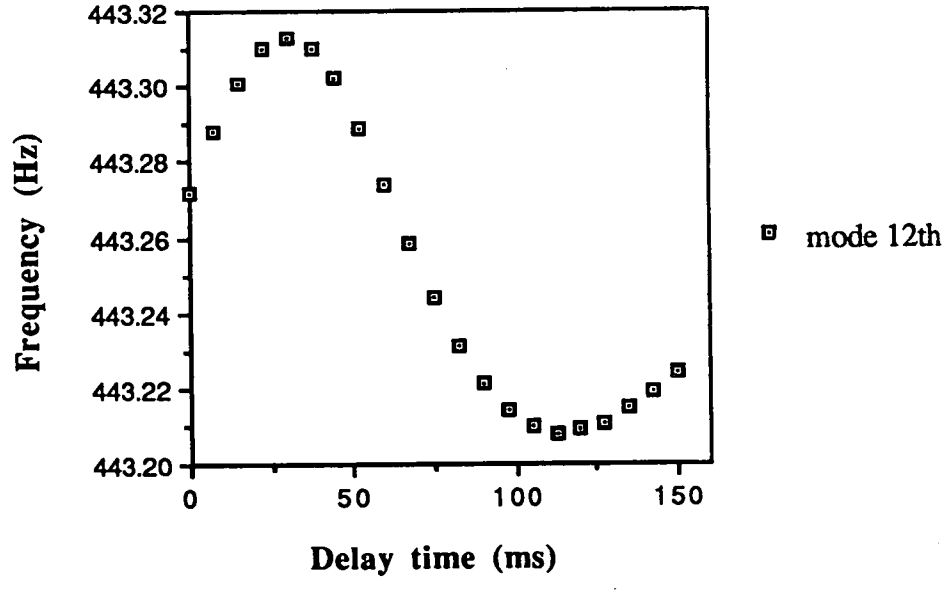

Graph 4.4 shows the time evolution of frequency of the 12th mode of the stepped overwound string on the monochord, S1(3).

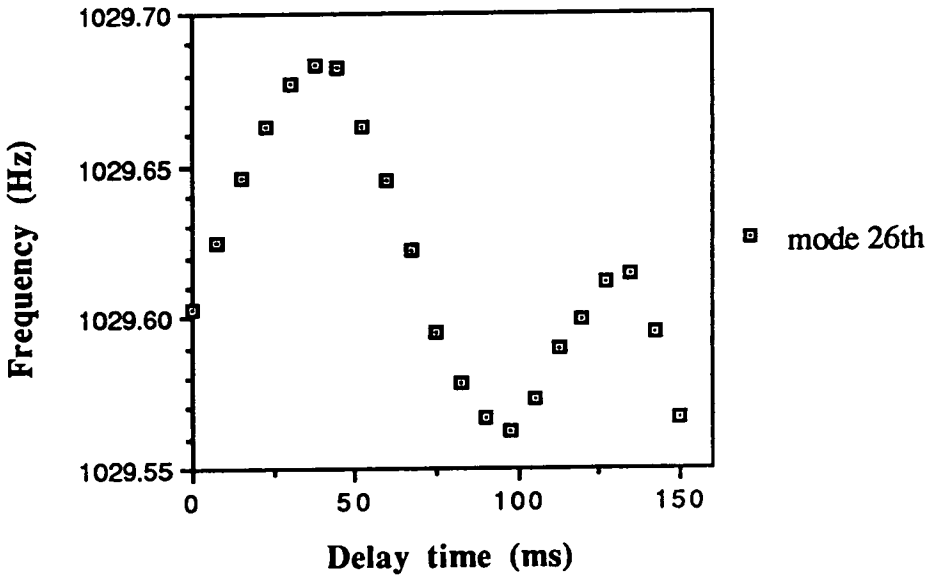

Graph 4.5 shows the time evolution of frequency of the 26th mode of the stepped overwound string on the monochord, S1(3).

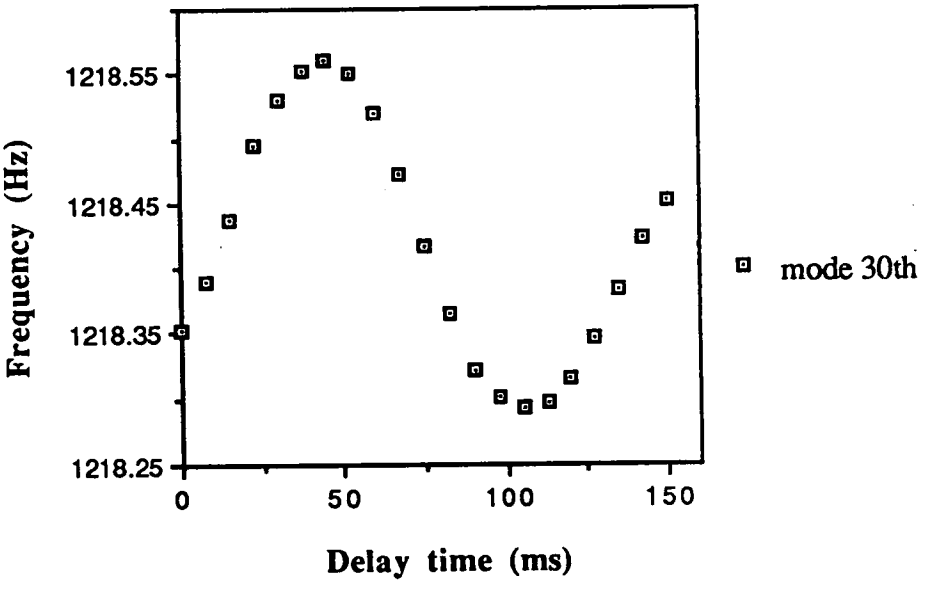

Graph 4.6 shows the time evolution of frequency of the 30th mode of the stepped overwound string on the monochord, S1(3).

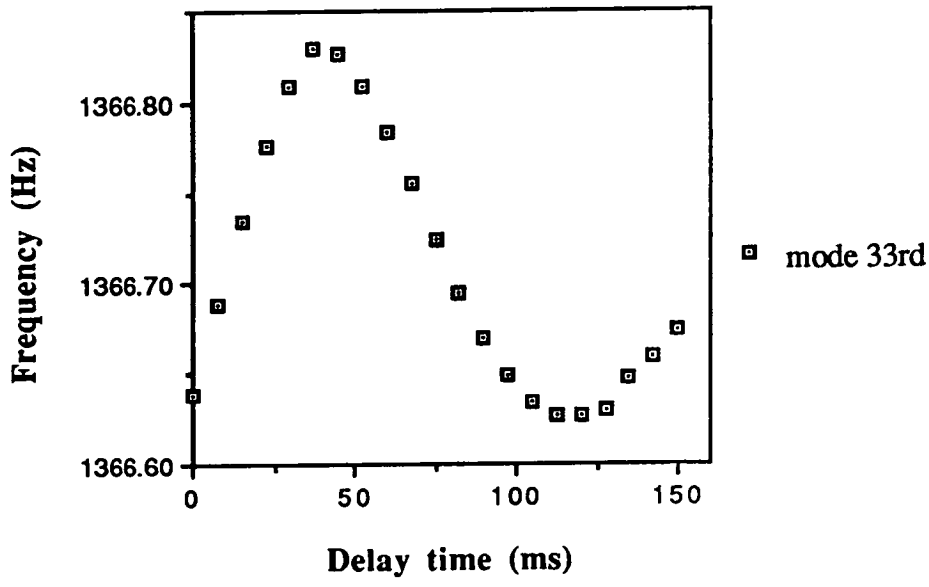

Graph 4.7 shows the time evolution of frequency of the 33rd mode of the stepped overwound string on the monochord, S1(3).

4.6 Experimental results.

In this section the measurements of the mode frequencies of overwound strings with and without step on the monochord are firstly presented. These are followed by the results of inharmonicity of the overwound strings on the monochord. Data of their experimental mode frequencies and the inharmonicity in cents are shown in Appendix D and E.

In order to consider vibration of overwound strings with and without step while eliminating other parameters affecting the strings such as bridges, soundboard vertical vibration of the strings, etc., the overwound strings on the monochord are studied as shown in Fig.4.1. The dimensions for the 18 uniform overwound strings, and for 18 2-segment overwound strings are shown in Table 3.1 and 3.2, respectively. The stepped overwound strings are

studied in order to provide a basis for the study of overwound piano strings that will be shown in Chapter 6.

Graph 4.8 presents the relation between the experimental inharmonicity and the mode number (n) for the six uniformly overwound strings on the monochord, U1(1), U1(2), U1(3), U1(4), U1(5) and U1(6). The six uniformly overwound strings on the monochord, U2(1), U2(2), U2(3), U2(4), U2(5) and U2(6) are presented in Graph 4.9 and U3(1), U3(2), U3(3), U3(4), U3(5) and U3(6) are presented in Graph 4.10.

In the case of the stepped overwound strings, the relation between inharmonicity and the mode number (n) for the six 2-segment overwound strings on the monochord, S1(1), S1(2), S1(3), S1(4), S1(5) and S1(6) are displayed in Graph 4.11. Graph 4.12 and Graph 4.13 display the six 2-segment overwound strings, S2(1), S2(2), S2(3), S2(4), S2(5) and S2(6) and the six 2-segment overwound strings, S3(1), S3(2), S3(3), S3(4), S3(5) and S3(6), respectively.

Discussion of the experimental results will be shown in next chapter with the comparison with the theoretical results.

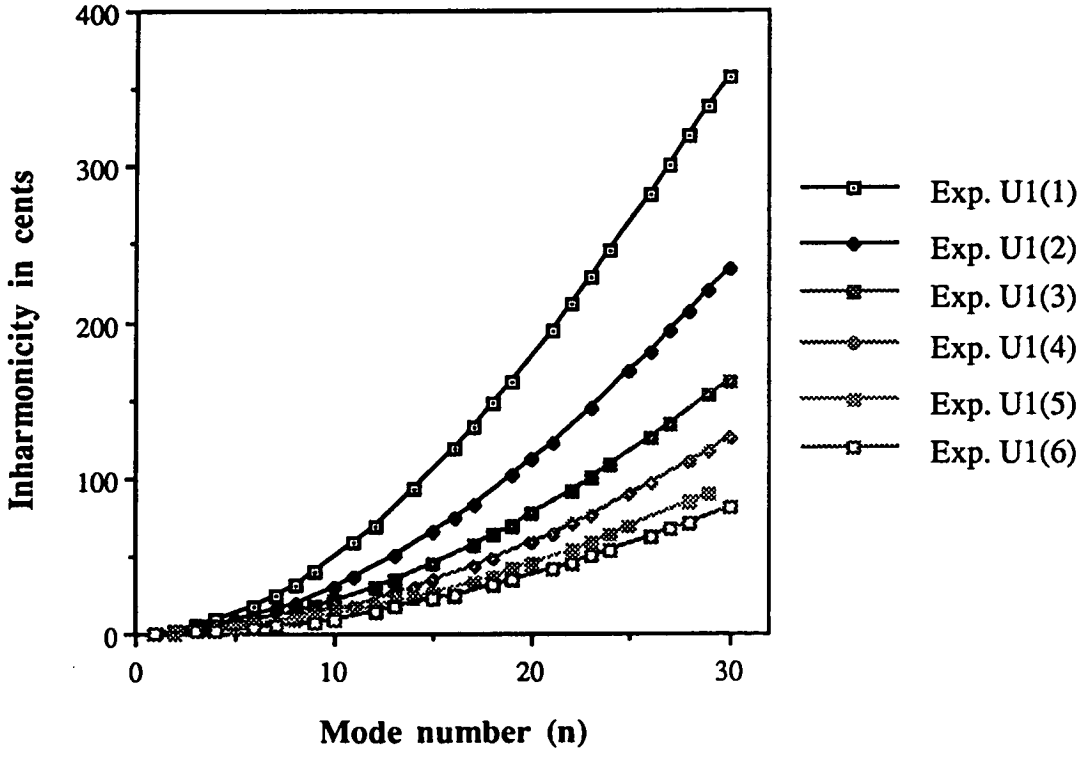

Graph 4.8 The relation between the experimental inharmonicity and the mode number (n) for the six uniformly overwound strings on the monochord, U1(1), U1(2), U1(3), U1(4), U1(5) and U1(6).

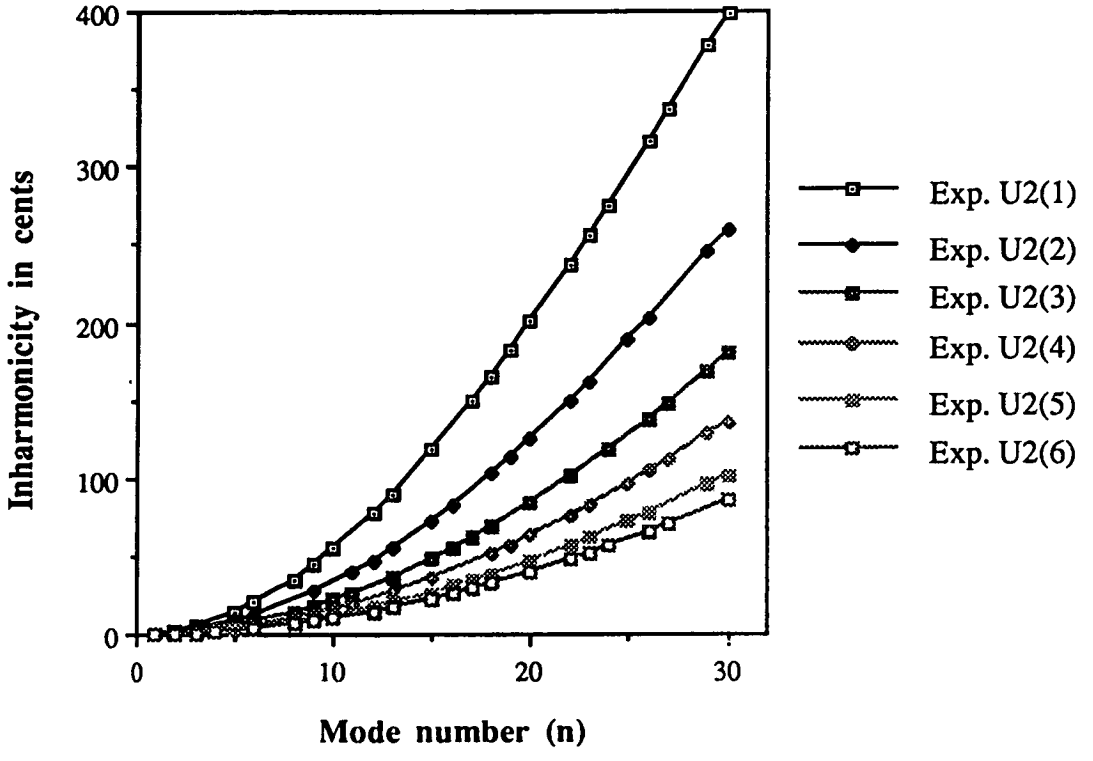

Graph 4.9 The relation between the experimental inharmonicity and the mode number (n) for the six uniformly overwound strings on the monochord, U2(1), U2(2), U2(3), U2(4), U2(5) and U2(6).

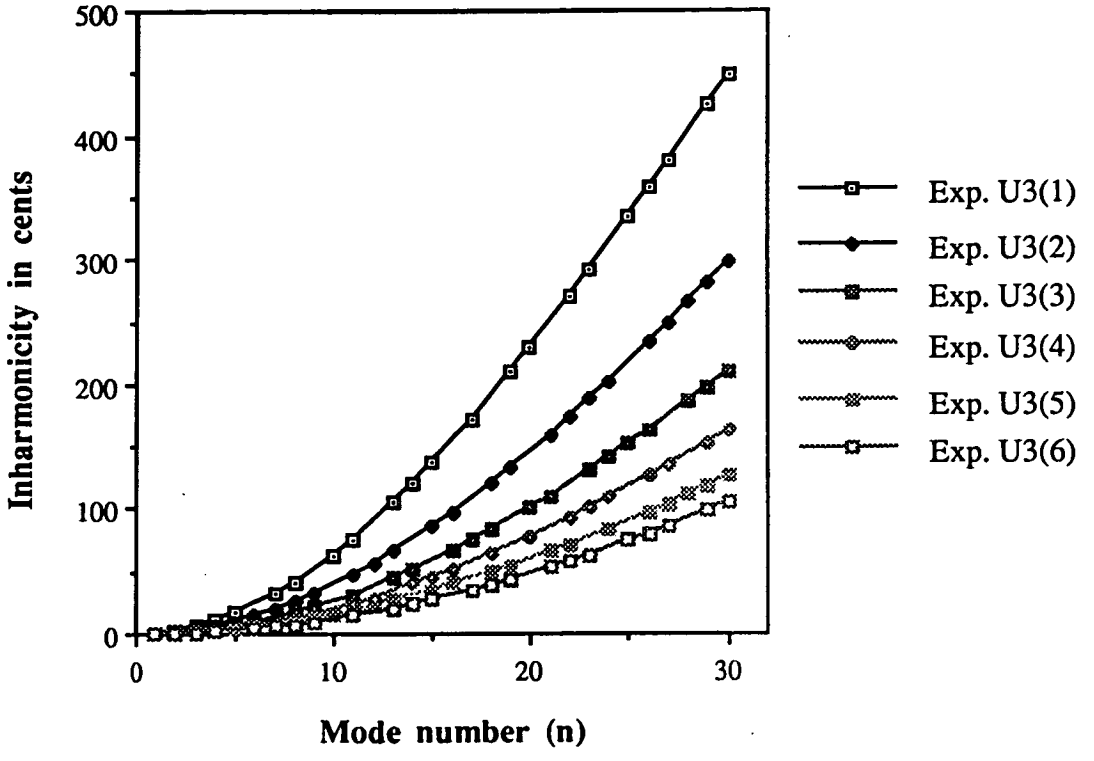

Graph 4.10 The relation between the experimental inharmonicity and the mode number (n) for the six uniformly overwound strings on the monochord, U3(1), U3(2), U3(3), U3(4), U3(5) and U3(6).

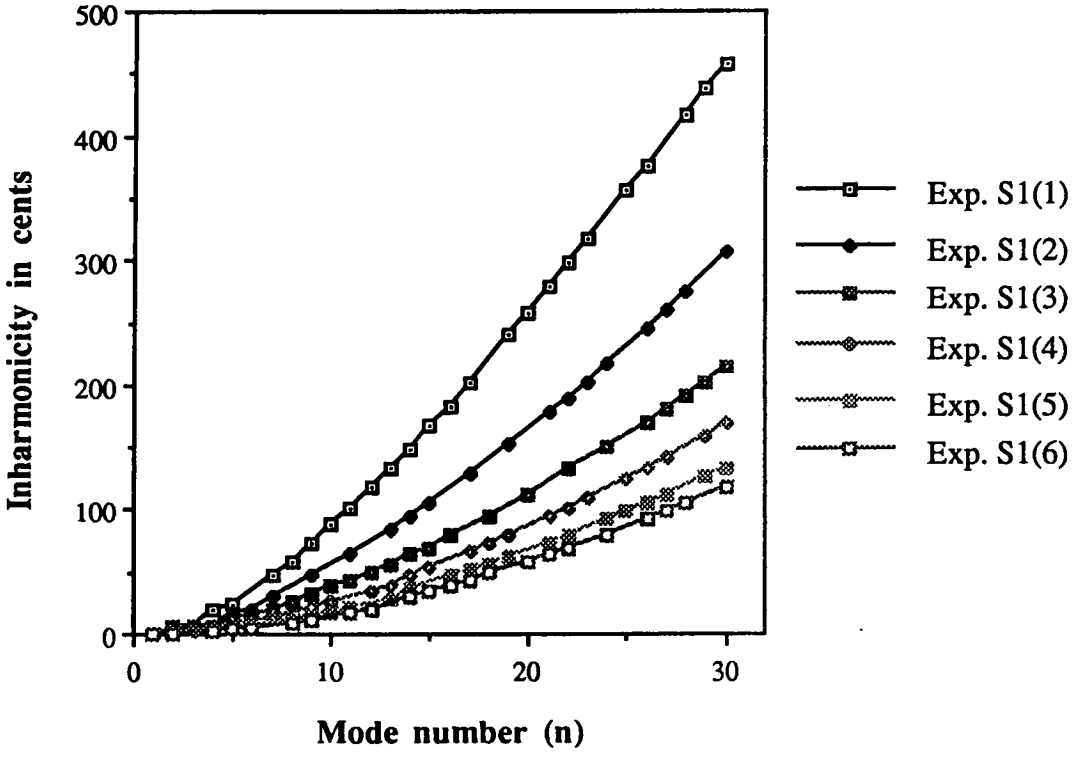

Graph 4.11 The relation between the experimental inharmonicity and the mode number (n) for the six 2-segment overwound strings on the monochord, S1(1), S1(2), S1(3), S1(4), S1(5) and S1(6).

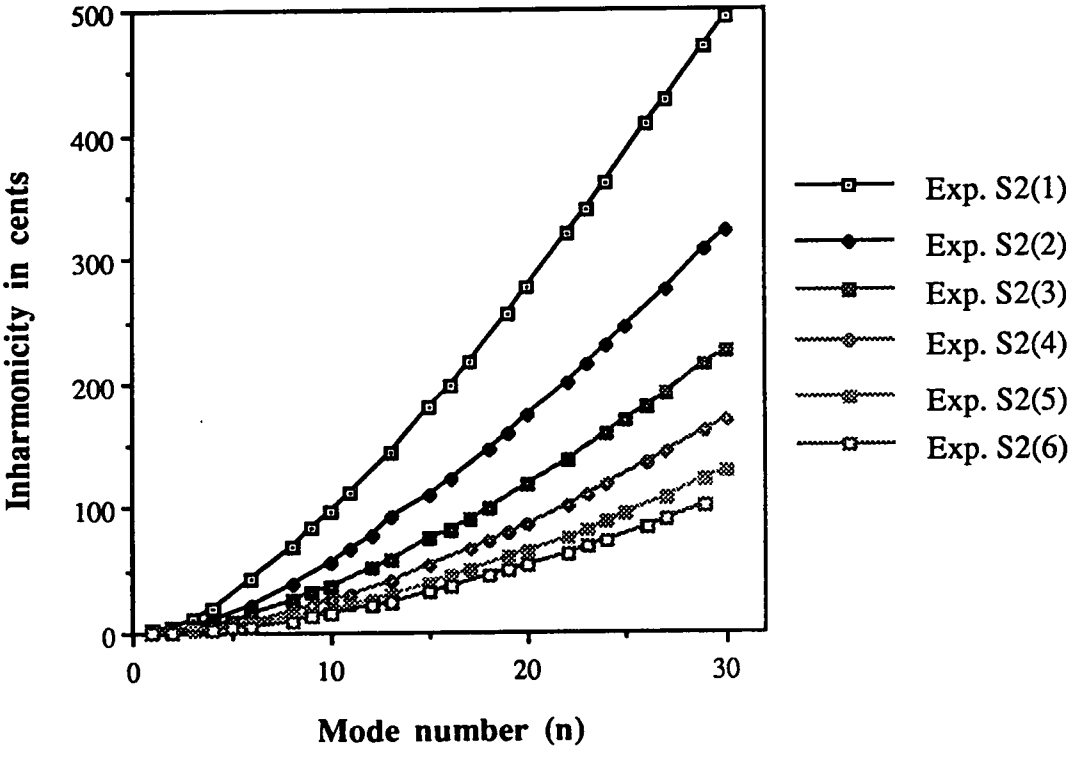

Graph 4.12 The relation between the experimental inharmonicity and the mode number (n) for the six 2-segment overwound strings on the monochord, S2(1), S2(2), S2(3), S2(4), S2(5) and S2(6).

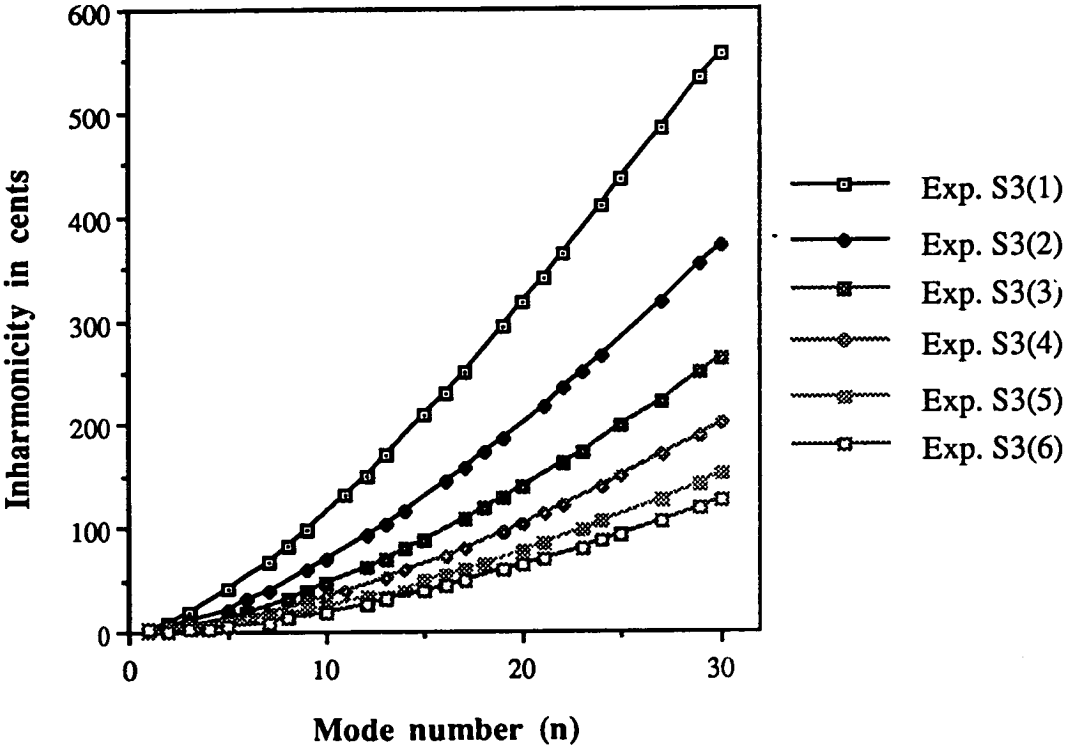

Graph 4.13 The relation between the experimental inharmonicity and the mode number (n) for the six 2-segment overwound strings on the monochord, S3(1), S3(2), S3(3), S3(4), S3(5) and S3(6).

CHAPTER 5

COMPARISON OF THEORY AND EXPERIMENT.

In this chapter the experimental inharmonicity for the uniformly overwound strings and for the stepped overwound strings discussed in Chapter 4 are compared with the theoretical inharmonicity calculated in Chapter 3. Experimental and theoretical values of the inharmonicity coefficient $B = (1/n^2)[(f_n/nf_0)^2 - 1]$ of each mode frequency of each string are compared. In order to probe in more detail the correspondence between calculated and measured frequencies, and to obtain a direct comparison with the predictions of the theory of Fletcher, it is useful to plot the parameter B as a function of mode number.

5.1 Comparison between the theoretical Inharmonicity and experimental Inharmonicity.

The theoretical inharmonicity values were presented for the 18 uniformly overwound strings and the 18 stepped overwound strings in Chapter 3, and the experimental inharmonicity values for the same 18 uniformly overwound strings and the same 18 stepped overwound strings on the monochord were shown in Chapter 4. Here we compare experimental and theoretical values for a given string.

Three representative pairs of strings, each pair having the same diameter and the same length as shown in Table 3.1 and Table 3.2 are chosen. The uniformly overwound string U1(3) and the stepped overwound string S1(3) have the same diameter and the same length; so do the pairs U2(3), S2(3) and U3(3), S3(3). The difference between the two strings in each pair is that one is uniformly wound while the other is stepped.

Graph 5.1 demonstrates a satisfactory level of agreement between theory and experiment for one uniformly wound string, U1(3) and one stepped overwound string, S1(3). A similar level of agreement is found for the other four strings shown in Graph 5.2 and Graph 5.3, demonstrating the comparison between theoretical and experimental inharmonicity for U2(3) and S2(3) and for U3(3) and S3(3), respectively. Each experimental point plotted in Graphs 5.1, 5.2 and 5.3 carries an error bar representing the standard error in the mean of 25 measurements, which was consistent with the calculated uncertainty due to noise corruption of the signal as described in Chapter 4. The magnitude of the error bar is 1 cent, too small to show on the graphs.

In Chapter 3 and Chapter 4 it was shown that the strings' inharmonicity decreases for the longer strings. The results presented in Graph 5.1 to 5.3 show that the inharmonicity for the stepped overwound strings is higher than the inharmonicity for the uniformly overwound string of the same length and diameter.

We can see that the effect of non-uniformity in the case of the stepped overwound strings is to increase the inharmonicity. As shown in the Graph 5.1 to Graph 5.3, experimental results agree very well with the theoretical results.

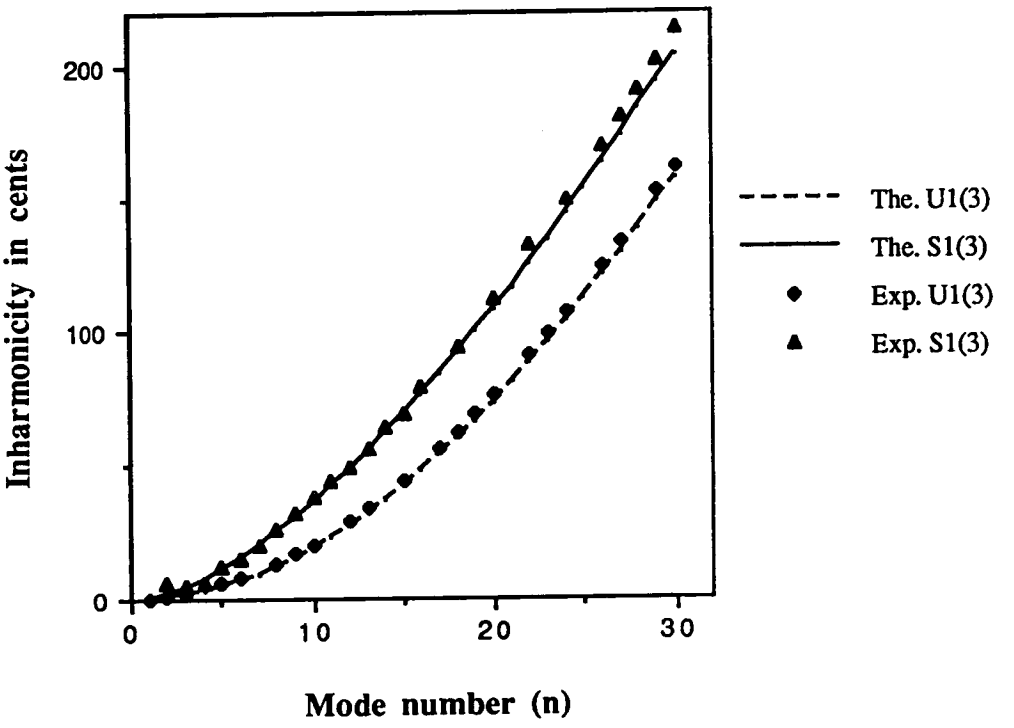

Graph 5.1 the relation between inharmonicity and the mode number (n), for the uniformly overwound string, U1(3), and for the stepped overwound string, S1(3). Solid line: present theory (U1(3)); broken line: present theory (S1(3)); triangles: experimental measurements (U1(3)); diamonds: experimental measurements (S1(3)).

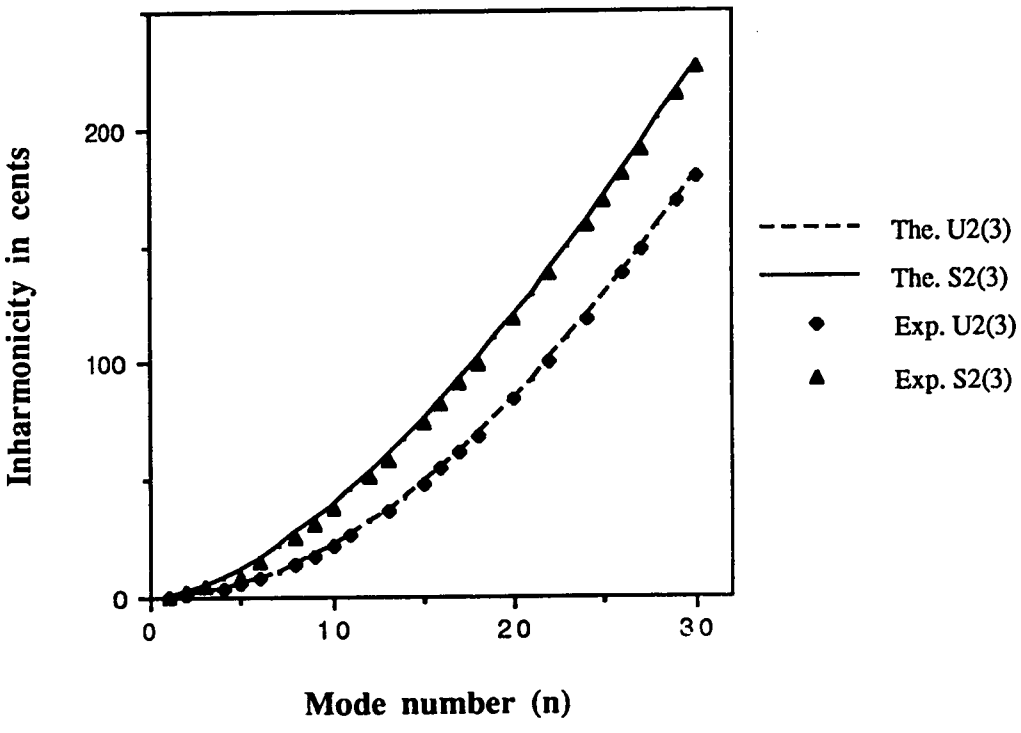

Graph 5.2 the relation between inharmonicity and the mode number (n), for the uniformly overwound string, U2(3), and for the stepped overwound string, S2(3). Solid line: present theory (U2(3)); broken line: present theory (S2(3)); triangles: experimental measurements (U2(3)); diamonds: experimental measurements (S2(3)).

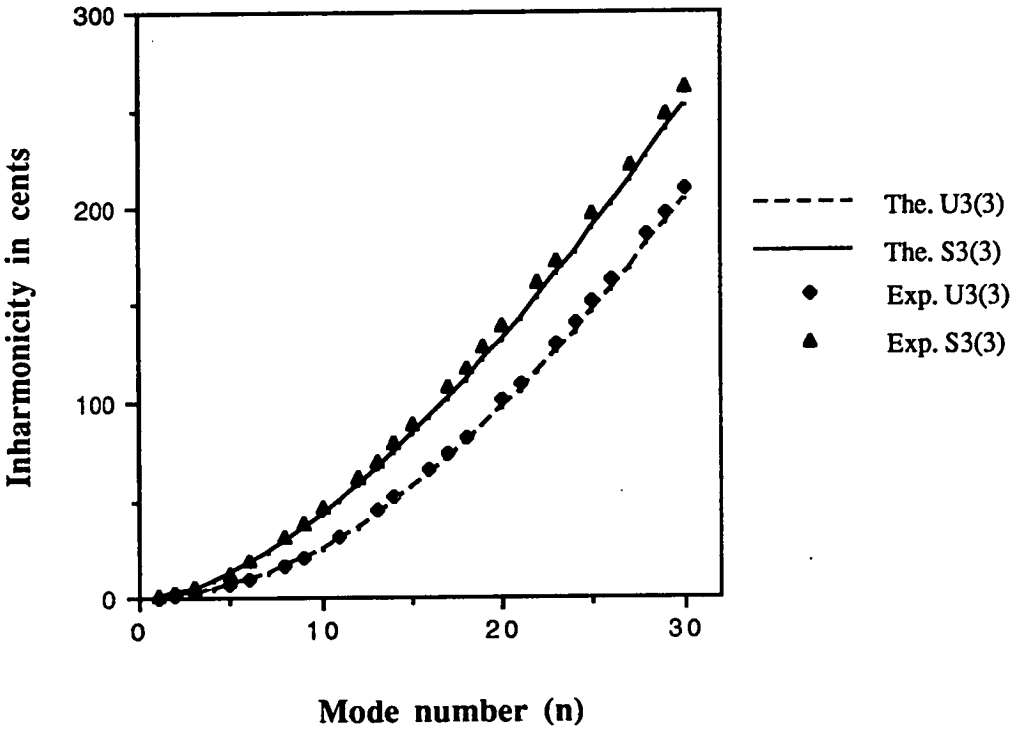

Graph 5.3 the relation between inharmonicity and the mode number (n), for the uniformly overwound string, U3(3), and for the stepped overwound string, S3(3). Solid line: present theory (U3(3)); broken line: present theory (S3(3)); triangles: experimental measurements (U3(3)); diamonds: experimental measurements (S3(3)).

5.2 Comparison of the B-coefficient from the theoretical results, experimental results and Fletcher's results.

In order to probe in more detail the correspondence between calculated and measured frequencies, and to obtain a direct comparison with the predictions of the theory of Fletcher, it is useful to plot the parameter $B=(1/n^2)[(f_n/nf_0)^2-1]$ as a function of mode number. This is done in Graph 5.4 for the first six uniformly overwound strings, U1(1), U1(2), U1(3), U1(4), U1(5) and U1(6), in Graph 5.5 for the second six uniformly overwound strings, U2(1), U2(2), U2(3), U2(4), U2(5) and U2(6), and in Graph 5.6 for the third six uniformly overwound strings, U3(1), U3(2), U3(3), U3(4), U3(5) and U3(6) described in Table 3.1. According to Fletcher's theory, B is a constant determined by the dimensions, constitution and tension of the string; values of B predicted by the Fletcher formula for each of the 18 strings under discussion are shown on the right hand axis of Graph 5.4, Graph 5.5 and Graph 5.6. The lines are fits to the theoretical values calculated in the present theoretical study, while the discrete points show values derived from the measurements.

It is clear from Graph 5.4, Graph 5.5 and Graph 5.6 that Fletcher's assumption that B is independent of mode number for a uniformly overwound string is consistent with the present calculations, although for the shorter strings our values of B are slightly higher than those of Fletcher. The experimental results agree well with our theoretical values. The inharmonicity coefficients B are lower when the strings are longer.

Our theoretical and experimental values of B are illustrated in Graph 5.7 for the first six partially overwound strings, S1(1), S1(2), S1(3), S1(4), S1(5) and S1(6), in Graph 5.8 for the second partially overwound strings, S2(1), S2(2), S2(3), S2(4), S2(5) and S2(6) and in Graph 5.9 for the third six partially

overwound strings, S3(1), S3(2), S3(3), S3(4), S3(5) and S3(6) described in Table 3.2. The deviation of B from the constancy characteristic of uniformly wound strings increases as the fractional length of unwound string increases. For mode numbers greater than 10, theory and experiment are in good agreement; for lower mode numbers and relatively large unwound fractions, it appears that the measured inharmonicity coefficient is slightly higher than that predicted by theory.

The error in the inharmonicity coefficient B, ΔB, is given by $(dB/df_n)\Delta f_n$, where Δf_n is the corresponding error in the mode frequency. With the expression of B-coefficient $B=(1/n^2)[(f_n/nf_0)^2-1]$ then $\Delta B=(2/n^2+2B)\Delta f_n/f_n$. Δf_n is evaluated at 2.5% of the frequency interval (0.1 Hz) for single measurement and 0.02 Hz for 25 measurements, and B is very small (of the order of 10^{-4}), so the error in the inharmonicity coefficient B mainly depends inversely on the square of mode number (n^2) and the mode frequency (f_n). If we consider the experimental mode frequency from 25 measurements of the stepped overwound string S1(1), for example, we can calculate the error in B-coefficient: on the second mode with $f_2=119.35$ Hz, ΔB is $\pm 8\times10^{-5}$, but on the tenth mode with $f_{10}=626.61$ Hz, ΔB is $\pm 6\times10^{-7}$. Correspondingly, error bars are shown on the graphs only for the first two modes; they are too small to see on the higher modes.

5.3 Uncertainty of experimental fundamental frequencies.

In the experimental measurements of mode frequencies for sets of strings of different lengths, the approximate value of the string tension was first estimated by plucking the string and observing the microphone signal on a digital storage oscilloscope. A low-pass filter was used to eliminate mode frequencies higher than that of the first mode, f_1, which was estimated to an

accuracy of 2% by measuring the period using the numerical cursor of the oscilloscope. Neglecting the small degree of inharmonicity in the first mode, f_1 was taken to be equal to f_0, and the string tension T derived from the equation $T = 4(a_1 + a_2)^2 f_0^2 \sigma_2$. As the length of the string was varied by moving the clamps, it was assumed that T remained constant, permitting values of f_0 to be calculated for each string length.

Although this relatively crude estimation of T was adequate for the evaluation of inharmonicities at the level of accuracy shown in Graphs 5.4 to 5.6, the inharmonicity coefficient B is much more sensitive to small variations in T (and f_0), especially at low mode numbers. In fact, the most sensible procedure is to fit the theoretically predicted values of B to those measured experimentally, using f_0 as a fitting parameter. This was done by varying the value of T used in deriving f_0. It should be noted that this altered not only the theoretical curve, but also the experimental values, since the latter depend on the value of f_0 assumed. Since Equation 2.48 contains the ratio $T/R_1 = T/QS\kappa^2$, it is possible that the fitting procedure also partially compensates for any error in the chosen value of the Young's modulus Q. The theoretical curves in Graph 5.7 to 5.9 were obtained in this way; in every case the value of T corresponding to the best fit was well within the experimental uncertainty in the measurement of T.

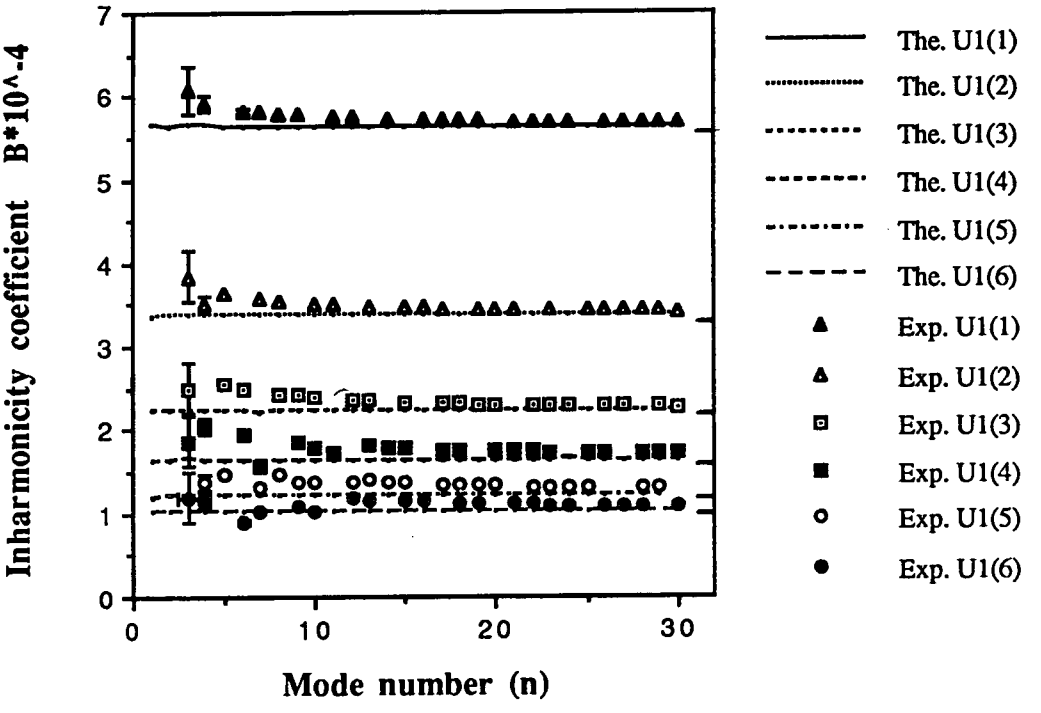

Graph 5.4 The relation between the inharmonicity coefficient B and the mode number (n) for the six uniform overwound strings, U1(1), U1(2), U1(3), U1(4), U1(5) and U1(6) is presented by lines for theoretical results and by points for experimental results.

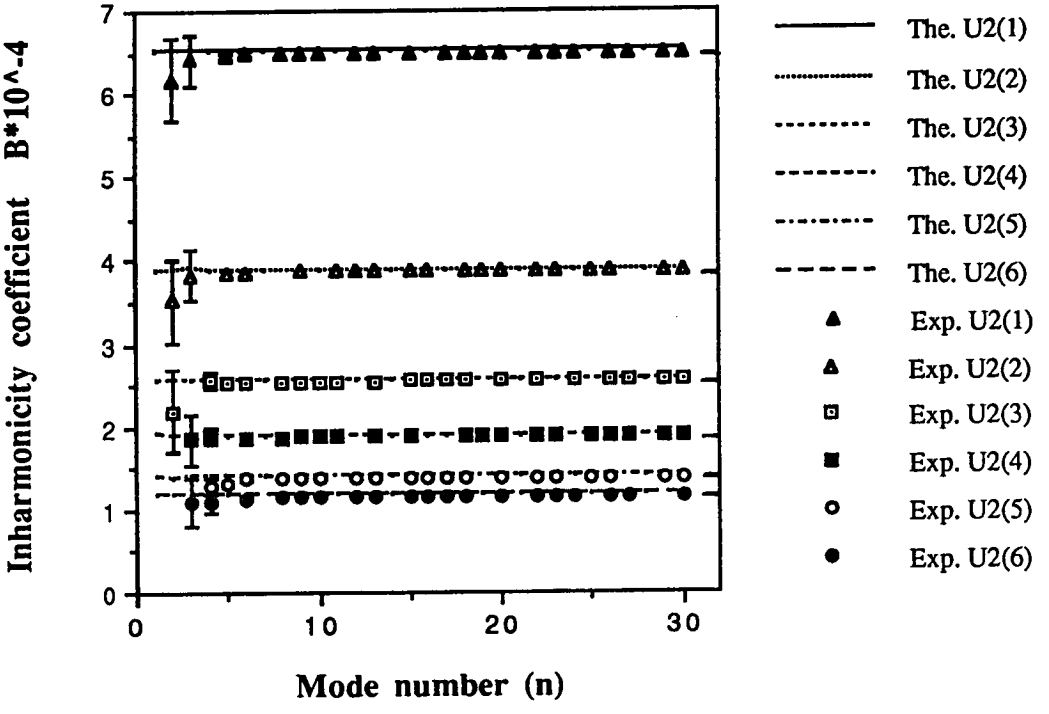

Graph 5.5 The relation between the inharmonicity coefficient B and the mode number (n) for the six uniform overwound strings, U2(1), U2(2), U2(3), U2(4), U2(5) and U2(6) is presented by lines for theoretical results and by points for experimental results.

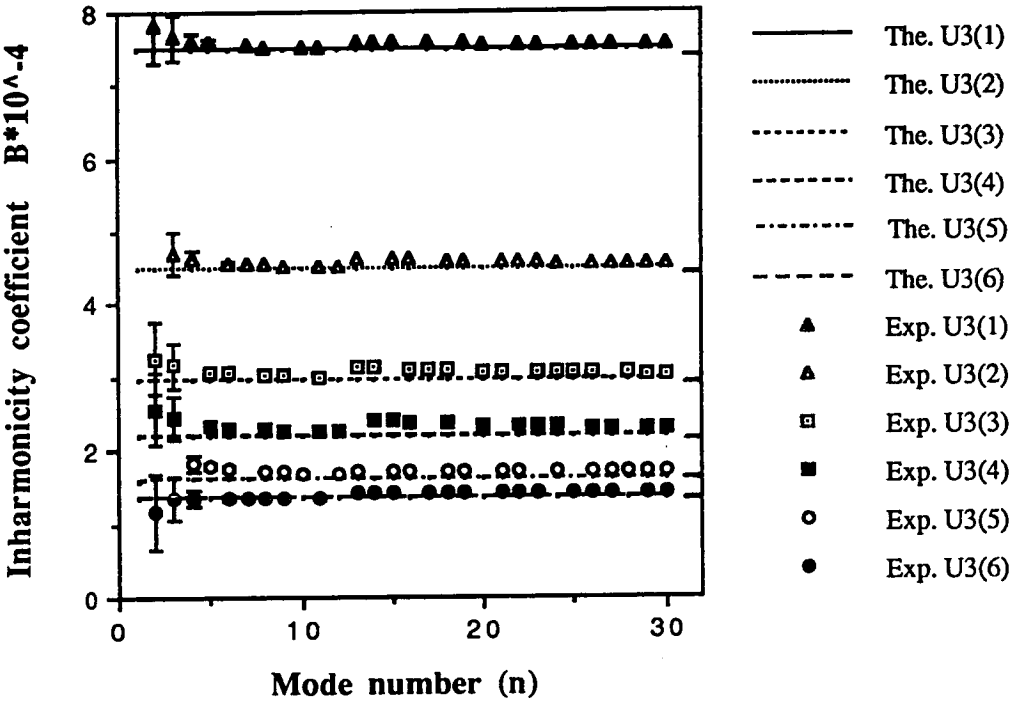

Graph 5.6 The relation between the inharmonicity coefficient B and the mode number (n) for the six uniform overwound strings, U3(1), U3(2), U3(3), U3(4), U3(5) and U3(6) is presented by lines for theoretical results and by points for experimental results.

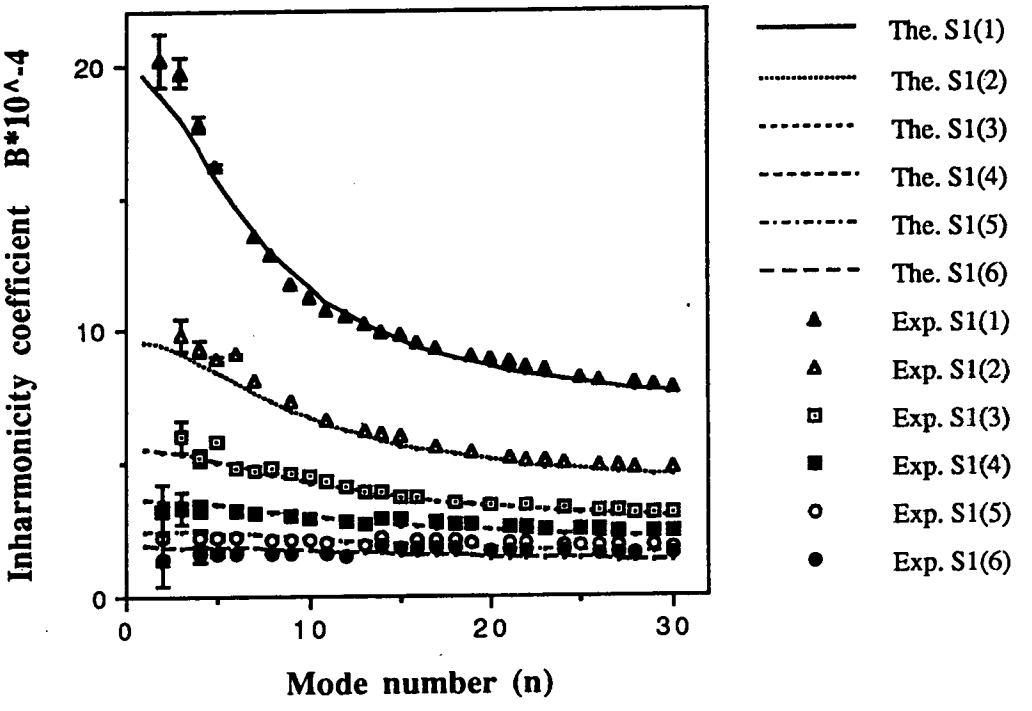

Graph 5.7 The relation between the inharmonicity coefficient B and the mode number (n) for the six 2-segment overwound strings, S1(1), S1(2), S1(3), S1(4), S1(5) and S1(6) is presented by lines for theoretical results and by points for experimental results.

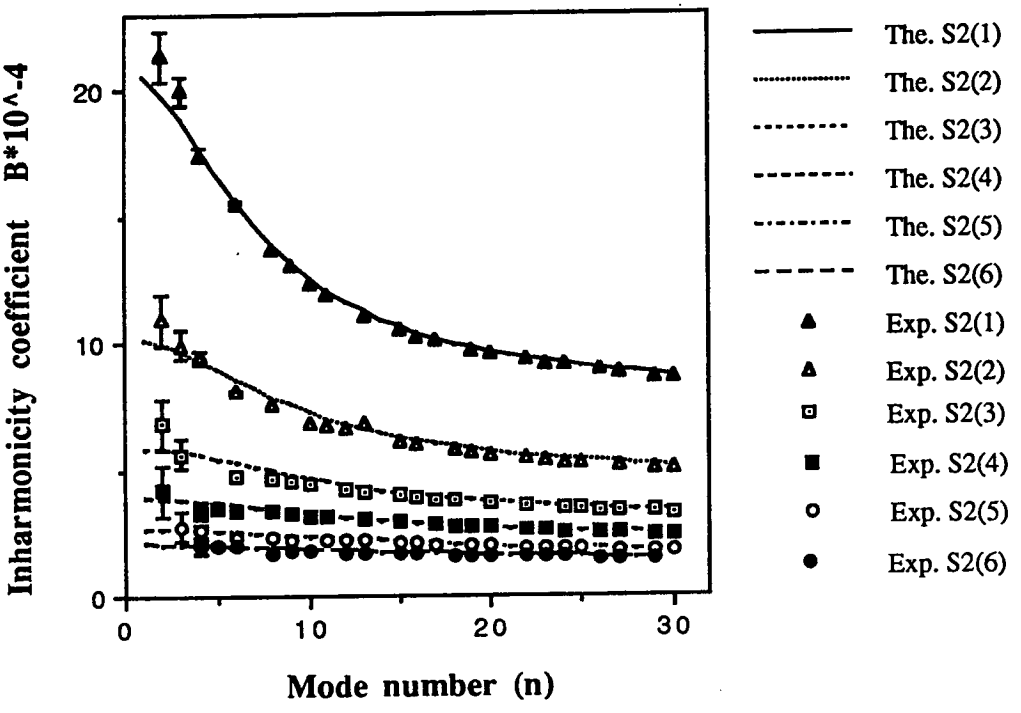

Graph 5.8 The relation between the inharmonicity coefficient B and the mode number (n) for the six 2-segment overwound strings, S2(1), S2(2), S2(3), S2(4), S2(5) and S2(6) is presented by lines for theoretical results and by points for experimental results.

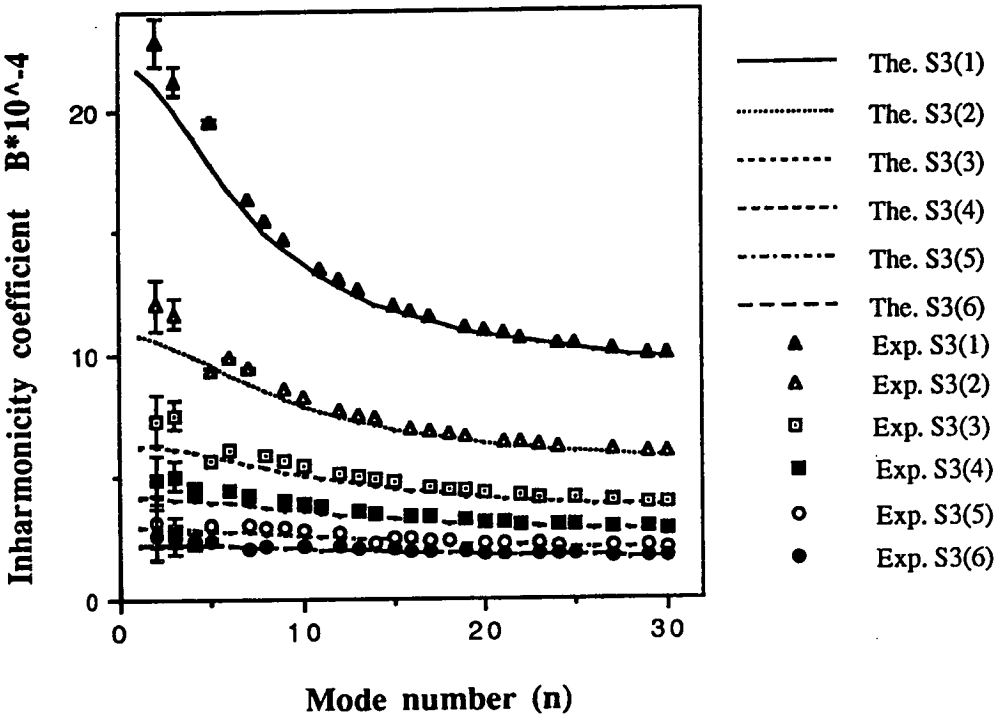

Graph 5.9 The relation between the inharmonicity coefficient B and the mode number (n) for the six 2-segment overwound strings, S3(1), S3(2), S3(3), S3(4), S3(5) and S3(6) is presented by lines for theoretical results and by points for experimental results.

CHAPTER 6

MEASUREMENT ON GRAND PIANO STRINGS.

The original motivation for this study was to determine the extent to which the non-uniformity of the overwinding on a bass piano string affected the inharmonicity of its mode frequencies. The theoretical treatment described in Chapters 2 and 3 assumed that the end supports of the string were completely rigid, and the experimental results given in Chapter 4 and 5 were obtained on a monochord which attempted to reproduce this ideal case. To examine the extent to which this work was relevant to the behaviour of overwound piano strings with the end support conditions typical of normal use, a series of measurements was performed on the bass strings of a broadwood grand piano in the Acoustics Laboratory of the Department of Physics at the University of Edinburgh. This piano was built in 1871, and was renovated and restrung in 1992.

6.1 Experimental technique on the grand piano.

The general arrangement of the experimental apparatus for the 2.5 m Broadwood grand piano is shown in Fig. 6.1. For the purposes of this experiment the piano strings were plucked rather than struck with the normal piano key and hammer mechanism. The position and material of a standard

piano hammer are such that certain modes of vibration are suppressed [54]. The use of the piano hammer would therefore have resulted in missing modes in the spectrum of modes of vibration of the string. It was found that plucking of the string at a position close to the end with the flesh and nail of the finger or thumb excited the greatest number of modes. The string damper was held far from the strings by putting a weight on the appropriate key.

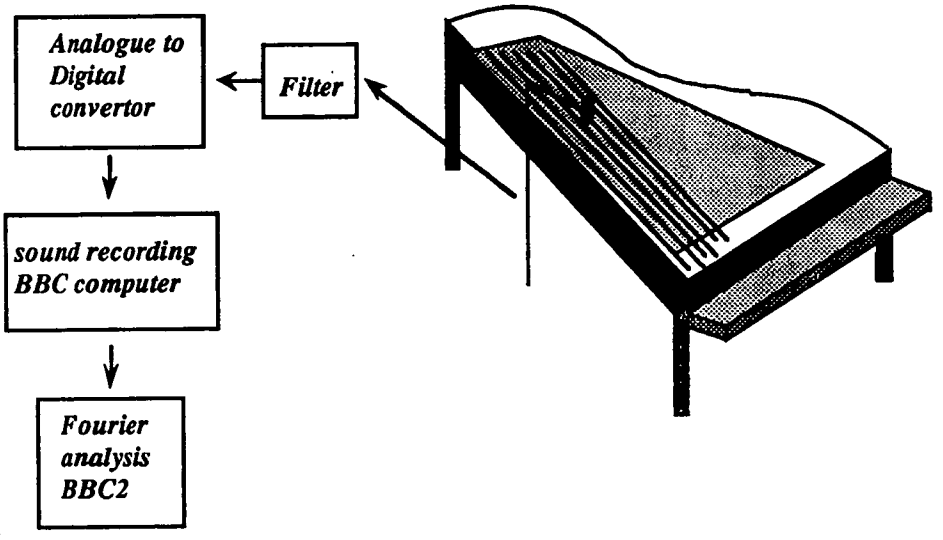

Fig. 6.1 The experimental apparatus for the 2.5 m Broadwood grand piano.

The sound was recorded and analysed using a SHURE SM94 condenser microphone mounted a short distance above the string at middle point using the same experimental technique as shown in Chapter 4.

The sound produced by a piano string on the monochord decays more slowly than the sound produced by the same string on the piano. The omission of the sounding board by no means eliminates the acoustical output of a piano. However, if the efficiency of conversion of mechanical energy into acoustical energy were the same for the sounding board as for the rest of the structure, one could assume from a comparison of the decay rates, with and without sounding board, that removal of the sounding board approximately

halves the rate of decay of piano tones. The effect is somewhat greater on low tones than on high ones [74]. The highest decay rate observed in the components studied here was 25 dB/sec. As shown in Chapter 4, the resulting uncertainty in the estimation of the frequency is still small in comparison with that arising from noise.

6.2 The experimental and theoretical results for the grand piano strings.

The dimensions for the 8 lowest bass strings on this piano are shown in Table 6.1.

Table 6.1 The dimensions of the bass piano strings on the Broadwood grand piano.

Piano strings	Core diameter d1 (mm.)	Overall diameter d2 (mm.)	Unwound length a1 (mm.)	Wound length a2 (mm.)	Total length a(mm.)	Unwound fraction a1:a2
A0	1.45	4.68	25	1845	1870	1:73.8
Bb0	1.40	4.41	23	1837	1860	1:79.9
B0	1.40	4.28	20	1818	1838	1:90.9
C1	1.30	3.98	22	1785	1807	1:81.1
Db1	1.30	3.77	18	1767	1785	1:98.2
D1	1.30	3.63	15	1755	1770	1:117
Eb1	1.23	3.44	13	1747	1760	1:134.4
E1	1.23	3.35	8	1738	1746	1:217.3

Typical sets of results are shown in Graph 6.1 to Graph 6.8. The dashed curves in Graph 6.1 to Graph 6.8 show the prediction of Fletcher's

theory on the assumption that the winding continued over the whole string length, while the solid lines take into account the effect of the short unwound section calculated from the frequency equation in Chapter 2 and Chapter 3. Each experimental point plotted in Graphs 6.1 to Graph 6.8 carries an error bar representing the standard error in the mean of 25 measurements, which was consistent with the calculated uncertainty due to noise corruption of the signal.

It is evident from Graph 6.1 that the major cause of the discrepancy between the Fletcher prediction and the measurement for the A0 string is indeed the non-uniformity of the winding. The present theory, which allows for the effect of non-uniformity, gives a much better agreement with the experimental results.

Surveying the remaining graphs, we see that in each case the present theory is closer to experiment than Fletcher, although for the shortest string E1 the effect of non-uniformity is small.

The reason for discrepancies between theory and experiment is possibly the increase in string stiffness due to the overwinding, which would have the effect of increasing the inharmonicity. It should be noted that a discrepancy of comparable magnitude (about 10 cents for $n = 30$) was found for the strings on the monochord.

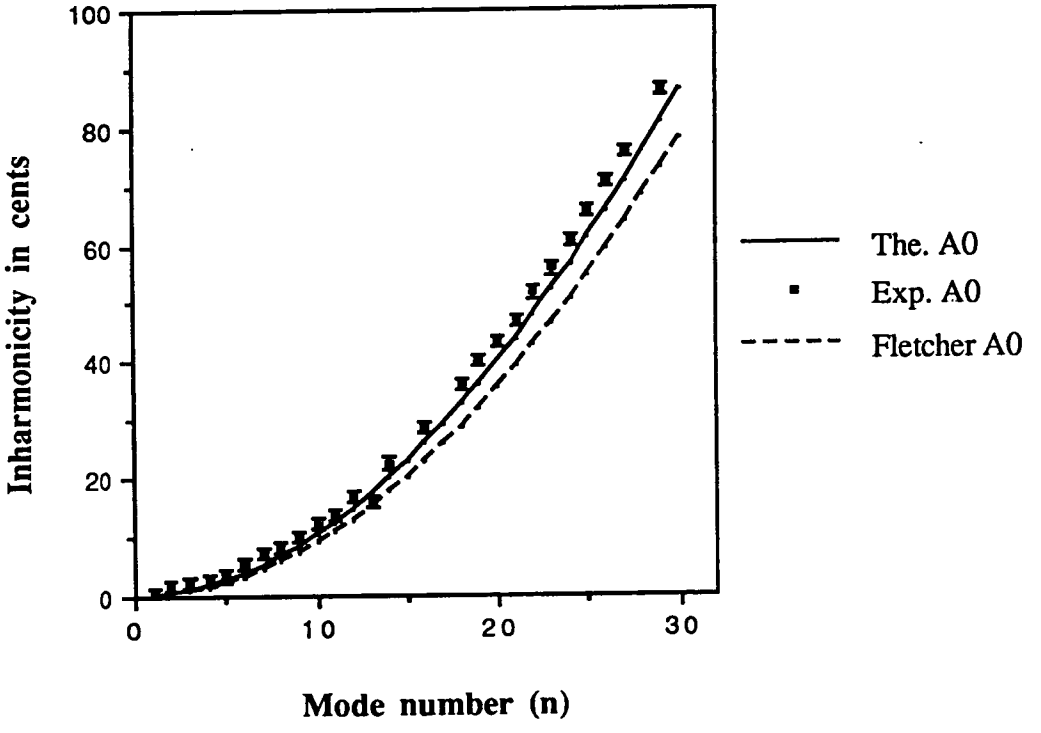

Graph 6.1 shows the measurement of the A0 strings on the piano. The ratio of unwound to wound length is 1:73.8. The dashed curve shows the prediction of Fletcher's theory on the assumption that the winding continued over the whole string length, while the solid lines take into account the effect of the short unwound section calculated from the frequency equation.

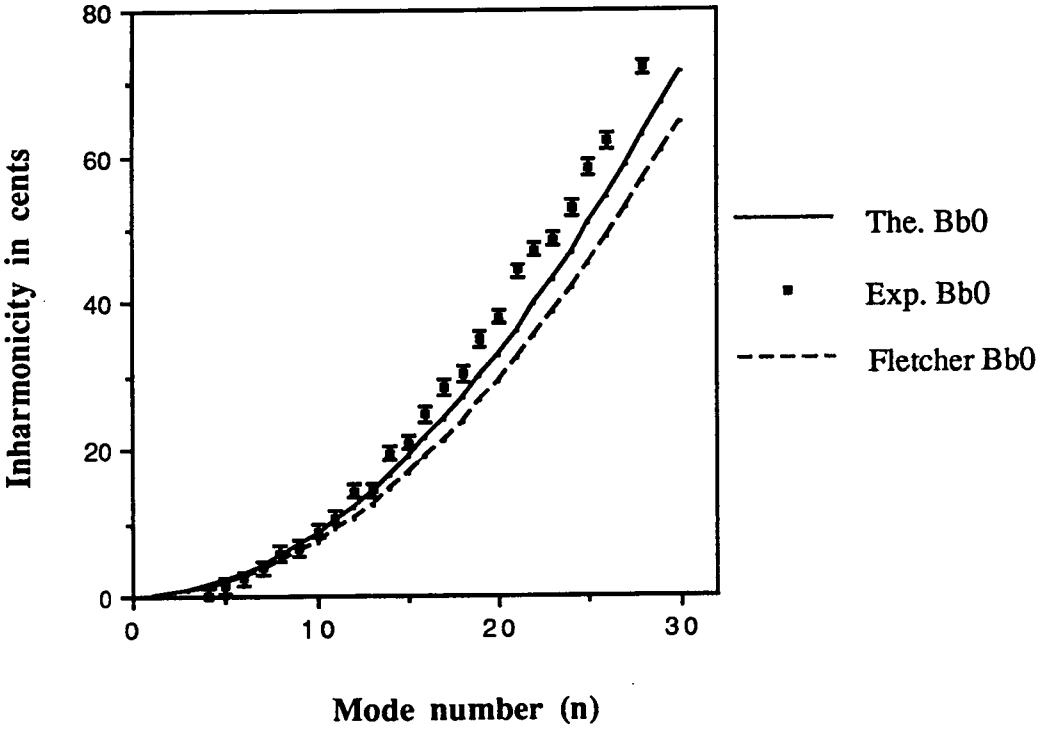

Graph 6.2 shows the measurement of the Bb0 strings on the piano. The ratio of unwound to wound length is 1:79.9. The dashed curve shows the prediction of Fletcher's theory on the assumption that the winding continued over the whole string length, while the solid lines take into account the effect of the short unwound section calculated from the frequency equation.

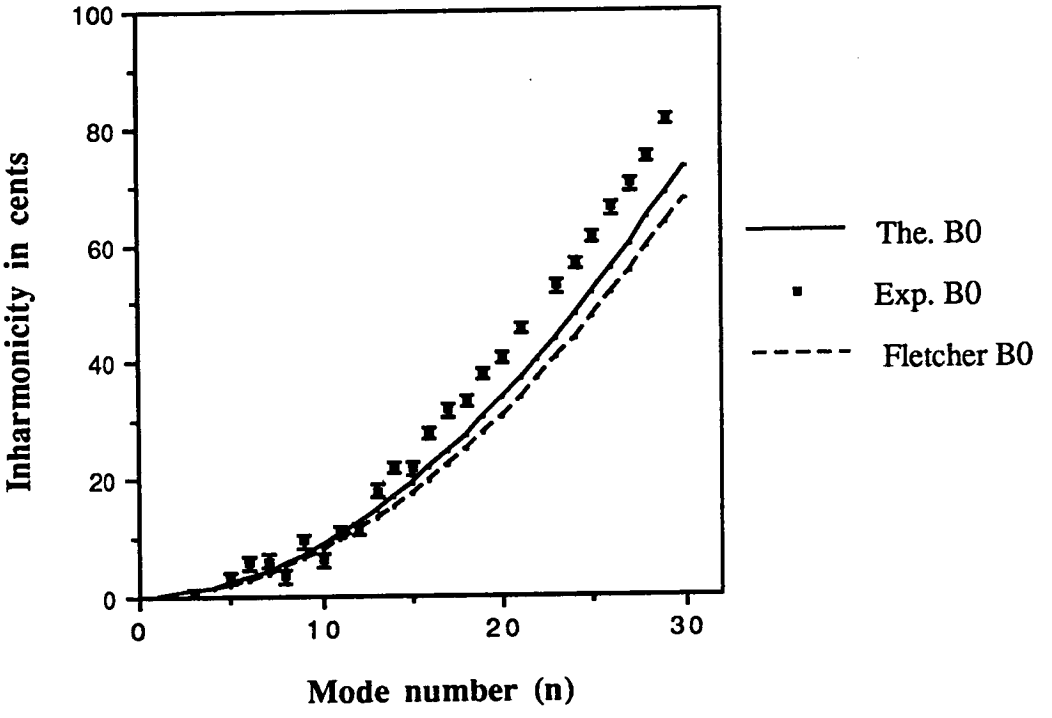

Graph 6.3 shows the measurement of the B0 strings on the piano. The ratio of unwound to wound length is 1:90.9. The dashed curve shows the prediction of Fletcher's theory on the assumption that the winding continued over the whole string length, while the solid lines take into account the effect of the short unwound section calculated from the frequency equation.

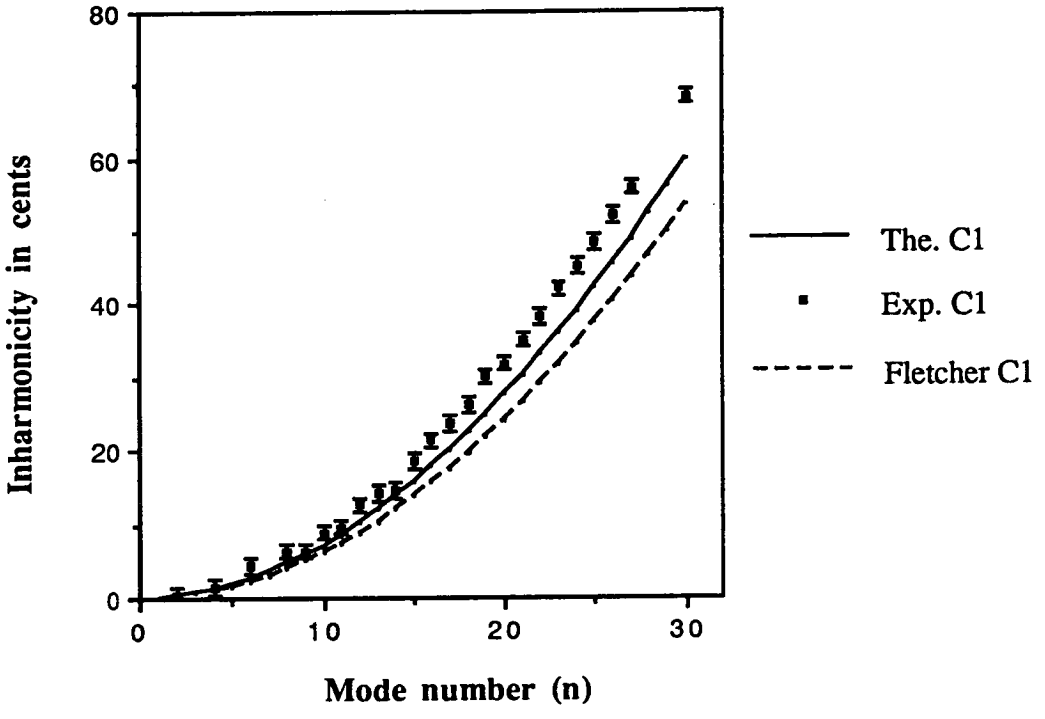

Graph 6.4 shows the measurement of the C1 strings on the piano. The ratio of unwound to wound length is 1:81.1. The dashed curve shows the prediction of Fletcher's theory on the assumption that the winding continued over the whole string length, while the solid lines take into account the effect of the short unwound section calculated from the frequency equation.

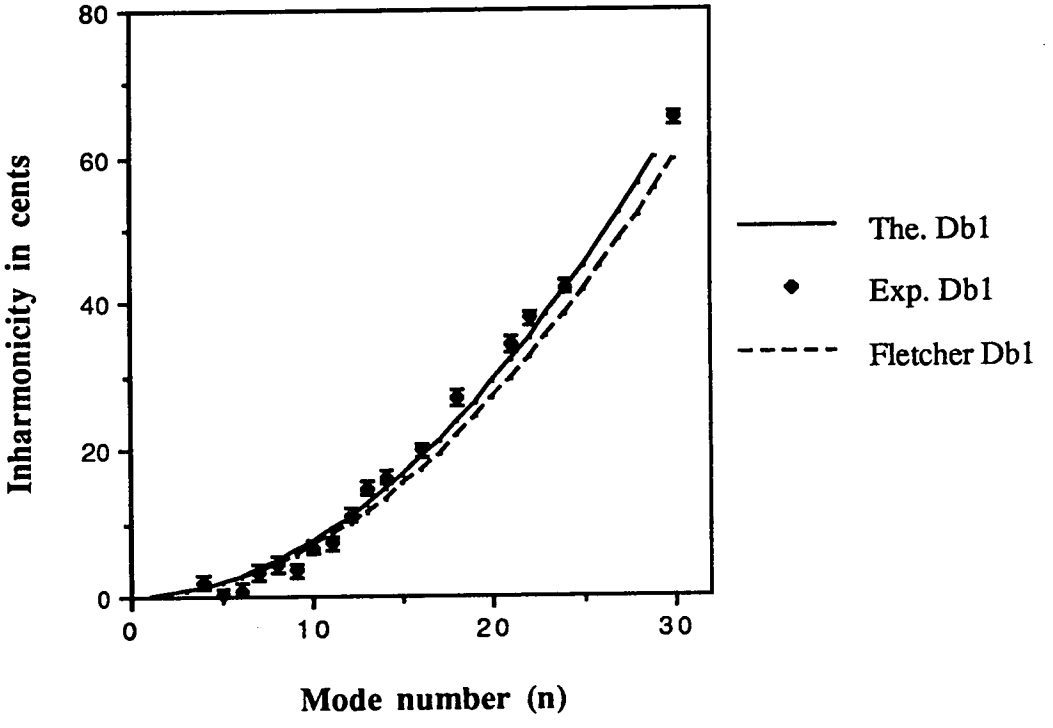

Graph 6.5 shows the measurement of the Db1 strings on the piano. The ratio of unwound to wound length is 1:98.2. The dashed curve shows the prediction of Fletcher's theory on the assumption that the winding continued over the whole string length, while the solid lines take into account the effect of the short unwound section calculated from the frequency equation.

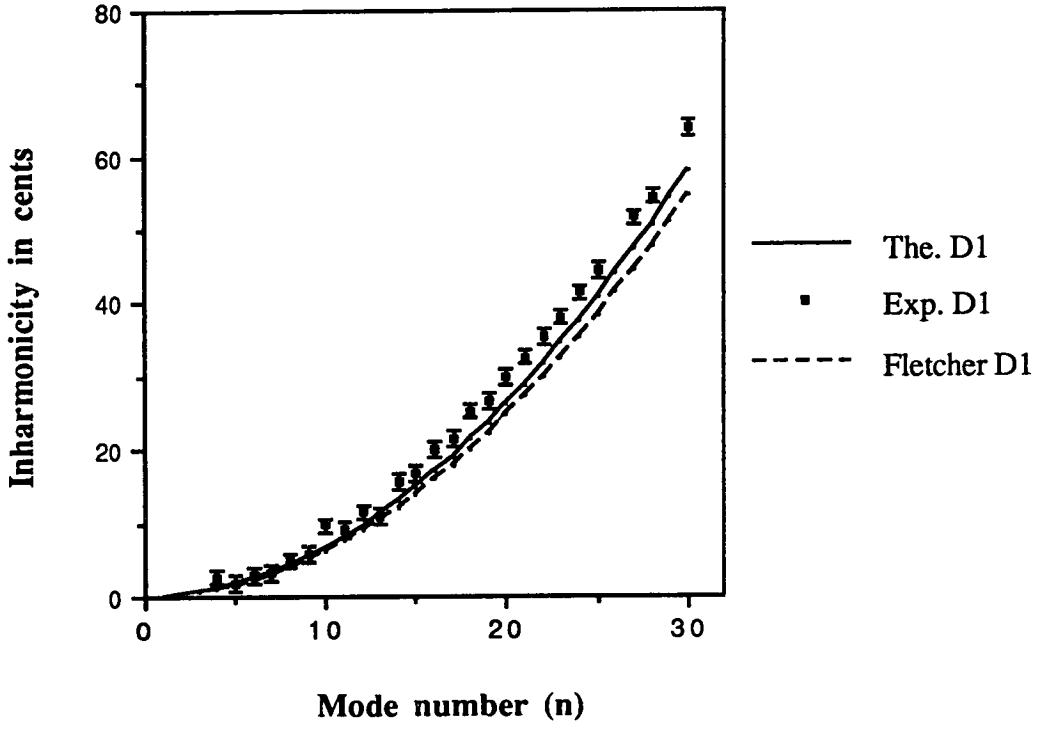

Graph 6.6 shows the measurement of the D1 strings on the piano. The ratio of unwound to wound length is 1:117.0. The dashed curve shows the prediction of Fletcher's theory on the assumption that the winding continued over the whole string length, while the solid lines take into account the effect of the short unwound section calculated from the frequency equation.

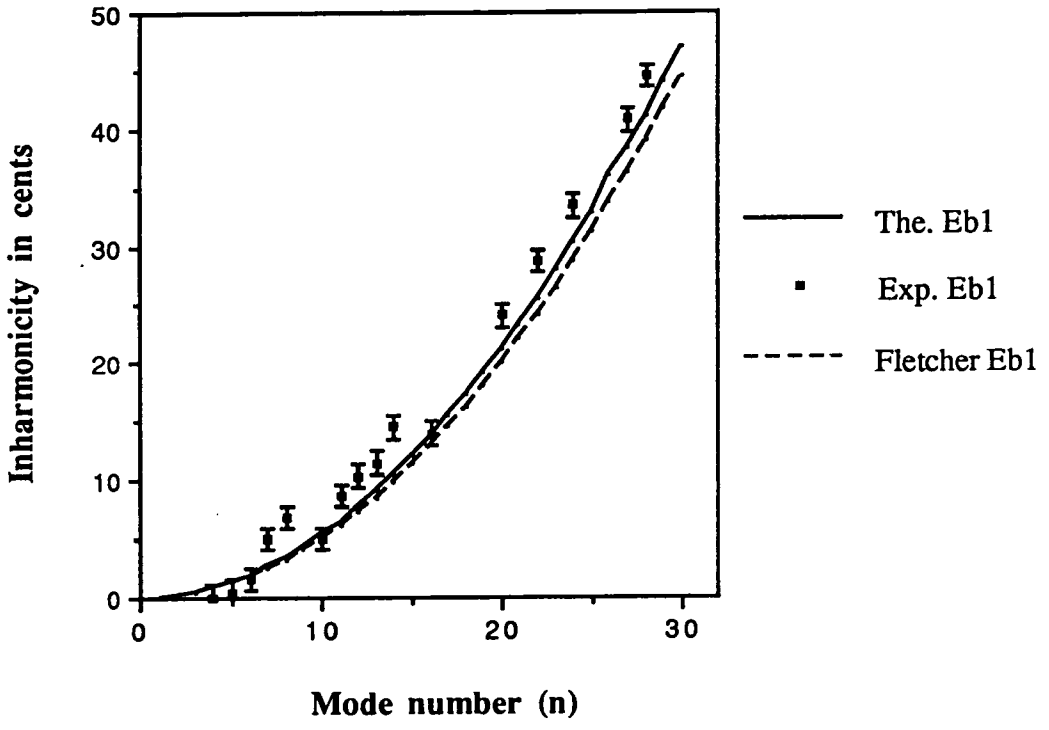

Graph 6.7 shows the measurement of the Eb1 strings on the piano. The ratio of unwound to wound length is 1:134.4. The dashed curve shows the prediction of Fletcher's theory on the assumption that the winding continued over the whole string length, while the solid lines take into account the effect of the short unwound section calculated from the frequency equation.

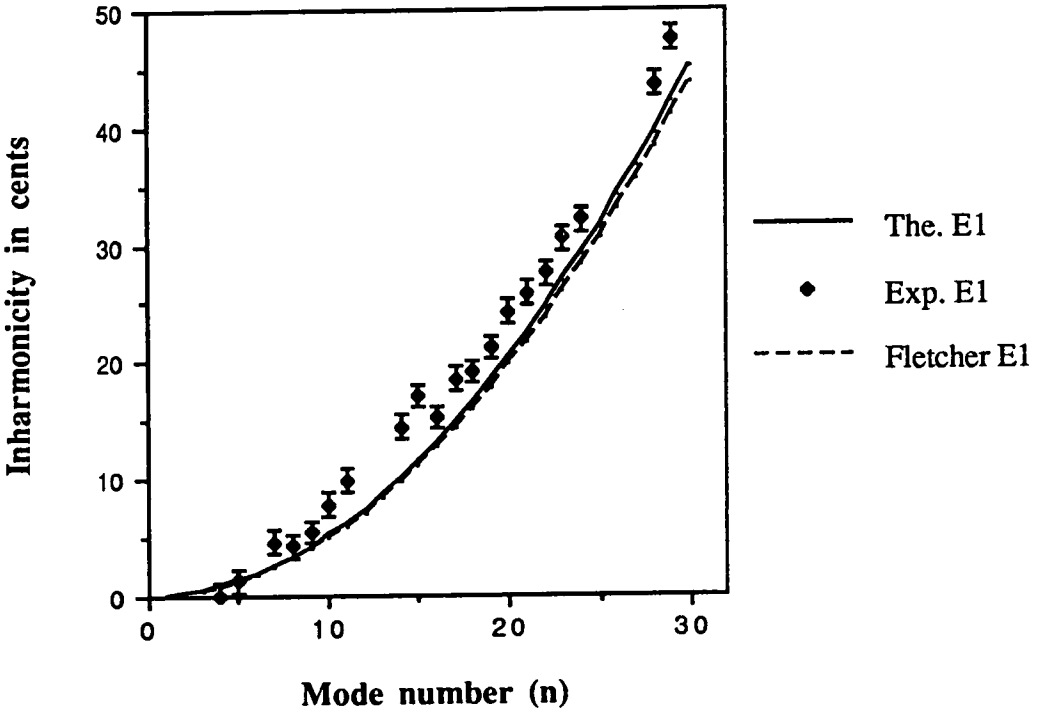

Graph 6.8 shows the measurement of the E1 strings on the piano. The ratio of unwound to wound length is 1:217.3. The dashed curve shows the prediction of Fletcher's theory on the assumption that the winding continued over the whole string length, while the solid lines take into account the effect of the short unwound section calculated from the frequency equation.

CHAPTER 7

SUMMARY AND CONCLUSIONS.

The work described in this thesis has been both theoretical and experimental. The objectives of the research programme have been achieved, with the development of an expression for the frequencies of vibration of a stepped overwound string and the confirmation of the theoretical results by experimental measurements of overwound strings with and without step on the monochord.

7.1 Conclusions.

The natural mode frequencies of piano strings are different from the harmonic series and the degree of inharmonicity has important relation for tone quality, tuning and the electronic synthesis of piano sounds. The stiffness of steel wire accounts almost entirely for the inharmonicity of the plain wire strings apart from effects due to the finite compliance of the supports. It has been shcwn, however that the string stiffness is not the only source of inharmonicity of the overwound piano strings. The effects of nonuniformity may contribute inharmonicity which cannot be explained by string stiffness alone.

The problem of the vibration of the nonuniform overwound stiff string has been treated in this thesis in a way which has not been described in other work. Fletcher proposed that his treatment of the plain string could be applied

to the overwound string by making the assumption that the overwinding increased only the linear mass density of the string. Discussions of the stepped string by Levinson, Sakata and Sakata and Gottlieb have not incorporated the stiffness of the stepped string.

In this thesis the derivation of the mode frequencies of the stepped string has been presented, taking into account the stiffness. We considered the vibration of the M-part string fixed at its ends and then applied this general theory to the specific case of the 2-segment string. The boundary conditions are for simple hinged supports.

The numerical calculations were undertaken to compute theoretical mode frequencies from the frequency equation for strings with varying degrees of overwinding. The theoretical results show that the inharmonicities of strings with the same core and overwinding diameters are decreased as the string length increases, in agreement with the predictions of more simple models. The inharmonicities for the stepped overwound strings are significantly higher than the inharmonicities for the uniformly overwound strings of the same length and the same core and overwinding diameters. The increase in inharmonicity is greatest for the string with the highest fraction of unwound length.

The experimental inharmonicities of overwound strings on the monochord have been measured, and compared with theoretical results. The rigid monochord has been designed in order to control the parameters and to reduce external effects disturbing the vibration of the strings. It is evident from the comparison that the theory presented here gives a better fit to measured inharmonicities than the analysis for the uniform overwound string by Fletcher. Apparently the stepped geometry of the overwound strings is significant.

Experimental and theoretical values of the inharmonicity coefficient B for each mode frequency of the uniformly and stepped overwound strings were derived, and compared with the constant inharmonicity coefficient B of

Fletcher's equation. It is clear that Fletcher's assumption that the inharmonicity coefficient B is independent of mode number for a given string is consistent with the present calculations for the uniform overwound string, although for the shorter strings our values of B are slightly higher than those of Fletcher. The experimental results agree well with our theoretical values. For stepped string the deviation of inharmonicity coefficient B from the constancy characteristic of uniformly wound strings increases as the fractional length of unwound string increases. For mode numbers greater than 10, theory and experiment are in good agreement; for lower mode numbers and relatively large unwound fractions, the measured inharmonicity coefficient is slightly higher than that predicted by theory.

The nonuniformity of the overwinding on the bass piano string, and the question of how it affects the inharmonicity of its mode frequencies, was the original motivation for this study. A series of measurements was performed on the bass strings of the Broadwood grand piano to examine the extent to which this work was relevant to the behaviour of overwound piano strings with the end support conditions typical of normal use. Our theory takes no account of any increase in inharmonicity due to the effect of the soundboard on the string. It is evident from the results that the major cause of the discrepancy between the Fletcher prediction and the measurement for the A0 string is indeed the non-uniformity of the winding. The present theory, which allows for the effect of non-uniformity, gives a much better agreement with the experimental results.

The present theory is closer to experiment than Fletcher, although for shortest string E1 the effect of non-uniformity is small.

The reason for discrepancies between theory and experiment is possibly the increase in string stiffness due to the overwinding, which would have the effect of increasing the inharmonicity. It should be noted that a discrepancy of comparable magnitude (about 10 cents for $n = 30$) was found for the strings on

the monochord. In addition, bass overwound piano strings often have more than 2 segments due to the double winding and the 2 cores left at the ends. The present theory can be readily extended to cover the case of the m-segment overwound stiff string by following Eqs.(2.33), (2.34) and (2.35) in chapter 2.

Actually, we should also keep in mind that the proper amount of inharmonicity in piano tone partials distributed in the frequency range of the piano enhances the tones and is not undesirable. However, The inharmonicity of the bass overwound strings on a grand piano is different from that on the small piano, upright piano. This study may suggest new manufacturing techniques for the bass overwound strings on the small piano in order to improve their tone quality.

The pitch glide effect in the low bass piano tones relies on the ability of the human hearing mechanism to detect frequency glides of short duration and indicates the complex ability of the ear-brain channel to discriminate between a range of sound stimuli requiring fast temporal pitch discrimination [86]. However, in order to obtain an assessment of the phenomenon, psycoacoustic evaluation of the respective presence and absence of the pitch-glide phenomenon would need to be observed during presentations of simulated inharmonic and harmonic tones to both musicians and non-musicians.

APPENDIX A

EXAMPLES FOR NUMERICAL CALCULATION

Examples of the application of the Mathematica FindRoot program to the frequency equation for the stepped overwound string, S1(1) and the uniformly overwound string, U1(1) are shown.

```
eqn = (u11[w]^2 + u22[w]^2)*
      (u12[w]^2 + u21[w]^2)*
      (u11[w]*Tanh[u21[w]*a2] +
       u21[w]*Tanh[u11[w]*a1])*
      (u12[w]*Tan[u22[w]*a2] +
       u22[w]*Tan[u12[w]*a1]) -
      (u11[w]^2 - u21[w]^2)*
      (u12[w]^2 - u22[w]^2)*
      (u11[w]*Tan[u22[w]*a2] +
       u22[w]*Tanh[u11[w]*a1])*
      (u12[w]*Tanh[u21[w]*a2] +
       u21[w]*Tan[u12[w]*a1]);

p1 = 7.85;

a1 = 0;

d1 = 0.135;

S1 = Pi*d1^2/4;

Q1 = 2.0*10^12;

p2 = 8.93;

a2 = 80.0;

d2 = 0.42;

S2 = Pi*d2^2/4;

k = d1/4;

d = (d2 - d1)/2;

dd = d + d1;

mass1 = Pi*d1^2*p1/4;

mass2 = mass1 + Pi^2*d*dd*p2/4;

f0 = 59.5;

T = 4*(a1+a2)^2*f0^2*mass2;

n = T;

P1 = mass1;

m = Q1*S1*k^2;

P2 = mass2;

u11[w] = Sqrt[Sqrt[n^2/((2*m)^2) +
         4*Pi^2*w^2*P1/m] + n/(2*m)];

u12[w] = Sqrt[Sqrt[n^2/((2*m)^2) +
         4*Pi^2*w^2*P1/m] - n/(2*m)];

u21[w] = Sqrt[Sqrt[n^2/((2*m)^2) +
         4*Pi^2*w^2*P2/m] + n/(2*m)];
```

```
u22[w] = Sqrt[Sqrt[n^2/((2*m)^2) +
          4*Pi^2*w^2*P2/m] - n/(2*m)];

FindRoot[eqn == 0, {w, 60}]

{w -> 59.5168}

FindRoot[eqn == 0, {w, 120}]

{w -> 119.134}

FindRoot[eqn == 0, {w, 180}]

{w -> 178.953}

FindRoot[eqn == 0, {w, 240}]

{w -> 239.072}

FindRoot[eqn == 0, {w, 302}]

{w -> 299.59}

FindRoot[eqn == 0, {w, 362}]

{w -> 360.606}

FindRoot[eqn == 0, {w, 424}]

{w -> 422.217}

FindRoot[eqn == 0, {w, 486}]

{w -> 484.516}

FindRoot[eqn == 0, {w, 550}]

{w -> 547.597}

FindRoot[eqn == 0, {w, 612}]

{w -> 611.551}

FindRoot[eqn == 0, {w, 675}]

{w -> 676.467}

FindRoot[eqn == 0, {w, 740}]

{w -> 742.432}

FindRoot[eqn == 0, {w, 808}]

{w -> 809.529}

FindRoot[eqn == 0, {w, 880}]

{w -> 877.84}

FindRoot[eqn == 0, {w, 945}]

{w -> 947.445}
```

```
FindRoot[eqn == 0, {w, 1015}]
{w -> 1018.42}
FindRoot[eqn == 0, {w, 1085}]
{w -> 1090.83}
FindRoot[eqn == 0, {w, 1160}]
{w -> 1164.76}
FindRoot[eqn == 0, {w, 1240}]
{w -> 1240.27}
FindRoot[eqn == 0, {w, 1320}]
{w -> 1317.43}
FindRoot[eqn == 0, {w, 1400}]
{w -> 1396.29}
FindRoot[eqn == 0, {w, 1482}]
{w -> 1476.92}
FindRoot[eqn == 0, {w, 1565}]
{w -> 1559.37}
FindRoot[eqn == 0, {w, 1650}]
{w -> 1643.69}
FindRoot[eqn == 0, {w, 1735}]
{w -> 1729.95}
FindRoot[eqn == 0, {w, 1820}]
{w -> 1818.18}
FindRoot[eqn == 0, {w, 1900}]
{w -> 1908.43}
FindRoot[eqn == 0, {w, 1990}]
{w -> 2000.75}
FindRoot[eqn == 0, {w, 2080}]
{w -> 2095.17}
FindRoot[eqn == 0, {w, 2173}]
{w -> 2191.75}
FindRoot[eqn == 0, {w, 2280}]
{w -> 2290.5}
```

```
FindRoot[eqn == 0, {w, 2380}]
{w -> 2391.48}
FindRoot[eqn == 0, {w, 2495}]
{w -> 2494.71}
FindRoot[eqn == 0, {w, 2600}]
{w -> 2600.22}
FindRoot[eqn == 0, {w, 2710}]
{w -> 2708.04}
FindRoot[eqn == 0, {w, 2810}]
{w -> 2818.2}
FindRoot[eqn == 0, {w, 2915}]
{w -> 2930.73}
FindRoot[eqn == 0, {w, 3045}]
{w -> 3045.66}
FindRoot[eqn == 0, {w, 3165}]
{w -> 3163.}
FindRoot[eqn == 0, {w, 3290}]
{w -> 3282.77}
FindRoot[eqn == 0, {w, 3420}]
{w -> 3405.}
FindRoot[eqn == 0, {w, 3550}]
{w -> 3529.72}
```

```
eqn = (u11[w]^2 + u22[w]^2)*
      (u12[w]^2 + u21[w]^2)*
      (u11[w]*Tanh[u21[w]*a2] +
       u21[w]*Tanh[u11[w]*a1])*
      (u12[w]*Tan[u22[w]*a2] +
       u22[w]*Tan[u12[w]*a1]) -
      (u11[w]^2 - u21[w]^2)*
      (u12[w]^2 - u22[w]^2)*
      (u11[w]*Tan[u22[w]*a2] +
       u22[w]*Tanh[u11[w]*a1])*
      (u12[w]*Tanh[u21[w]*a2] +
       u21[w]*Tan[u12[w]*a1]);

p1 = 7.85;

a1 = 5.0;

d1 = 0.135;

S1 = Pi*d1^2/4;

Q1 = 2.0*10^12;

p2 = 8.93;

a2 = 75.0;

d2 = 0.42;

S2 = Pi*d2^2/4;

k = d1/4;

d = (d2 - d1)/2;

dd = d + d1;

mass1 = Pi*d1^2*p1/4;

mass2 = mass1 + Pi^2*d*dd*p2/4;

f0 = 59.58;

T = 4*(a1+a2)^2*f0^2*mass2;

n = T;

P2 = mass2;

m = Q1*S1*k^2;

P1 = mass1;

u11[w] = Sqrt[Sqrt[n^2/((2*m)^2) +
          4*Pi^2*w^2*P1/m] + n/(2*m)];

u12[w] = Sqrt[Sqrt[n^2/((2*m)^2) +
          4*Pi^2*w^2*P1/m] - n/(2*m)];

u21[w] = Sqrt[Sqrt[n^2/((2*m)^2) +
          4*Pi^2*w^2*P2/m] + n/(2*m)];

u22[w] = Sqrt[Sqrt[n^2/((2*m)^2) +
          4*Pi^2*w^2*P2/m] - n/(2*m)];
```

```
FindRoot[eqn == 0, {w, 60}]
{w -> 59.6384}
FindRoot[eqn == 0, {w, 120}]
{w -> 119.61}
FindRoot[eqn == 0, {w, 180}]
{w -> 180.177}
FindRoot[eqn == 0, {w, 242}]
{w -> 241.508}
FindRoot[eqn == 0, {w, 304}]
{w -> 303.698}
FindRoot[eqn == 0, {w, 367}]
{w -> 366.806}
FindRoot[eqn == 0, {w, 432}]
{w -> 430.88}
FindRoot[eqn == 0, {w, 498}]
{w -> 495.97}
FindRoot[eqn == 0, {w, 565}]
{w -> 562.135}
FindRoot[eqn == 0, {w, 632}]
{w -> 629.441}
FindRoot[eqn == 0, {w, 703}]
{w -> 697.957}
FindRoot[eqn == 0, {w, 775}]
{w -> 767.76}
FindRoot[eqn == 0, {w, 835}]
{w -> 838.928}
FindRoot[eqn == 0, {w, 910}]
{w -> 911.536}
FindRoot[eqn == 0, {w, 985}]
{w -> 985.664}
FindRoot[eqn == 0, {w, 1060}]
{w -> 1061.39}
FindRoot[eqn == 0, {w, 1138}]
{w -> 1138.78}
```

```
FindRoot[eqn == 0, {w, 1217}]
{w -> 1217.91}
FindRoot[eqn == 0, {w, 1297}]
{w -> 1061.39}
FindRoot[eqn == 0, {w, 1380}]
{w -> 1381.64}
FindRoot[eqn == 0, {w, 1465}]
{w -> 1466.37}
FindRoot[eqn == 0, {w, 1551}]
{w -> 1553.07}
FindRoot[eqn == 0, {w, 1641}]
{w -> 1641.81}
FindRoot[eqn == 0, {w, 1731}]
{w -> 1732.6}
FindRoot[eqn == 0, {w, 1824}]
{w -> 1825.49}
FindRoot[eqn == 0, {w, 1926}]
{w -> 1920.5}
FindRoot[eqn == 0, {w, 2016}]
{w -> 2017.63}
FindRoot[eqn == 0, {w, 2116}]
{w -> 2116.87}
FindRoot[eqn == 0, {w, 2216}]
{w -> 2218.19}
FindRoot[eqn == 0, {w, 2317}]
{w -> 2321.54}
FindRoot[eqn == 0, {w, 2418}]
{w -> 2426.81}
FindRoot[eqn == 0, {w, 2530}]
{w -> 2533.85}
FindRoot[eqn == 0, {w, 2637}]
{w -> 2642.47}
FindRoot[eqn == 0, {w, 2753}]
{w -> 2752.46}
```

```
FindRoot[eqn == 0, {w, 2865}]
{w -> 2863.64}
FindRoot[eqn == 0, {w, 2980}]
{w -> 2976.07}
FindRoot[eqn == 0, {w, 3085}]
{w -> 3090.15}
FindRoot[eqn == 0, {w, 3198}]
{w -> 3206.63}
FindRoot[eqn == 0, {w, 3313}]
{w -> 3326.27}
FindRoot[eqn == 0, {w, 3437}]
{w -> 3449.57}
FindRoot[eqn == 0, {w, 3560}]
{w -> 3576.69}
```

APPENDIX B

THEORETICAL MODE FREQUENCIES

In this Appendix the theoretical mode frequencies obtained by numerical solution of the frequency equation are tabulated. Table B-1 shows the theoretical mode frequencies of the uniformly overwound strings, U1(1), U1(2), U1(3), U1(4), U1(5) and U1(6). Table B-2 shows the theoretical mode frequencies of the uniformly overwound strings, U2(1), U2(2), U2(3), U2(4), U2(5) and U2(6). Table B-3 shows the theoretical mode frequencies of the uniformly overwound strings, U3(1), U3(2), U3(3), U3(4), U3(5) and U3(6). Table B-4 shows the theoretical mode frequencies of the stepped overwound strings, S1(1), S1(2), S1(3), S1(4), S1(5) and S1(6). Table B-5 shows the theoretical mode frequencies of the stepped overwound strings, S2(1), S2(2), S2(3), S2(4), S2(5) and S2(6). And Table B-6 shows the theoretical mode frequencies of the stepped overwound strings, S3(1), S3(2), S3(3), S3(4), S3(5) and S3(6). Details of the string dimensions see Table 3.1 and 3.2 in chapter 3.

Table B-1 The theoretical mode frequencies for the uniformly overwound strings, U1(1), U1(2), U1(3), U1(4), U1(5) and U1(6).

Mode number	Mode frequencies					
(n)	U1(1)	U1(2)	U1(3)	U1(4)	U1(5)	U1(6)
1	59.52	44.61	35.90	29.35	25.40	21.36
2	119.13	89.26	71.83	58.72	50.81	42.73
3	178.95	134.00	107.81	88.12	76.24	64.11
4	239.07	178.88	143.86	117.55	101.70	85.51
5	299.59	223.94	180.00	147.05	127.19	106.94
6	360.61	269.23	216.26	176.62	152.73	128.39
7	422.22	314.78	252.66	206.28	178.33	149.89
8	484.52	360.64	289.24	236.03	203.98	171.43
9	547.60	406.86	326.00	265.90	229.72	193.03
10	611.55	453.48	362.97	295.90	255.53	214.68
11	676.47	500.54	400.17	326.05	281.43	236.40
12	742.43	548.08	437.64	356.35	307.44	258.19
13	809.53	596.14	475.38	386.82	333.55	280.05
14	877.84	644.77	513.43	417.47	359.78	302.00
15	947.45	693.99	551.80	448.33	386.14	324.04
16	1018.42	743.86	590.51	479.39	412.64	346.17
17	1090.83	794.40	629.59	510.67	439.27	368.41
18	1164.76	845.65	669.06	542.20	466.06	390.75
19	1240.27	897.66	708.93	574.00	493.01	413.21
20	1317.43	950.44	749.23	606.01	520.13	435.79
21	1396.29	1004.04	789.98	638.32	547.42	458.49
22	1476.92	1058.49	831.19	670.91	574.90	481.33
23	1559.37	1113.81	872.88	703.81	602.57	504.30
24	1643.69	1170.05	915.08	737.08	630.45	527.41
25	1729.95	1227.23	957.80	770.55	658.53	550.68
26	1818.18	1285.37	1001.05	804.41	686.83	574.10
27	1908.43	1344.51	1044.86	838.62	715.40	597.68
28	2000.75	1404.68	1089.25	873.19	744.11	621.42
29	2095.17	1465.89	1134.22	908.12	773.10	645.38
30	2191.75	1528.17	1179.79	943.43	802.36	669.43

Table B-2 The theoretical mode frequencies for the uniformly overwound strings, U2(1), U2(2), U2(3), U2(4), U2(5) and U2(6).

Mode number	Mode frequencies					
(n)	U2(1)	U2(2)	U2(3)	U2(4)	U2(5)	U2(6)
1	56.76	42.57	34.22	27.95	24.19	20.34
2	113.63	85.19	68.48	55.92	48.39	40.69
3	170.72	127.90	102.78	83.92	72.62	61.05
4	228.14	170.77	137.16	111.97	96.87	81.44
5	286.00	213.83	171.65	140.08	121.16	101.85
6	344.41	257.15	206.27	168.27	145.51	122.30
7	403.46	300.75	241.04	196.56	169.91	142.79
8	463.28	344.86	276.00	224.96	194.38	163.33
9	523.95	389.04	311.17	253.48	218.94	183.93
10	585.58	433.82	346.56	282.15	243.58	204.59
11	648.25	479.08	382.22	310.97	268.33	225.33
12	712.08	524.86	418.16	339.96	293.19	246.14
13	777.13	571.22	454.41	369.15	318.16	267.03
14	843.51	618.19	490.98	398.53	343.27	288.02
15	911.30	665.81	527.91	428.13	368.51	309.11
16	980.56	714.13	565.22	457.97	393.90	330.30
17	1051.40	763.19	602.93	488.05	419.45	351.60
18	1123.87	813.02	641.06	518.38	445.17	373.02
19	1198.04	863.67	679.63	548.99	417.06	394.57
20	1273.99	915.16	718.67	579.89	497.14	416.25
21	1351.78	967.54	758.20	611.09	523.41	438.06
22	1431.47	1020.84	798.23	642.60	549.88	460.03
23	1513.11	1075.09	838.79	674.44	576.57	482.14
24	1596.76	1130.32	879.89	706.62	603.47	504.41
25	1682.47	1186.56	921.61	739.15	630.60	526.84
26	1770.29	1243.85	963.81	772.04	657.97	549.44
27	1860.27	1302.22	1006.67	805.31	685.61	572.21
28	1952.45	1361.67	1050.14	838.95	713.46	595.17
29	2046.87	1422.25	1094.25	873.02	741.58	618.33
30	2143.56	1483.32	1139.01	907.49	769.98	641.65

Table B-3 The theoretical mode frequencies for the uniformly overwound strings, U3(1), U3(2), U3(3), U3(4), U3(5) and U3(6).

Mode number	Mode frequencies					
(n)	U3(1)	U3(2)	U3(3)	U3(4)	U3(5)	U3(6)
1	53.49	40.11	32.25	26.34	22.79	19.17
2	107.10	80.27	64.54	52.70	45.59	38.35
3	160.95	120.54	96.88	79.10	68.42	57.55
4	215.16	160.98	129.30	105.55	91.28	76.76
5	269.84	201.62	161.84	132.06	114.18	96.01
6	325.12	242.54	194.53	158.66	137.14	115.30
7	381.10	283.77	227.38	185.38	160.16	134.63
8	437.90	325.38	260.43	212.19	183.26	154.02
9	495.62	367.40	293.70	239.16	206.44	173.47
10	554.37	409.90	327.23	266.27	229.73	192.99
11	614.26	452.92	361.03	293.56	253.13	212.59
12	675.37	496.51	395.15	321.03	276.63	232.27
13	737.81	540.72	429.56	348.70	300.27	252.04
14	801.67	585.62	464.39	376.60	324.05	271.91
15	867.03	631.15	499.61	404.72	347.98	291.89
16	934.00	677.47	535.16	433.10	372.08	311.98
17	1002.59	724.59	571.17	461.74	396.34	332.20
18	1072.95	772.52	607.65	490.66	420.78	352.54
19	1145.12	821.32	644.61	519.88	445.41	373.01
20	1219.18	871.04	682.04	549.66	470.24	393.63
21	1295.18	921.70	720.01	579.25	495.28	414.40
22	1373.18	973.34	758.53	609.43	520.54	435.32
23	1453.25	1025.99	797.60	639.97	546.04	456.41
24	1535.44	1079.69	837.26	670.87	571.75	477.66
25	1619.80	1134.46	877.53	702.15	597.73	499.09
26	1706.37	1190.34	918.41	733.81	623.94	520.70
27	1795.20	1247.36	959.94	765.88	650.43	542.50
28	1886.34	1305.53	1002.12	798.36	677.18	564.49
29	1979.82	1364.89	1044.99	831.27	704.22	586.69
30	2075.67	1425.47	1088.54	864.61	731.54	609.09

Table B-4 The theoretical mode frequencies for the stepped overwound strings, S1(1), S1(2), S1(3), S1(4), S1(5) and S1(6).

Mode number	Mode frequencies					
(n)	S1(1)	S1(2)	S1(3)	S1(4)	S1(5)	S1(6)
1	59.64	44.71	35.91	29.36	25.40	21.36
2	119.61	89.55	71.88	58.74	50.82	42.74
3	180.18	134.62	107.96	88.19	76.28	64.13
4	241.51	180.01	144.20	117.72	101.79	85.56
5	303.70	225.78	180.63	147.37	127.37	107.04
6	366.81	271.98	217.29	177.15	153.03	128.57
7	430.88	318.63	254.19	207.07	178.79	150.16
8	495.97	365.77	291.37	237.15	204.64	171.83
9	562.14	413.43	328.82	267.41	230.61	193.56
10	629.44	461.62	366.58	297.85	256.70	215.39
11	697.96	510.38	404.65	328.49	282.91	237.30
12	767.76	559.75	443.05	359.34	309.26	259.30
13	838.93	609.75	481.81	390.40	335.75	281.41
14	911.54	660.42	520.93	421.69	362.39	303.62
15	985.66	711.80	560.44	453.21	389.19	325.94
16	1061.39	763.91	600.35	484.99	416.15	348.38
17	1138.78	816.81	640.68	517.03	443.27	370.94
18	1217.91	870.51	681.45	549.34	470.58	393.63
19	1298.94	925.06	722.69	581.93	498.07	416.45
20	1381.64	980.48	764.40	614.78	525.75	439.40
21	1466.37	1036.83	806.61	648.02	553.63	462.50
22	1553.07	1094.11	849.34	681.53	581.72	485.74
23	1641.81	1152.38	892.61	715.38	610.03	509.14
24	1732.60	1211.65	936.43	749.57	638.55	532.69
25	1825.49	1271.98	980.82	784.11	667.30	556.41
26	1920.50	1333.68	1025.80	819.01	696.29	580.30
27	2017.63	1395.81	1071.39	854.30	725.53	604.36
28	2116.87	1459.39	1117.60	889.96	755.01	628.60
29	2218.19	1524.12	1164.45	926.03	784.76	653.02
30	2321.54	1590.00	1211.95	962.50	814.77	677.64

Table B-5 The theoretical mode frequencies for the stepped overwound strings, S2(1), S2(2), S2(3), S2(4), S2(5) and S2(6).

Mode number	Mode frequencies					
(n)	S2(1)	S2(2)	S2(3)	S2(4)	S2(5)	S2(6)
1	56.80	42.58	34.23	27.96	24.19	20.34
2	113.93	85.29	68.52	55.94	48.41	40.70
3	171.66	128.23	102.92	83.99	72.66	61.07
4	230.16	171.51	137.49	112.13	96.96	81.49
5	289.55	215.17	172.25	140.39	121.33	101.95
6	349.89	259.27	207.25	168.78	145.79	122.47
7	411.25	303.85	242.51	197.32	170.35	143.05
8	473.68	348.94	278.04	226.03	195.01	163.70
9	537.26	394.57	313.87	254.92	219.79	184.44
10	602.07	440.78	350.03	284.01	244.70	205.27
11	668.19	487.61	386.52	313.31	269.74	226.21
12	735.69	535.24	423.36	342.83	294.93	247.20
13	804.67	585.24	460.58	372.58	320.27	268.33
14	875.22	632.12	498.20	402.58	345.77	289.57
15	947.40	681.77	536.24	432.83	371.43	310.93
16	1021.31	732.21	574.71	463.36	397.27	332.42
17	1097.03	783.50	613.64	494.16	423.30	354.03
18	1174.62	835.67	653.04	525.26	449.51	375.79
19	1254.16	888.76	692.95	556.67	475.93	397.68
20	1335.71	942.79	733.37	588.40	502.55	419.72
21	1419.33	997.82	774.34	620.47	529.39	441.92
22	1505.07	1053.87	815.87	652.88	556.46	464.28
23	1592.99	1110.97	857.98	685.64	583.76	486.80
24	1683.11	1169.17	900.69	718.78	611.30	509.49
25	1775.83	1228.48	944.01	752.31	639.09	532.37
26	1870.10	1288.87	987.98	786.23	667.13	555.42
27	1966.98	1350.57	1032.60	820.55	695.44	578.67
28	2066.11	1413.40	1077.89	855.30	724.03	602.11
29	2167.45	1477.46	1123.88	890.09	752.89	625.75
30	2270.93	1542.76	1170.57	926.09	782.04	649.69

Table B-6 The theoretical mode frequencies for the stepped overwound strings, S3(1), S3(2), S3(3), S3(4), S3(5) and S3(6).

Mode number	Mode frequencies					
(n)	S3(1)	S3(2)	S3(3)	S3(4)	S3(5)	S3(6)
1	53.53	40.12	32.26	26.35	22.79	19.17
2	107.39	80.37	64.58	52.72	45.61	38.36
3	161.84	120.86	97.02	79.17	68.46	57.57
4	217.08	161.67	129.62	105.70	91.36	76.81
5	273.22	202.89	162.42	132.35	114.34	96.11
6	330.33	244.55	195.46	159.14	137.41	115.46
7	388.51	286.71	228.77	186.09	160.58	134.88
8	447.81	329.40	262.28	213.21	183.85	154.38
9	508.33	372.67	296.28	240.52	207.25	173.96
10	570.15	416.54	330.52	268.04	230.79	193.63
11	633.36	461.06	365.12	295.78	254.46	213.40
12	698.05	506.27	400.10	323.75	278.29	233.28
13	764.32	552.21	435.48	351.97	302.27	253.28
14	832.25	598.93	471.28	380.45	326.43	273.39
15	901.93	646.46	507.52	409.20	350.76	293.63
16	973.45	694.84	544.23	438.24	375.28	314.00
17	1046.88	744.13	581.43	467.58	400.00	334.51
18	1122.32	794.35	619.14	497.24	424.92	355.17
19	1199.81	845.55	657.38	527.23	450.06	375.98
20	1279.44	897.76	696.18	557.55	475.42	396.95
21	1361.27	951.03	735.56	588.24	501.01	418.08
22	1445.33	1005.39	775.53	619.30	526.83	439.38
23	1531.69	1060.87	816.13	650.74	552.91	460.86
24	1620.38	1117.51	857.36	682.57	579.25	482.53
25	1711.43	1175.33	899.26	714.82	605.85	504.38
26	1804.86	1234.39	941.83	747.49	632.73	526.43
27	1900.67	1294.65	985.10	780.59	659.89	548.69
28	1998.85	1356.65	1029.09	814.14	687.35	571.15
29	2099.35	1419.04	1073.81	848.15	715.10	593.83
30	2202.11	1483.19	1119.28	882.64	743.17	616.73

APPENDIX C

THEORETICAL INHARMONICITY

In this Appendix, theoretical values of inharmonicity calculated from the mode frequencies in Appendix B are tabulated. Table C-1 shows the theoretical inharmonicity for the uniformly overwound strings, U1(1), U1(2), U1(3), U1(4), U1(5) and U1(6). Table C-2 shows the theoretical inharmonicity for the uniformly overwound strings, U2(1), U2(2), U2(3), U2(4), U2(5) and U2(6). Table C-3 shows the theoretical inharmonicity for the uniformly overwound strings, U3(1), U3(2), U3(3), U3(4), U3(5) and U3(6). Table C-4 shows the theoretical inharmonicity for the stepped overwound strings, S1(1), S1(2), S1(3), S1(4), S1(5) and S1(6). Table C-5 shows the theoretical inharmonicity for the stepped overwound strings, S2(1), S2(2), S2(3), S2(4), S2(5) and S2(6). And Table C-6 shows the theoretical inharmonicity for the stepped overwound strings, S3(1), S3(2), S3(3), S3(4), S3(5) and S3(6). For details of the string dimensions see Table 3.1 and 3.2 in chapter 3.

Table.C-1 The theoretical inharmonicity in cents for the six uniformly overwound strings, U1(1), U1(2), U1(3), U1(4), U1(5) and U1(6).

Mode number	U1(1)	U1(2)	Inharmonicity in cents U1(3)	U1(4)	U1(5)	U1(6)
1	0	0	0	0	0	0
2	2	1	1	1	0	0
3	4	3	2	1	1	1
4	8	5	3	2	2	1
5	12	7	5	4	3	2
6	17	10	7	5	4	3
7	23	14	9	7	5	4
8	31	19	12	9	7	6
9	39	23	15	11	8	7
10	48	29	19	14	10	9
11	57	35	23	17	13	11
12	68	41	27	20	15	13
13	79	48	32	24	17	15
14	91	56	37	27	20	17
15	103	64	42	31	23	20
16	117	72	48	36	26	22
17	131	81	52	40	30	25
18	145	90	60	45	33	28
19	160	100	67	50	37	31
20	176	110	74	55	41	34
21	192	120	81	61	45	38
22	209	131	88	66	49	42
23	226	142	96	72	54	45
24	244	154	104	79	58	49
25	261	166	113	85	63	53
26	280	178	121	91	68	57
27	298	191	130	98	73	62
28	317	204	139	105	78	66
29	336	217	148	112	84	71
30	355	230	158	120	89	76

Table.C-2 The theoretical inharmonicity in cents for the six uniformly overwound strings, U2(1), U2(2), U2(3), U2(4), U2(5) and U2(6).

Mode number	Inharmonicity in cents					
	U2(1)	U2(2)	U2(3)	U2(4)	U2(5)	U2(6)
1	1	0	0	0	0	0
2	2	1	1	1	0	0
3	5	3	2	1	1	1
4	9	5	4	3	2	2
5	14	8	6	4	3	3
6	20	12	8	6	4	4
7	27	16	11	8	6	5
8	35	22	14	10	8	6
9	44	27	18	13	10	8
10	55	33	22	16	12	10
11	66	40	26	20	15	12
12	78	47	31	23	17	15
13	90	55	37	24	20	17
14	104	64	42	32	23	20
15	118	73	49	36	27	23
16	133	82	55	41	30	26
17	149	92	62	46	34	29
18	166	103	69	52	38	32
19	183	114	77	58	43	36
20	200	125	85	64	47	40
21	218	137	93	70	52	44
22	237	150	101	76	57	48
23	256	162	110	83	62	52
24	276	175	119	90	67	57
25	295	189	129	97	72	61
26	316	202	138	105	78	66
27	336	217	148	112	84	71
28	357	231	159	120	90	76
29	378	245	169	129	96	82
30	399	260	180	137	103	87

Table.C-3 The theoretical inharmonicity in cents for the six uniformly overwound strings, U3(1), U3(2), U3(3), U3(4), U3(5) and U3(6).

Mode number	Inharmonicity in cents					
	U3(1)	U3(2)	U3(3)	U3(4)	U3(5)	U3(6)
1	1	0	0	0	0	0
2	3	2	1	1	1	0
3	6	3	2	2	1	1
4	10	6	4	3	2	2
5	16	10	6	5	3	3
6	23	14	9	7	5	4
7	31	19	12	9	7	6
8	41	25	16	12	9	7
9	51	31	20	15	11	9
10	63	38	25	19	14	12
11	75	46	30	23	17	14
12	89	54	36	27	20	17
13	103	63	42	31	23	20
14	119	73	49	36	27	23
15	135	83	56	42	31	26
16	152	94	63	47	35	29
17	170	106	71	53	39	33
18	188	118	79	59	44	37
19	207	130	88	66	49	41
20	227	143	97	73	54	46
21	247	156	106	80	59	50
22	268	170	116	87	65	55
23	289	184	126	95	71	60
24	311	199	136	103	77	65
25	332	214	147	111	83	70
26	346	229	158	120	89	76
27	377	245	169	128	96	81
28	400	261	180	137	103	87
29	423	277	192	146	110	93
30	446	294	204	156	117	99

Table.C-4 The theoretical inharmonicity in cents for the six stepped overwound strings, S1(1), S1(2), S1(3), S1(4), S1(5) and S1(6).

Mode number	S1(1)	S1(2)	Inharmonicity in cents S1(3)	S1(4)	S1(5)	S1(6)
1	2	1	1	0	0	0
2	7	3	2	1	1	1
3	14	7	4	3	2	1
4	23	12	7	5	3	3
5	33	18	11	7	5	4
6	45	25	15	10	7	6
7	56	32	20	14	10	7
8	69	40	25	17	12	10
9	82	48	30	21	15	12
10	95	56	36	25	18	14
11	109	65	42	30	22	17
12	123	74	49	35	25	20
13	138	84	55	40	29	23
14	154	94	62	45	33	26
15	170	104	69	50	37	30
16	186	114	76	56	41	33
17	202	125	84	62	45	37
18	220	137	92	68	50	41
19	238	148	100	74	55	45
20	256	160	108	80	59	49
21	275	173	117	87	64	53
22	294	185	126	94	70	57
23	313	198	135	100	75	62
24	332	211	144	108	80	66
25	352	225	154	115	86	71
26	372	239	163	122	92	76
27	392	252	173	130	97	81
28	412	266	183	138	103	86
29	432	281	194	146	110	91
30	453	295	204	154	116	97

Table.C-5 The theoretical inharmonicity in cents for the six stepped overwound strings, S2(1), S2(2), S2(3), S2(4), S2(5) and S2(6).

Mode number	S2(1)	S2(2)	Inharmonicity in cents S2(3)	S2(4)	S2(5)	S2(6)
1	2	1	1	0	0	0
2	7	3	3	1	1	1
3	15	7	5	3	2	2
4	24	13	9	5	4	3
5	35	19	13	8	5	4
6	47	26	17	11	8	6
7	60	34	22	15	10	8
8	74	42	28	19	13	10
9	88	51	34	23	16	13
10	103	61	40	28	20	16
11	118	70	47	33	24	19
12	134	81	54	38	28	22
13	151	91	60	43	32	25
14	168	102	69	49	36	29
15	186	114	77	55	40	33
16	204	126	85	61	45	37
17	223	138	93	68	50	41
18	242	151	102	75	55	45
19	262	164	111	82	60	50
20	282	177	121	89	66	54
21	303	191	130	96	71	59
22	324	205	140	104	77	64
23	345	210	150	112	83	69
24	367	234	161	120	89	74
25	389	249	171	128	96	79
26	411	264	182	136	102	85
27	433	280	193	145	109	91
28	455	295	205	154	115	96
29	477	311	216	163	122	102
30	499	328	228	172	129	109

Table.C-6 The theoretical inharmonicity in cents for the six stepped overwound strings, S3(1), S3(2), S3(3), S3(4), S3(5) and S3(6).

Mode number	S3(1)	S3(2)	Inharmonicity S3(3)	in cents S3(4)	S3(5)	S3(6)
1	2	1	1	0	0	0
2	7	4	2	1	1	1
3	15	8	5	3	2	2
4	26	14	8	6	4	3
5	38	20	12	9	6	5
6	51	28	17	12	8	7
7	65	37	23	16	11	9
8	79	46	29	20	14	11
9	95	56	36	25	18	14
10	111	66	43	30	22	17
11	128	77	50	36	26	21
12	146	88	58	42	30	24
13	164	100	66	48	35	28
14	183	112	74	54	40	32
15	203	125	83	61	45	36
16	224	138	92	68	50	41
17	244	152	102	75	55	45
18	266	166	112	82	61	50
19	288	180	122	90	67	55
20	310	195	132	98	73	60
21	333	211	143	107	79	65
22	356	226	154	115	86	71
23	380	242	165	124	92	77
24	404	259	177	133	99	82
25	428	275	189	142	106	88
26	452	292	201	152	114	95
27	476	309	214	161	121	101
28	500	328	226	171	129	108
29	524	345	236	181	136	114
30	549	362	252	192	144	121

APPENDIX D

EXPERIMENTAL MODE FREQUENCIES

Table D-1 shows the experimental mode frequencies of the uniformly overwound strings, U1(1), U1(2), U1(3), U1(4), U1(5) and U1(6). Table D-2 shows the experimental mode frequencies of the uniformly overwound strings, U2(1), U2(2), U2(3), U2(4), U2(5) and U2(6). Table D-3 shows the experimental mode frequencies of the uniformly overwound strings, U3(1), U3(2), U3(3), U3(4), U3(5) and U3(6). Table D-4 shows the experimental mode frequencies of the stepped overwound strings, S1(1), S1(2), S1(3), S1(4), S1(5) and S1(6). Table D-5 shows the experimental mode frequencies of the stepped overwound strings, S2(1), S2(2), S2(3), S2(4), S2(5) and S2(6). And Table D-6 shows the experimental mode frequencies of the stepped overwound strings, S3(1), S3(2), S3(3), S3(4), S3(5) and S3(6). Details of the string dimensions see Table 3.1 and 3.2 in chapter 3.

Table D-1 The experimental mode frequencies for the uniformly overwound strings, U1(1), U1(2), U1(3), U1(4), U1(5) and U1(6).

Mode number	Mode frequencies					
(n)	U1(1)	U1(2)	U1(3)	U1(4)	U1(5)	U1(6)
1	59.52	44.61	35.90	29.35	25.40	21.36
2	119.14	89.27	71.84	58.73	50.82	
3	178.99	134.03	107.82	88.12		64.11
4	239.12	178.90		117.59	101.71	85.52
5		224.02	180.08		127.23	
6	360.73		216.37	176.72		128.37
7	422.38	314.93		206.23	178.37	149.89
8	484.73	360.84	289.43		204.14	
9	547.87		326.24	266.13	229.86	193.10
10		453.79	363.27	296.11	255.74	214.68
11	676.87	500.91		326.22		
12	742.92		438.08		307.78	258.48
13		596.66	475.90	387.33	334.07	280.40
14	878.50			418.07	360.38	
15		694.68	552.49	449.02	386.83	324.50
16	1019.28	744.64				346.70
17	1091.80	795.29	630.48	511.56	440.16	
18	1165.85		670.05	543.19	467.05	391.42
19	1241.49	898.76	710.04		494.11	413.95
20		951.66	750.45	607.23	521.35	
21	1397.78	1005.39		639.67		459.40
22	1478.55		832.67	672.39	576.38	482.32
23	1561.15	1115.43	874.50	705.43	604.19	505.39
24	1645.63		916.84		632.21	528.63
25		1229.14		772.46	660.44	
26	1820.46	1287.44	1003.12	806.48		575.49
27	1910.88	1346.74	1047.09			599.18
28	2003.39	1407.08		875.59	746.51	623.04
29	2098.00	1468.46	1136.79	910.70	775..68	
30	2194.78	1530.93	1182.55	946.19		671.29

Table D-2 The experimental mode frequencies for the uniformly overwound strings, U2(1), U2(2), U2(3), U2(4), U2(5) and U2(6).

Mode number	Mode frequencies					
(n)	U2(1)	U2(2)	U2(3)	U2(4)	U2(5)	U2(6)
1	56.76	42.57	34.23	27.96	24.20	20.35
2	113.62	85.18	68.47	55.92	48.39	40.69
3	170.71	127.90		83.92		61.05
4			137.16	111.97	96.86	81.43
5	285.98	213.82	171.64		121.15	
6	344.39	257.13	206.25	168.26	145.50	122.29
7						
8	463.24		275.98	224.94	194.37	163.32
9	523.90	389.01	311.14	253.46	218.92	183.91
10	585.52		346.53	282.12	243.56	204.57
11		479.02	382.18	310.94		
12	711.98	524.80			293.15	246.11
13	777.04	571.14	454.35	369.10	318.12	266.99
14						
15	911.18	665.72	527.84	428.07	368.46	309.06
16		714.03	565.13	457.90	393.84	330.25
17	1051.25		602.83		419.38	351.54
18	1123.70	812.89	640.95	518.29	445.09	372.96
19	1197.86	863.52		548.89		
20	1273.79	915.00	718.54	579.78	497.04	416.17
21						
22	1431.23	1020.65	798.07	642.47	549.77	459.93
23	1512.85	1074.88		674.30	576.44	482.03
24	1596.48		879.71			504.29
25		1186.32		738.98	630.46	
26	1769.97	1243.59	963.60	771.86	657.82	549.31
27	1859.93		1006.44	805.12		572.07
28						
29	2046.49	1421.94	1093.99	872.80	741.39	
30	2143.15	1482.99	1138.73	907.26	769.77	641.47

Table D-3 The experimental mode frequencies for the uniformly overwound strings, U3(1), U3(2), U3(3), U3(4), U3(5) and U3(6).

Mode number	Mode frequencies					
(n)	U3(1)	U3(?)	U3(3)	U3(4)	U3(5)	U3(6)
1	53.49	40.11	32.26	26.34	22.79	19.17
2	107.11		64.54	52.72	45.60	38.35
3	160.96	120.56	96.89	79.12		57.55
4	215.18	161.00			91.29	76.76
5	269.88		161.87	132.09	114.20	
6		242.58	194.56	158.70	137.17	115.30
7	381.16	283.82				134.63
8	437.96	325.45	260.49	212.26	183.32	154.02
9		367.48	293.78	239.24	206.52	173.47
10	554.47				229.83	
11	614.38	453.04	361.16	293.68		212.59
12		496.66		321.17	276.78	
13	738.49	541.39	430.26		300.95	252.16
14	802.45		465.17	377.38		272.08
15	867.93	632.05		405.62	348.88	292.12
16		678.49	536.18	434.12	373.10	
17	1003.75		572.33			332.55
18		773.81	608.94	491.96	422.08	352.97
19	1146.56	822.77			446.86	373.53
20	1220.78		683.64	551.00		
21		923.47	721.78		497.05	415.09
22	1375.12	975.28		611.37	522.48	436.11
23	1455.37	1028.11	799.72	642.09		457.30
24		1081.99	839.57	673.17	574.05	
25	1622.30		880.03			500.21
26	1709.07	1193.04	921.12	736.52	626.65	521.95
27	1798.12	1250.28		768.80	653.34	543.88
28		1308.67	1005.26		680.32	
29	1983.18	1368.25	1048.35	834.63	707.58	588.34
30	2079.27	1429.07	1092.14	868.21	735.14	610.89

Table D-4 The experimental mode frequencies for the stepped overwound strings, S1(1), S1(2), S1(3), S1(4), S1(5) and S1(6).

Mode number	Mode frequencies					
(n)	S1(1)	S1(2)	S1(3)	S1(4)	S1(5)	S1(6)
1	59.58	44.69	35.89	29.35	25.40	21.36
2	119.35		72.05	58.74	50.82	42.73
3	179.30	134.51	108.04	88.18		
4	240.96	179.44	144.08	117.71	101.78	85.56
5	301.87	225.59	180.80		127.35	107.04
6		271.00	217.28	177.11	153.00	128.58
7	428.40	318.37	254.18	207.02		
8	492.93		291.57		204.59	171.87
9	559.41	413.11	329.08	267.33	230.54	193.64
10	626.61		366.99	297.75	256.61	
11	694.68	509.95	405.03		282.80	237.46
12	765.07		443.34	359.19		259.52
13	836.51	609.64	482.04	390.23	335.59	
14	909.01	661.05	521.66	422.51	363.23	303.87
15	984.35	712.59	560.35	454.23		326.25
16	1059.81		601.17		417.39	348.76
17	1137.88	817.92		518.50	444.77	371.39
18			682.45	551.09	472.35	394.16
19	1299.83	926.75		583.99	500.15	
20	1383.24		766.08			440.15
21	1469.72	1039.76		650.80	556.43	463.36
22	1556.96	1096.82	852.46	684.73	584.94	486.74
23	1646.37	1155.31		719.03		
24		1215.34	939.31		642.72	534.01
25	1828.93			788.80	672.02	
26	1924.42	1338.94	1029.61	824.29	701.59	582.00
27		1402.43	1075.84	860.20	731.46	606.28
28	2121.89	1466.35	1122.35			630.75
29	2223.83		1170.10	933.35	792.10	
30	2327.84	1599.78	1218.56	970.60	822.90	680.32

Table D-5 The experimental mode frequencies for the stepped overwound strings, S2(1), S2(2), S2(3), S2(4), S2(5) and S2(6).

Mode number	Mode frequencies					
(n)	S2(1)	S2(2)	S2(3)	S2(4)	S2(5)	S2(6)
1	56.78	42.57	34.23	27.95	24.19	20.342
2	113.79	85.22	68.52	55.92	48.39	40.696
3	171.36	128.07	102.92		72.64	
4	229.54	171.28		111.98	96.89	81.448
5			171.88	140.20		101.899
6	348.98	258.69	207.05	168.55	145.69	122.405
7						
8	472.27	348.17	277.77	225.73	194.88	163.623
9	535.69		313.58	254.59	219.61	184.349
10	600.05	439.42	349.70	283.64		205.164
11	666.01	486.36		312.90	269.56	
12		533.70	422.96		294.73	247.084
13	801.43	583.76	460.16	372.10	320.05	268.202
14						
15	944.15	680.06	535.79	432.283	371.18	310.783
16	1017.84	730.42	574.20		397.01	332.258
17	1093.41		613.09	493.55	423.02	
18		833.71	652.49	524.61		375.607
19	1250.16	886.75		555.99	475.62	397.491
20	1331.15	940.793	732.79	587.68	502.23	419.525
21						
22	1500.68	1050.78	815.29	652.09	556.104	464.059
23	1587.80	1107.64		684.83	583.387	486.573
24	1678.01	1165.70	900.05	717.94	610.911	509.259
25		1225.04	943.23		638.684	
26	1866.22		987.22	785.32		555.169
27	1960.62	1346.96	1031.81	819.61	695.011	578.405
28						
29	2159.52	1473.20	1123.14	889.48	752.431	625.468
30	2263.16	1538.42	1169.96	925.07	781.571	

Table D-6 The experimental mode frequencies for the stepped overwound strings, S3(1), S3(2), S3(3), S3(4), S3(5) and S3(6).

Mode number	Mode frequencies					
(n)	S3(1)	S3(2)	S3(3)	S3(4)	S3(5)	S3(6)
1	53.53	40.13	32.27	26.35	22.80	19.19
2	107.47	80.39	64.60	52.73	45.62	38.36
3	161.994	120.93	97.08	79.20	68.45	57.58
4				105.74		76.83
5	273.90	202.85	162.39		114.38	96.14
6		244.85	195.61	159.32		
7	389.14	287.12		186.31	160.73	134.88
8	448.62		262.81		184.05	154.41
9	509.33	373.34	296.84	240.90	207.50	
10		417.37	331.22	268.51	231.20	193.74
11	634.82			296.34		
12	699.75	507.47	401.10		278.73	233.58
13	766.29	553.62	436.65	352.75		253.63
14		600.56	472.64	381.36	326.04	
15	904.53		509.08		351.46	294.09
16	976.37	696.98		439.43	376.07	314.53
17	1050.16	746.53	583.44	468.92	400.89	335.11
18		797.05	621.39		425.92	
19	1203.87	848.55	659.89	528.90		376.72
20	1283.92		698.957	559.41	476.65	397.77
21	1366.19	954.71		590.28	502.37	418.98
22	1450.71	1009.42	778.89	621.54		
23		1065.28	819.80		554.55	461.95
24	1626.75	1122.31		685.24	581.03	483.71
25	1718.32		903.60	717.71		505.67
26						
27	1908.67	1300.73	990.16	783.97	662.14	550.19
28						
29	2108.55	1426.05	1079.65	852.05	717.70	595.56
30	2211.94	1490.69	1125.53	886.80	745.94	618.58

APPENDIX E

EXPERIMENTAL INHARMONICITY

In this Appendix, experimental values of inharmonicity calculated from the mode frequencies in Appendix D are tabulated. Table E-1 shows the experimental inharmonicity for the uniformly overwound strings, U1(1), U1(2), U1(3), U1(4), U1(5) and U1(6). Table E-2 shows the experimental inharmonicity for the uniformly overwound strings, U2(1), U2(2), U2(3), U2(4), U2(5) and U2(6). Table E-3 shows the experimental inharmonicity for the uniformly overwound strings, U3(1), U3(2), U3(3), U3(4), U3(5) and U3(6). Table E-4 shows the experimental inharmonicity for the stepped overwound strings, S1(1), S1(2), S1(3), S1(4), S1(5) and S1(6). Table E-5 shows the experimental inharmonicity for the stepped overwound strings, S2(1), S2(2), S2(3), S2(4), S2(5) and S2(6). And Table E-6 shows the experimental inharmonicity for the stepped overwound strings, S3(1), S3(2), S3(3), S3(4), S3(5) and S3(6). Details of the string dimensions see Table 3.1 and 3.2 in chapter 3.

Table.E-1 The experimental inharmonicity in cents for the six uniformly overwound strings, U1(1), U1(2), U1(3), U1(4), U1(5) and U1(6).

Mode number	U1(1)	U1(2)	Inharmonicity in cents U1(3)	U1(4)	U1(5)	U1(6)
1	1	0	0	0	0	0
2	2	1	1	1	1	
3	5	3	2	1		1
4	8	5		3	2	2
5		8	6		3	
6	18		8	6		3
7	24	15		7	6	4
8	31	19	13		8	
9	40		17	13	10	8
10		30	20	15	12	9
11	58	36		18		
12	69		29		17	15
13		50	34	26	20	17
14	92			30	23	
15		65	44	34	26	22
16	118	74				24
17	132	83	56	43	33	
18	147		63	48	37	30
19	162	102	69		41	34
20		112	77	59	45	
21	194	123		64		41
22	211		91	70	54	45
23	228	145	99	76	58	49
24	246		107		63	53
25		169		89	68	
26	282	181	125	96		62
27	300	194	134			66
28	319	207		110	84	70
29	338	220	152	117	89	
30	358	233	162	125		80

Table.E-2 The experimental inharmonicity in cents for the six uniformly overwound strings, U2(1), U2(2), U2(3), U2(4), U2(5) and U2(6).

Mode number	U2(1)	U2(2)	Inharmonicity U2(3)	in cents U2(4)	U2(5)	U2(6)
1	1	0	0	0	0	0
2	2	1	1	0	0	0
3	5	3		1		1
4			4	3	2	1
5	14	8	5		3	
6	20	12	8	6	4	4
7						
8	35		14	10	8	6
9	44	27	18	13	10	8
10	54		22	16	12	10
11		40	26	20		
12	77	47			17	14
13	90	55	37	27	20	17
14						
15	118	73	48	36	27	22
16		82	55		30	25
17	149		62		34	29
18	165	103	69	51	38	32
19	182	114		57		
20	200	125	84	63	47	39
21						
22	237	149	101	76	56	48
23	256	162		83	61	52
24	275		119			56
25		188		97	72	
26	315	202	138	104	78	66
27	336		148	112		71
28						
29	378	245	169	128	96	
30	399	259	179	136	102	87

Table.E-3 The experimental inharmonicity in cents for the six uniformly overwound strings, U3(1), U3(2), U3(3), U3(4), U3(5) and U3(6).

Mode number	Inharmonicity in cents					
	U3(1)	U3(2)	U3(3)	U3(4)	U3(5)	U3(6)
1	1	0	0	0	0	0
2	3		1	1	1	0
3	6	4	2	2		1
4	10	6			3	2
5	16		7	5	4	
6		14	9	7	5	4
7	31	19				6
8	41	25	17	13	9	7
9		31	21	16	12	9
10	63				15	
11	75	46	31	23		14
12		55		28	21	
13	105	65	45		27	20
14	120		52	40		24
15	137	86		46	35	27
16		97	66	51	40	
17	172		74			35
18		120	83	64	49	39
19	209	133			54	44
20	229		101	78		
21		160	110		66	53
22	270	174		93	71	58
23	292	188	130	101		63
24		203	141	109	84	
25	335		152			74
26	357	233	163	126	97	80
27	380	249		135	104	86
28		265	186		112	
29	426	282	198	153	118	98
30	449	298	210	163	126	105

Table.E-4 The experimental inharmonicity in cents for the six stepped overwound strings, S1(1), S1(2), S1(3), S1(4), S1(5) and S1(6).

Mode number	S1(1)	S1(2)	Inharmonicity in cents S1(3)	S1(4)	S1(5)	S1(6)
1	0	0		0	0	0
2	3		6	1	1	1
3	5	6	5	3		
4	19	7	6	5	3	2
5	23	16	12		5	4
6		18	15	10	7	6
7	46	30	20	13		
8	58		26		12	10
9	73	46.31	32	21	15	13
10	87		38	25	18	
11	101	63.49	44		21	18
12	117		50	34		22
13	133	83	56	39	28	
14	149	95	64	48	37	28
15	167	106	69	54		31
16	183		78		46	35
17	201	128		67	51	39
18			94	73	56	43
19	239	151		80	62	
20	258		112			52
21	279	177		94	73	56
22	298	189	132	102	79	61
23	318	202		109		
24		216	149		92	71
25	355			125	98	
26	376	245	170	134	105	81
27		260	181	142	112	87
28	416	275	191			92
29	437		202	160	126	
30	457	306	214	169	133	104

Table.E-5 The experimental inharmonicity in cents for the six stepped overwound strings, S2(1), S2(2), S2(3), S2(4), S2(5) and S2(6).

Mode number	S2(1)	S2(2)	Inharmonicity S2(3)	in cents S2(4)	S2(5)	S2(6)
1	1	0	0	0	0	0
2	5	2	2	1	0	1
3	12	5	4		2	
4	20	11		3	2	2
5			8	6		3
6	43	22	15	9	7	5
7						
8	69	39	25	16	12	10
9	83		31	21	15	12
10	97	55	38	25		15
11	112	66		30	22	
12		76	51		26	21
13	144	93	59	41	30	25
14						
15	180	109	74	53	39	32
16	198	121	82		44	36
17	217		91	66	49	
18		146	100	72		44
19	256	160		79	59	49
20	276	173	118	87	65	53
21						
22	319	200	138	102	76	63
23	340	214		110	82	68
24	362	229	159	118	88	73
25		244	169		95	
26	407		180	134		84
27	427	275	191	143	108	90
28						
29	471	306	214	161	121	101
30	493	323	226	170	128	

Table.E-6 The experimental inharmonicity in cents for the six stepped overwound strings, S3(1), S3(2), S3(3), S3(4), S3(5) and S3(6).

Mode number	S3(1)	S3(2)	Inharmonicity in cents S3(3)	S3(4)	S3(5)	S3(6)
1	2	1	1	1	1	0
2	9	4	3	2	1	1
3	17	9	6	4	2	2
4				6		3
5	42	20	12		6	5
6		30	19	14		
7	67	39		18	13	9
8	82		32		16	12
9	98	59	39	28	20	
10		69	46	33	24	18
11	132			39		
12	150	92	62		33	26
13	169	104	70	51		30
14		117	79	58	37	
15	208		88		48	39
16	229	143		72	53	44
17	250	157	108	80	59	48
18		172	118		65	
19	294	186	128	96		58
20	316		139	104	77	64
21	340	217		113	84	69
22	363	233	162	121		
23		249	173		98	81
24	411	266		140	105	87
25	435		197	149		93
26						
27	483	318	222	169	127	106
28						
29	532	353	249	189	143	119
30	556	371	262	200	151	126

APPENDIX F

PIANO STRINGS' THEORETICAL AND EXPERIMENTAL MODE FREQUENCIES

Table F-1 shows the theoretical mode frequencies of the piano strings, A0, Bb0, B0 and C1. Table F-2 shows the theoretical mode frequencies of the piano strings, Db1, D1, Eb1 and E1. Table F-3 shows the experimental mode frequencies of the piano strings, A0, Bb0, B0 and C1. Table F-4 shows the experimental mode frequencies of the piano strings, Db1, D1, Eb1 and E1. For details of the string dimensions see Table 6.1 in chapter 6.

Table F-1 The theoretical mode frequencies for the piano strings, A0, Bb0, B0 and C1.

Mode number (n)	Mode frequencies			
	A0	Bb0	B0	C1
1	25.86	28.50	29.40	31.80
2	51.73	57.01	58.81	63.61
3	77.62	85.54	88.24	95.44
4	103.54	114.09	117.69	127.28
5	129.50	142.68	147.18	159.17
6	155.50	171.31	176.72	191.08
7	181.56	199.98	206.30	223.05
8	207.68	228.72	235.95	255.07
9	233.87	257.52	265.67	287.16
10	260.15	286.40	295.46	319.31
11	286.52	315.36	325.34	351.54
12	312.99	344.42	355.32	383.85
13	339.57	373.56	385.40	416.26
14	366.26	402.82	415.59	448.76
15	393.08	432.19	445.90	481.37
16	420.02	461.67	476.34	514.09
17	447.35	491.29	506.91	546.93
18	474.35	521.04	537.63	579.89
19	501.74	550.93	568.49	612.99
20		580.98	599.52	646.23
21	557.03	611.17	630.71	679.61
22	584.93	641.54	662.62	713.14
23	613.02	672.07		746.83
24	641.31	702.77	725.35	780.69
25	669.79	733.66	757.28	814.71
26	698.48	764.74	789.41	848.91
27	727.39	796.02	821.75	883.30
28		827.499	854.31	917.87
29	785.87	859.187	887.09	952.64
30	815.45	891.09	920.104	987.61

Table F-2 The theoretical mode frequencies for the piano strings, Db1, D1, Eb1 and E1.

Mode number (n)	Mode frequencies			
	Db1	D1	Eb1	E1
1	32.60	35.90	37.84	39.80
2	65.21	71.81	75.69	79.61
3	97.84	107.74	113.55	119.43
4	130.49	143.69	151.44	159.28
5	163.18	179.67	189.35	199.15
6	195.90	215.70	227.29	239.06
7	228.68	251.78	265.28	279.01
8	261.52	287.91	303.32	319.01
9	294.43	324.11	341.42	359.06
10	327.41	360.39	379.58	399.18
11	360.47	396.75	417.80	439.37
12	393.62	433.20	456.11	479.64
13	426.88	469.75	494.50	520.00
14	460.24	506.40	532.98	560.44
15	493.72	543.17	571.56	600.99
16	527.32	580.07	610.24	641.63
17	561.05	617.09	649.03	682.40
18	594.92	654.25	687.94	723.28
19	628.93	691.56	726.98	764.28
20	663.10	729.02	766.15	805.42
21	697.43	766.65	805.45	846.70
22	731.93	804.44	844.90	888.13
23	766.60	842.41	884.50	929.70
24	801.46	880.56	924.25	971.44
25	836.506	918.90	964.17	1013.34
26		957.44	1004.26	1055.42
27	907.197	996.19	1044.52	1097.67
28	942.86	1035.15	1084.97	1140.11
29	978.731	1074.33	1125.6	1182.74
30		1113.73	1166.43	1225.57

Table F-3 The experimental mode frequencies for the piano strings, A0, Bb0, B0 and C1.

Mode number (n)	Mode frequencies			
	A0	Bb0	B0	C1
1	25.87			
2	51.78			63.62
3	77.69	85.51	88.31	
4	103.60	114.09		127.31
5	129.56	142.72	147.42	
6	155.65	171.36	177.17	191.29
7	181.78	200.09	206.74	
8	207.88	228.93	235.91	255.33
9	234.08	257.66	266.31	287.26
10	260.45	286.67	295.35	319.64
11	286.72	315.67	325.80	351.75
12	313.36	345.10	355.47	384.40
13	339.28	373.88	386.58	416.82
14	366.79	403.80	417.30	448.96
15		433.02	447.03	482.18
16	420.69	462.93	478.50	515.14
17		492.89	509.57	548.09
18	475.28	522.42	540.05	581.17
19	502.85	552.99	571.53	614.83
20	530.28	583.09	602.58	647.83
21	558.02	614.50	634.54	681.51
22	586.22	644.81		715.27
23	614.34	674.70	697.86	749.48
24	642.80	705.72	729.85	783.41
25	671.48	737.51	762.24	817.66
26	700.43	768.64	794.93	852.13
27	729.46		827.48	886.82
28		832.59	860.45	992.48
29	788.31		894.54	1028.10
30				1100.10

Table F-4 The experimental mode frequencies for the piano strings, Db1, D1, Eb1 and E1.

Mode number (n)	Mode frequencies			
	Db1	D1	Eb1	E1
1		35.96	37.85	
2		71.79	75.64	79.62
3	101.12	108.33	113.90	
4	134.36	143.43	151.88	158.88
5	167.78	179.18	189.91	198.75
6	201.40	215.17	228.03	241.24
7	235.29	251.08	266.56	278.78
8	269.08	287.22	304.96	318.54
9	302.56	323.31		358.62
10	336.81	360.01	380.80	398.99
11	370.58	395.87	419.76	439.42
12	405.19	432.47	458.38	478.74
13	439.88	468.34	496.91	517.85
14	474.11	505.77	536.08	560.74
15		542.21		601.73
16	543.03	579.51	612.47	641.15
17		616.25		682.52
18	613.38	653.92		722.92
19		690.75		764.00
20		728.52	770.06	805.62
21	718.68	766.13		846.70
22	754.42	803.90	849.34	887.86
23		841.75		929.83
24	825.06	880.06	929.08	971.12
25		918.32		
26				
27		995.94	1049.65	
28		1034.52	1090.87	1140.60
29				1183.95
30	1045.14	1114.37		

APPENDIX G

PIANO STRINGS' THEORETICAL AND EXPERIMENTAL INHARMONICITY

Table G-1 shows the theoretical inharmonicity for the piano strings, A0, Bb0, B0 and C1. Table G-2 shows the theoretical inharmonicity for the piano strings, Db1, D1, Eb1 and E1. Table G-3 shows the experimental inharmonicity for the piano strings, A0, Bb0, B0 and C1. Table G-4 shows the experimental inharmonicity in cents for the piano strings, Db1, D1, Eb1 and E1. For details of the string dimensions see Table 6.1 in chapter 6.

Table G-1 The theoretical inharmonicity in cents for the piano strings, A0, Bb0, B0 and C1.

Mode number (n)	Inharmonicity in cents			
	A0	Bb0	B0	C1
1	0	0	0	0
2	0	0	0	0
3	1	1	1	1
4	2	1	1	1
5	3	2	2	2
6	4	3	3	3
7	5	4	4	4
8	7	5	6	5
9	8	7	7	6
10	10	9	9	7
11	13	10	10	9
12	15	12	12	10
13	17	14	14	12
14	20	16	17	14
15	23	19	19	16
16	26	21	22	18
17	30	24	24	20
18	33	27	27	23
19	36	30	30	25
20		33	34	28
21	44	36	37	30
22	48	40	42	33
23	52	43		36
24	57	47	48	39
25	61	51	52	42
26	66	55	56	46
27	71	59	60	49
28		63	64	53
29	81	67	69	56
30	86	72	73	60

Table G-2 The theoretical inharmonicity in cents for the piano strings, Db1, D1, Eb1 and E1.

Mode number (n)	Inhamonicity in cents			
	Db1	D1	Eb1	E1
1	0	0	0	0
2	0	0	0	0
3	1	1	0	0
4	1	1	1	1
5	2	2	1	1
6	3	2	2	2
7	4	3	3	3
8	5	4	3	3
9	6	5	4	4
10	7	7	5	5
11	9	8	6	6
12	11	10	8	7
13	13	11	9	9
14	15	13	10	10
15	17	15	12	12
16	19	17	14	13
17	21	19	15	15
18	24	21	17	17
19	26	24	19	18
20	29	26	21	20
21	32	29	23	22
22	35	32	26	25
23	38	35	28	27
24	42	38	30	30
25	45	41	33	32
26		44	36	34
27	52	47	38	37
28	56	51	41	39
29	60	54	44	42
30		58	47	45

Table G-3 The experimental inharmonicity in cents for the piano strings, A0, Bb0, B0 and C1.

Mode number (n)	Inharmonicity in cents			
	A0	Bb0	B0	C1
1	0			
2	2			0
3	2	0	2	
4	3	1		1
5	3	3	5	
6	5	4	8	4
7	7	5	8	
8	8	7	5	6
9	10	8	11	6
10	12	10	8	9
11	14	12	13	10
12	17	16	13	13
13	16	16	20	14
14	23	21	24	15
15		22	24	19
16	29	26	30	21
17		30	34	24
18	36	31	35	26
19	40	36	40	30
20	45	39	42	32
21	47	46	47	35
22	52	48		38
23	56	50	55	42
24	61	54	59	45
25	66	60	63	49
26	71	63	68	52
27	76		72	56
28		73	77	
29	86		83	
30				68

Table G-4 The experimental inharmonicity in cents for the piano strings, Db1, D1, Eb1 and E1.

Mode number (n)	Inharmonicity in cents			
	Db1	D1	Eb1	E1
1				
2				
3	0			
4	2	3	0	0
5	0	2	1	1
6	1	3	2	
7	3	3	5	5
8	4	5	7	4
9	3	6		6
10	7	10	5	8
11	7	9	9	10
12	11	12	10	
13	15	11	12	
14	16	16	15	14
15		17		17
16	20	20	14	15
17		22		19
18	27	25		19
19		27		21
20		30	24	24
21	34	33		26
22	38	35	29	28
23		38		31
24	42	42	33	32
25		45		
26				
27		52	41	
28		55	45	44
29				48
30	65	64		

BIBLIOGRAPHY

1. Alembert, D. *Hist. Acad. Sci.* **3**, 214-219 (1747).
2. Alfredson, R.J. & Steinke, S. *Acustica* **39**, 130-132 (1978).
3. Askenfelt, A. & Jansson, E.V. *Journal of Acoustical Society of America* **88**, 52-63 (1990).
4. Askenfelt, A. & Jansson, E.V. *Journal of Acoustical Society of America* **90**, 2383-2393 (1991).
5. Askenfelt, A. & Jansson, E.V. *Journal of Acoustical Society of America* **93**, 2181-2196 (1991).
6. Bachmann, W., Bucker, H. & Kohl, B. *Acustica* **68**, 123-130 (1989).
7. Backus, J. *Journal of Acoustical Society of America* **58**, 1078-1081 (1975).
8. Bacon, R.A. & Bowsher, J.M. *Acustica* **41**, 21-27 (1978).
9. Baker, C.G.B., Thair, C.M. & Gough, C.E. *Acustica* **44**, 70-77 (1980).
10. Bariaux, D., Cornelissen, G., Prins, J.D., Guisset, J.L. & Willems, J. *Acustica* **32**, 307-313 (1975).
11. Barrett, T.W. *Journal of Sound and Vibration* **20**, 407-412 (1972).
12. Bell, A.J. & Parks, R. *Proc. of the Inst. of Acoustics.* **12**, 753-755 (1990).
13. Benade, A.H. *Fundamentals of Musical Acoustics.* (McGraw-Hill., New York, 1968).
14. Bilhuber, P.H. & Johnson, C.A. *Journal of Acoustical Society of America* **11**, 311-320 (1940).
15. Blackham, E.D. *Scientific American* 24-33 (1965).
16. Bokaian, A. *Journal of Sound and Vibration* **126**, 49-65 (1988).

17. Boutillon, X., Radier, J., Valette, C. & Castellengo, M. *Comptes Rendus Acad. Sci. Paris.* **298**, 815-820 (1984).

18. Boutillon, X. *Journal of Acoustical Society of America* **83**, 746-754 (1988).

19. Brigham, E.O. *The Fast Fourier Transform.* (Prentice-Hall., 1974).

20. Buchmann, W., Bucker, H. & Kohl, B. *Acustica* **68**, 123-130 (1989).

21. Calder, J. *Journal of Catgut Acoustical Society.* **1**, 17-29 (1991).

22. Campbell, D.M., Greated, C. & Parks, R. *Physics Education.* **25**, 20-29 (1990).

23. Capron, M.D. & Williams, F.W. *Journal of Sound and Vibration* **124**, 453-466 (1988).

24. Chaigne, A. & Askenfelt, A. *Journal of Acoustical Society of America* **95**, 1112-1118 (1994).

25. Chaigne, A. & Askenfelt, A. *Journal of Acoustical Society of America* **95**, 1631-1640 (1994).

26. Clarke, R.J. *Acustica* **40**, 34-39 (1978).

27. College, F.J. *Journal of Acoustical Society of America* **21**, 318-322 (1946).

28. Cooley, J.W. & Turkey, J.W. *Math Computation.* **19 (April)**, 297-381 (1965).

29. Cranch, E.T. & Adler, A.A. *Journal of Applied Mechanics.* **March**, 103-108 (1956).

30. Cuesta, C. & Valette, C. *Acustica* **66**, 37-45 (1988).

31. Cuesta, C. & Valette, C. *Acustica* **68**, 112-122 (1989).

32. Cuesta, C. & Valette, C. *Acustica* **71**, 28-40 (1990).

33. Dasarathy, B.V. & Srinivasan, P. *Journal of Sound and Vibration* **9**, 49-52 (1969).

34. Deb, K.K. *Journal of Sound and Vibration* **20**, 1-7 (1972).

35. Exley, K.A. *Journal of Sound and Vibration* **9**, 420-437 (1969).

36. Filipich, C.P. & Laura, P.A.A. *Journal of Sound and Vibration* **125**, 393-396

(1988).

37. Filipich, C.P. & Laura, P.A.A. *Journal of Sound and Vibration* **126**, 1-8 (1988).

38. Firth, I.M. *Acustica* **39**, 252-263 (1978).

39. Fletcher, H., Blackham, E., Donnell & R., S. *Journal of Acoustical Society of America* **34**, 749-761 (1962).

40. Fletcher, H. *Journal of Acoustical Society of America* **36**, 203-209 (1964).

41. Fletcher, N.H. *Acustica* **37**, 139-147 (1977).

42. Fletcher, N.H. *Journal of Acoustical Society of America* **64**, 1566-1569 (1978).

43. George, W.H. *Acustica* **4**, 224-225 (1954).

44. Ghosh, R.N. *Journal of Acoustical Society of America* **7**, 254-260 (1936).

45. Gottlieb, H.P.W. *Journal of Sound and Vibration* **108**, 63-72 (1986).

46. Gottlieb, H.P.W. *Journal of Sound and Vibration* **118**, 283-290 (1987).

47. Gough, C.E. *Acustica* **44**, 113-123 (1980).

48. Gough, C.E. *Acustica* **48**, 124-141 (1981).

49. Gutierrez, R.H., Laura, P.A.A. & Rossi, R.E. *Journal of Sound and Vibration* **145**, 341-344 (1991).

50. Hall, D.E. *Journal of Acoustical Society of America* **79**, 141-147 (1986).

51. Hall, D.E. *Journal of Acoustical Society of America* **81**, 535-546 (1987).

52. Hall, D.E. *Journal of Acoustical Society of America* **81**, 547-555 (1987).

53. Hall, D.E. *Journal of Acoustical Society of America* **82**, 1913-1918 (1987).

54. Hall, D.E. *Journal of Acoustical Society of America* **83**, 1627-1638 (1988).

55. Hall, D.E. *Journal of Acoustical Society of America* **92**, 95-105 (1992).

56. Harris, F.J. *Proceedings of the IEEE.* **66**, 51-83 (1978).

57. Huang, C.L.D. & Walker, H.S.J. *Journal of Sound and Vibration* **126**, 9-17 (1988).

58. Hundley, M. & Benioff. *Proceedings of the Second International Congress on*

Acoustics. 159 (1957).

59. James, C.J. & Chivers, R.C. *Acustica* **69**, 13-16 (1989).

60. Jaroszewski, A. *Acustica* **77**, 106-110 (1992).

61. Jaroszewski, A. *Acustica* **76**, 137-141 (1992).

62. Kalotas, T.M. & Lee, A.R. *Acustica* **76**, 20-26 (1992).

63. Karp, C. *Acustica* **54**, 209-216 (1984).

64. Karp, C. *Acustica* **60**, 295-299 (1986).

65. Keeler, J.S. *IEEE Transaction on Audio and Electroacoustics*. **AU-20**, 338-344 (1972).

66. Kent, E.L. *Dokumentation Europiano Kongress Berlin*. 58-68 (1965).

67. Kirk, R.E. *Journal of Acoustical Society of America* **31**, 1644-1648 (1959).

68. Kock, W.E. *Journal of Acoustical Society of America* **8**, 227-233 (1937).

69. Lagrange, J.L. *Oenvre de Lagrange*. **1**, 39 (1867).

70. Laura, P.A.A. & Verniere de Irassar, P.L. *Journal of Sound and Vibration* **124**, 1-12 (1988).

71. Levinson, M. *Journal of Sound and Vibration* **49**, 287-291 (1976).

72. Lieber, E. *Acustica* **33**, 324-335 (1975).

73. Linsay, R.B. *Acoustics: Historical and Philosoplical Development*. 96-102 (1973).

74. Martin, D.W. *Journal of Acoustical Society of America* **19**, 535-541 (1947).

75. Martin, D.W. & Ward, W.D. *Journal of Acoustical Society of America* **33**, 582-585 (1961).

76. Maurizi, M.J. & Belles, P.M. *Journal of Sound and Vibration* **145**, 345-347 (1991).

77. McIntyre, M.E. & Woodhouse, J. *Acustica* **43**, 93-108 (1979).

78. Metyger, E. *Journal of Acoustical Society of America* **42**, 896 (1967).

79. Miller, F.J. *Journal of Acoustical Society of America* **21**, 318-322 (1949).

80. Moore, B.C.J., Peters, R.W. & Glasberg, B.R. *Journal of Acoustical Society*

of America **77**, 1861-1867 (1985).

81. Morse, M. *Vibration and Sound.* (McGraw-Hill., New York., 1936).

82. Orduna-Bustamante, F. & Boullosa, R.R. *Journal of Acoustical Society of America* **93**, 3265-3270 (1993).

83. Palmer, C. & Brown, J.C. *Journal of Acoustical Society of America* **90**, 60-66 (1991).

84. Parks, R. *Proceeding of the Institute of Acoustics.* **15**, 673-680 (1993).

85. Podlesak, M. & Lee, A.R. *Journal of Acoustical Society of America* **83**, 305-317 (1988).

86. Podlesak, M. & Lee, A.R. *Acustica* **68**, 61-66 (1989).

87. Rabiner, L.R., *et al. IEEE Transsactions Audio and Electroacoustics.* **AU-20**, 322-337 (1972).

88. Rayleigh, J.W.S.L. *Theory of Sound.* (Dover Publication, 1954).

89. Ross, M.J. *Acustica* **24**, 273-283 (1971).

90. Rossi, R.E., Gutierrez, R.H. & Laura, P.A.A. *Journal of Acoustical Society of America* **89**, 2456-2458 (1991).

91. Sakata, T. & Sakata, Y. *Journal of Sound and Vibration* **71**, 315-317 (1980).

92. Schuck, O.H. & Young, R.W. *Journal of Acoustical Society of America* **15**, 1-11 (1943).

93. Schumacher, R.T. *Acustica* **43**, 109-120 (1979).

94. Shankland, R.S. & Coltman, J.W. *Journal of Acoustical Society of America* **10**, 161-166 (1939).

95. Sloane, C. *Journal of Sound and Vibration* **125**, 185-186 (1988).

96. Spyridis, H., Roumeliotis, E. & Papadimitraki-Chlichlia, H. *Acustica* **51**, 180-182 (1982).

97. Spyridis, H. & Roumeliotis, E. *Acustica* **52**, 255-256 (1983).

98. Stevens, K.K. *Journal of Sound and Vibration* **20**, 257-268 (1972).

99. Suzuki, H. *Journal of Acoustical Society of America* **82**, 1145-1151 (1987).

100. Taylor, B. *Phil. Trans. Roy. Soc.* **28**, 26-32 (1713).

101. Terhardt, E. & Zick, M. *Acustica* **32**, 268-274 (1975).

102. Terhardt, E. *Acustica* **64**, 61-72 (1987).

103. Terhardt, E. *Acustica* **70**, 179-188 (1990).

104. Thwaites, S. & Fletcher, N.H. *Journal of Acoustical Society of America* **69**, 1476-1483 (1981).

105. Tsay, H.S. & Kinsbury, H.B. *Journal of Sound and Vibration* **124**, 539-554 (1988).

106. Von Helmholtz, H. *On the Sensations of Tone*. (Dover, New York, 1954).

107. Watkinson, P.S., Shepherd, R. & Bowsher, J.M. *Acustica* **51**, 213-221 (1982).

108. Weinreich, G. *Journal of Acoustical Society of America* **62**, 1474-1484 (1977).

109. Weinreich, G. *Journal of Acoustical Society of America* **62**, 1474-1484 (1977).

110. Weyer, R.D. *Acustica* **35**, 232-252 (1976).

111. Weyer, R.D. *Acustica* **36**, 241-258 (1976).

112. Winckel, F. *Music, sound and sensation.* (Dover Publications., New York., 1967).

113. Wolf, D. & Muller, H. *Journal of Acoustical Society of America* **44**, 1093-1097 (1968).

114. Young, R.W. *Journal of Acoustical Society of America* **24**, 267-273 (1952).

115. Young, R.W. *Acustica* **4**, 259-262 (1954).

116. Zhu, G.H., Crocker, M.J. & Roa, M.D. *Journal of Acoustical Society of America* **85**, 171-177 (1989).

Proceedings of the Institute of Acoustics

INHARMONICITY OF STEPPED STIFF STRINGS.

P Chumnantas, C A Greated & D M Campbell.

University of Edinburgh, Department of Physics, Edinburgh, UK.

1. INTRODUCTION

The problem of the vibration of flexible strings with uniform characteristics has been treated by many investigators and the results are well established. Vibration characteristics of stiff strings are also quite well understood and the predicted mode frequencies are in closed agreement with observations [1]. In this paper, the vibration of nonuniform stiff strings is considered.

In the late 19th century, Lord Rayleigh [2] described a theory for the vibration of strings, showing that in the piano, the stiffness of the strings affects the restoring force to a significant degree. He derived a formula to predict how the stiffness of a piano string can cause it to vibrate at frequencies somewhat greater than those of the ideal string.

The more general theory for the stiff string, often encountered in the literature, was developed by Morse [3], and by Shankland and Coltman [4]. They derived expressions for the frequencies of a string of uniform diameter and density in free transverse vibration between rigid supports. Shankland and Coltman predicted a progressive sharpening of the partials as the mode number increases, the extent of the sharpening being dependent on the ratio of the string diameter to its length; the greater this ratio, the greater will be the sharpening. Robert W. Young [5, 6, 7] and his colleagues found that the sharpening follows approximately a square law with respect to mode number. They observed that the departure from the harmonic series of the plain steel strings was about the same in all the pianos they tested and was consistently less in large pianos than in small ones. More recently, many other investigators have studied the piano string inharmonicity problem with plain steel strings and overwound bass strings [8].

All piano bass strings are characterised by a steel wire core wrapped with copper, or sometimes iron, used to increase the string's linear mass density. While the tight coiling of the copper wire ensures close coupling to the core, the windings contribute considerably more to the increase in the string's linear mass density than to its bending stiffness. Most bass strings have a single winding of copper wire, and it is usually only within the lowest octave that double winding is used. A double-wound string consists of a bare steel core wrapped with a small diameter copper wire, which is then overspun with a second winding of larger diameter. A small part of the steel core is left exposed near the end of the string. Thus only the outer winding is visible and the existence of the inner winding is evident only from the small change in the diameter of the overall covering near the ends.

A theoretical relationship for inharmonicity that can be applied to wrapped strings was derived by Harvey Fletcher [9]. He showed that the formula $f_n = nf\sqrt{1+Bn^2}$ gives values

INHARMONICITY OF STEPPED STIFF STRINGS.

of the partial frequencies of the solid piano strings close to his observed values, where n is the number of the partial. The constant B, the inharmonicity coefficient calculated from the dimensions of the wire, is $B = (\pi^2 Q S \kappa^2 / 4 l^2 \sigma f_0^2)$, where f_0 is the fundamental frequency, Q the Young's modulus of elasticity, S the area of the cross section, l the length, σ the linear density, and κ the radius of gyration of the string. Fletcher had the idea of applying this to overwound strings by taking σ to be the linear density of the overwound string (core and windings). He suggested that the value of linear density of the overwound string would be

$$\sigma = \rho_{cu} \frac{\pi^2}{16} D^2 + (\rho_s \frac{\pi}{4} - \rho_{cu} \frac{\pi^2}{16}) d^2$$

for a steel core of diameter d with volume mass density ρ_s and copper winding with volume mass density ρ_{cu} and wire diameter D.

Fletcher's formula has previously been applied [1] to predict the inharmonicity of strings on a 2.5 m Broadwood grand piano (1871) in the Physics Department at the University of Edinburgh. It was found that for the full range of plain solid strings the predicted and observed inharmonicities were in close agreement. However for the overwound strings the observed inharmonicity was higher than predicted, taking the string as being uniform over its length. The deviation was up to some 30% for the most heavily overwound, A0 string. This has led us to investigate the effect of string nonuniformity, caused by the windings not continuing over the entire string length.

Some discussions about this problem have appeared over the last few years by Levinson [10], Sakata and Sakata [11], and Gottlieb [12]. Levinson studied the free vibration of a string with stepped mass density and derived an exact equation for calculating the natural frequency, but did not obtain any numerical solutions. Sakata and Sakata derived an exact frequency equation for a string with stepped mass density and proposed an approximate formula for estimating the fundamental natural frequency of the string. In Gottlieb's work, the three-part string, with two step discontinuities in density, was investigated in some detail for both fixed and free end conditions. Aspects of the "four-part" and "m-part" string problems were also discussed. However, these derivations have not taken into account the stiffness of the stepped string.

2. THEORETICAL CONSIDERATION

In this section we derive an expression for the frequencies of vibration of a stepped stiff string. Consider the vibration of an M-part string fixed at its ends. The (displacement) finite element formulation of the one-dimensional fourth-order differential equation [2] is

$$T_i \frac{\partial^2 w_i}{\partial x_i^2} - (QS\kappa^2)_i \frac{\partial^4 w_i}{\partial x_i^4} = \rho_i S_i \frac{\partial^2 w_i}{\partial t^2} \qquad \mathbf{i = 1, 2, 3, ..., m} \qquad (1)$$

INHARMONICITY OF STEPPED STIFF STRINGS.

where w_i is the (small) transverse displacement of the string originally lying on the x-axis, t is the time, T is the Tension, S_i is the area of cross-section, κ_i its radius of gyration. ρ_i and Q_i are the density and modulus of elasticity of the material for $a_{i-1} \le x_i \le a_i$ where x_i is the length of the i-th segment of the string. $a_0 = 0$ and $a_m = \sum_{i=1}^{m} a_i = a$, the total length of the string.

The ends of the string are considered to be clamped. Then the boundary conditions are

$$\begin{aligned} w_1(0) &= w_m(a) = 0 \\ w_1'(0) &= w_m'(a) = 0 \end{aligned} \tag{2}$$

and the junction conditions

$$\begin{aligned} w_i(a_i) &= w_{i+1}(a_i) \\ w_i'(a_i) &= w_{i+1}'(a_i) \\ (QS\kappa^2)_i w_i''(a_i) &= (QS\kappa^2)_{i+1} w_{i+1}''(a_i) \\ T_i w_i'(a_i) + (QS\kappa^2)_i w_i'''(a_i) &= T_{i+1} w_{i+1}'(a_i) + (QS\kappa^2)_{i+1} w_{i+1}'''(a_i). \end{aligned} \tag{3}$$

The boundary conditions are those for simple supports and the junction conditions express the continuity of the displacement, slope, moment, and shear at the junctions of the M segments of the stiff string.

In the case of a two segment stiff string, the normal mode frequencies can be found from the equation (afterwards, called the frequency equation):

$$\begin{aligned} &\left(\frac{(QS\kappa^2)_1}{(QS\kappa^2)_2}\frac{\mu_{11}^2}{\mu_{22}^2} + 1\right)(\mu_{11}\tanh(\mu_{21}a_2) + \mu_{21}\tanh(\mu_{11}a_1)) \\ &\quad \times\left\{\frac{(QS\kappa^2)_1}{(QS\kappa^2)_2}\frac{\mu_{12}^2}{\mu_{21}^2} + 1\right\}\{\mu_{12}\tan(\mu_{22}a_2) + \mu_{22}\tan(\mu_{12}a_1)\} \\ &\quad -\left\{\frac{(QS\kappa^2)_1}{(QS\kappa^2)_2}\frac{\mu_{11}^2}{\mu_{21}^2} - 1\right\}\{\mu_{11}\tan(\mu_{22}a_2) + \mu_{22}\tanh(\mu_{11}a_1)\} \\ &\quad \times\left\{\frac{(QS\kappa^2)_1}{(QS\kappa^2)_2}\frac{\mu_{12}^2}{\mu_{22}^2} - 1\right\}\{\mu_{12}\tanh(\mu_{21}a_2) + \mu_{21}\tan(\mu_{12}a_1)\} = 0 \end{aligned} \tag{4}$$

Equation (4) contains four parameters $\mu_{11}, \mu_{12}, \mu_{21}, \mu_{22}$ which are functions of the frequency, f.

INHARMONICITY OF STEPPED STIFF STRINGS.

$$\mu_{jk} = \{\sqrt{(\frac{T_j}{2(QS\kappa^2)_j})^2 + (2\pi f)^2 \frac{\rho_j}{(Q\kappa^2)_j}} + (-1)^k \frac{T_j}{2(QS\kappa^2)_j})^{\frac{1}{2}} \qquad (5)$$

$$: j,k = 1,2.$$

In the case of the stepped stiff string it is considered that its tension and stiffness are constant along its length due to the core. Its frequency equation is

$$\begin{aligned}&(\frac{\mu_{11}^2}{\mu_{22}^2}+1)(\frac{\mu_{12}^2}{\mu_{21}^2}+1)\{\frac{\mu_{11}}{\mu_{21}}\frac{\tanh(\mu_{21}a_2)}{\tanh(\mu_{11}a_1)}+1\}\{\frac{\mu_{12}}{\mu_{22}}\frac{\tan(\mu_{22}a_2)}{\tan(\mu_{12}a_1)}+1\}\\ &-(\frac{\mu_{11}^2}{\mu_{21}^2}-1)(\frac{\mu_{12}^2}{\mu_{22}^2}-1)\{\frac{\mu_{11}}{\mu_{22}}\frac{\tan(\mu_{22}a_2)}{\tanh(\mu_{11}a_1)}+1\}\{\frac{\mu_{12}}{\mu_{21}}\frac{\tanh(\mu_{21}a_2)}{\tan(\mu_{12}a_1)}+1\}=0 \qquad (6)\end{aligned}$$

The allowed frequencies, f_n : (n = 1, 2, 3, 4, ...) can be found from equation (5) & (6).

3. NUMERICAL RESULT

Numerical calculations have been undertaken to compute theoretical mode frequencies for strings on the Edinburgh Broadwood grand piano. Only the single overwound strings in the lowest octave, sounding A0 to A1 were considered; results here are presented for two of the strings, Bb0 and Db1.

Fig I shows the notation used for defining the parameters of the overwound string. This was clamped at both ends and the linear density was calculated using the method of W T Goddard [13].

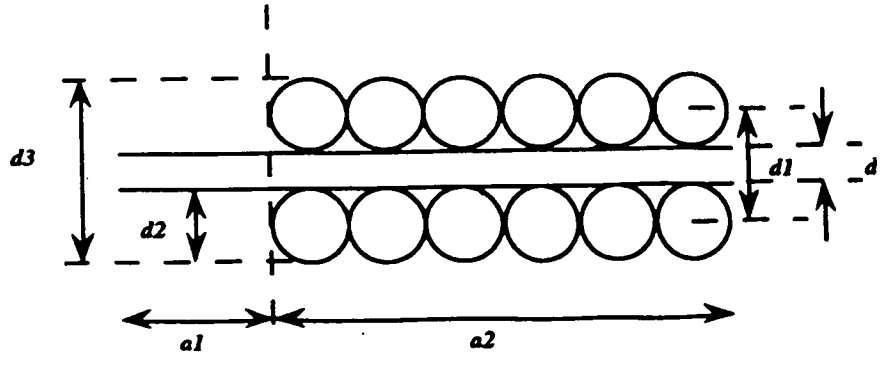

Fig. I the single overwound string.

INHARMONICITY OF STEPPED STIFF STRINGS.

The 1-st segment is the bare string and the 2-nd segment has both the steel core and the wrapped copper wire. Table I shows the dimensions for the two strings Bb0 and Db1.

Table I The dimensions of the strings. Bb0 and Db1

Strings' parameters	Bb0	Db1
d (mm.)	0.140	0.130
d_2(mm.)	0.441	0.377
a_1(mm.)	23.00	18.00
a_2(mm.)	1837.00	1767.00
σ_1(g/mm.)	0.0121	0.0104
σ_2(g/mm.)	0.1084	0.0794

The mode frequencies were found numerically from Equation 5 & 6 by applying Newton's method; this was programmed on an Apple Macintosh computer using the Mathematica package. The results of these computations are shown in Tables II and III. Figures II and III present these results graphically.

Table II The departure of the natural frequencies from the harmonic series for Bb0 string with Fletcher's formula, Observation and Theory (Eqs. 5 & 6).

Mode number (n)	Bb0		
	Fletcher's formula	Observation	Theory (Eqs. 5 & 6)
1	1.0000	1.0000	1.0000
2	2.0003	2.0005	2.0004
3	3.0011	3.0016	3.0015
4	4.0026	4.0037	4.0035
5	5.0052	5.0072	5.0069
6	6.0089	6.0125	6.0119
7	7.0142	7.0198	7.0190
8	8.0212	8.0296	8.0283
9	9.0301	9.0421	9.0403
10	10.0413	10.0578	10.0552
11	11.0549	11.0769	11.0734
12	12.0713	12.0997	12.0953

INHARMONICITY OF STEPPED STIFF STRINGS.

Fig II

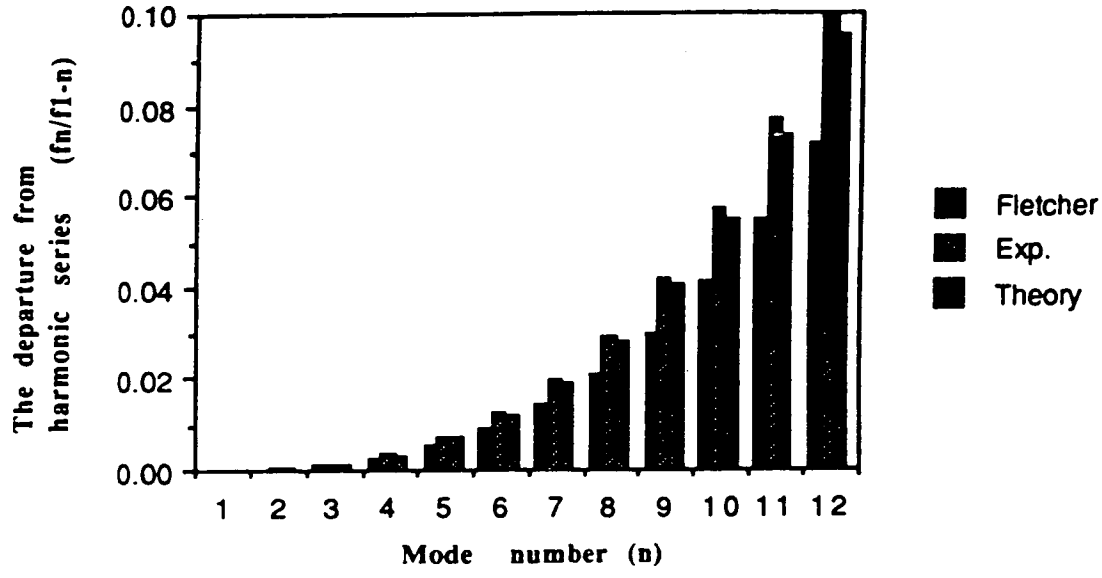

Table III The departure of the natural frequencies from the harmonic series for Db1 string with Fletcher's formula, Observation and Theory (Eqs. 5 & 6).

Mode number (n)	Db1		
	Fletcher's formula	Observation	Theory (Eqs. 5 & 6)
1	1.0000	1.0000	1.0000
2	2.0003	2.0004	2.0004
3	3.0009	3.0012	3.0012
4	4.0022	4.0028	4.0028
5	5.0044	5.0055	5.0054
6	6.0076	6.0095	6.0093
7	7.0120	7.0151	7.0148
8	8.0226	8.0226	8.0221
9	9.0255	9.0321	9.0314
10	10.0350	10.0441	10.0430
11	11.0466	11.0586	11.0573
12	12.0604	12.0761	12.0743

INHARMONICITY OF STEPPED STIFF STRINGS.

Fig III

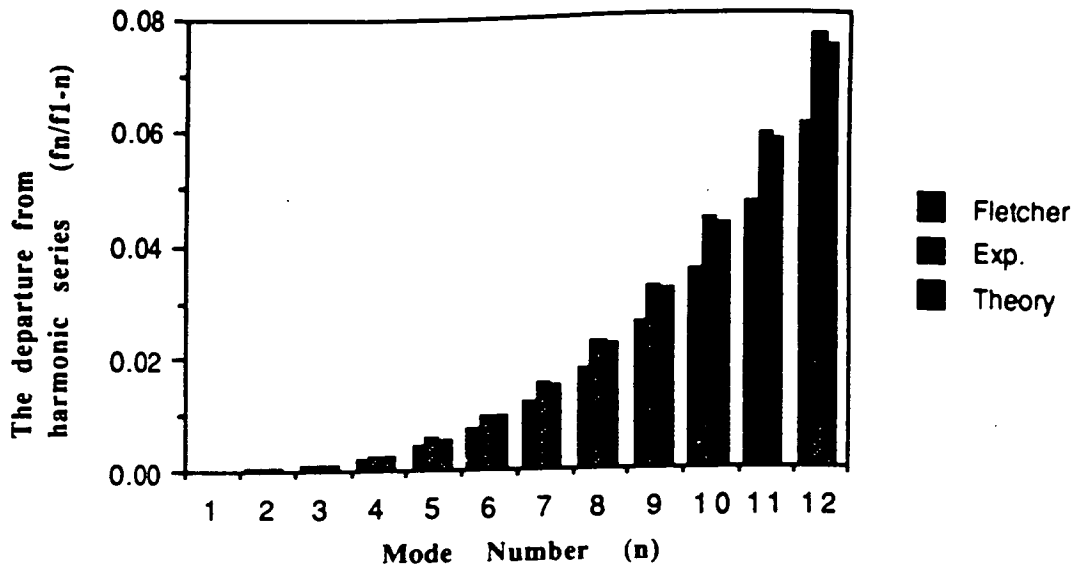

4. INHARMONICITY MEASUREMENTS

In order to validate the theory developed in section 2 of this paper, experiments were conducted to measure the inharmonicity of the single overwound strings on the Edinburgh Broadwood. The key of the note under study was held down with a weight in order to retract the damper and allow the string to vibrate freely; on this piano the dampers are below the strings. The string was then plucked with the finger at a position close to the end and the sound was recorded at a point near to the centre of the string using a microphone mounted a short distance above. The acoustic signal was captured digitally using a Barry Box (a unit specially designed for collecting sound samples) and was analysed on a BBC B computer using an FFT routine developed at Edinburgh [1]. This program generates a high resolution spectrum and accurately locates the peaks, from which the inharmonicity of any particular mode can be determined.

The measured peak frequencies for the first twelve modes for string Bb0 are shown in Table II and are displayed graphically in Figure II. These can be compared with the theoretical frequency values, together with the corresponding frequencies calculated from Fletcher's formula. Corresponding results for the note Db1 are given in Table III and Figure III. It is seen that stepped stiff string theory gives a very good match, the error in the twelfth mode being only 5%. The error using Fletcher's theory is approximately six times as great.

Similar results have been measured for the other single overwound strings and the results show generally the same trends.

5. CONCLUSIONS

It is evident from the results that the theory presented here gives a better fit to measured inharmonicities than Fletcher's analysis for a uniform string. Apparently the stepped geometry of the overwound strings is significant. However, our predictions still underestimate the inharmonicity by about 5% in the twelfth mode. This could be due to a number of factors. The winding itself may tend to increase the stiffness of the string i.e. the stiffness of a length of overwound string is slightly greater than the stiffness of the core by itself. The flexibility of the supports may also be important. Neither of these factors are included in the analysis.

In order to study the problem further, a purpose-designed monochord has now been constructed at Edinburgh. With this it will be possible to measure the tension precisely and to vary the support rigidity.

6. REFERENCE

[1] D.M. Campbell, C.A. Greated and R. Parks, *Proc. of the Inst. of Acoustics*, 12(1), 743-752 (1990).
[2] J.W. Strutt Lord Rayleigh, "The Theory of Sound", 2nd ed. Dover Publications, New-York, 1954.
[3] P.M. Morse, "Vibration and Sound", 2nd ed. McGraw-Hill, New York, 1948.
[4] R.S. Shankland and J.W. Coltman, *J. Acoust. Soc. Amer.*, 10(3), 161-1666 (1939).
[5] O.H. Shuck & R.W. Young, *J. Acoust. Soc. Amer.*, 15(1), 1-11 (1943).
[6] R.W. Young, *J. Acoust. Soc. Amer.*, 24(3), 267-273 (1952).
[7] R.W. Young, *Acustica*, 4, 259-262 (1954).
[8] A.J. Bell & R. Parks, *Proc. of the Inst. of Acoustics*, 12(1), 753-755 (1990).
[9] H. Fletcher, *J. Acoust. Soc. Amer.*, 36(1), 203-210 (1964).
[10] M. Levinson, *J. of Sound and Vibration*, 49(2), 287-291 (1976).
[11] T. Sakata & Y. Sakata, *J. of Sound and Vibration*, 71(2), 315-317 (1980).
[12] H.P.W. Gottlieb, *J. of Sound and Vibration*, 118(2), 283-290 (1987).
[13] W. Trow Goddard, "A handbook on the strings of the pianoforte and other keyboard instruments with design formulae", Billingham Press, Billingham, England, 1985.

JOURNAL DE PHYSIQUE IV
Colloque C5, supplément au Journal de Physique III, Volume 4, mai 1994

Inharmonicity of nonuniform overwound strings

P. CHUMNANTAS, C.A. GREATED and R. PARKS

Department of Physics, University of Edinburgh, Edinburgh EH9 3JZ, U.K.

In our previous paper [10], the transverse wave equation for the case of a stepped stiff string was described, and the numerical results of the frequency equation were compared with data from experiments on piano strings. It was evident from these results that the theory presented there gave a better fit to measured inharmonicities than Fletcher's analysis for a uniform overwound string. In this paper, we describe measurements of inharmonicity carried out on nonuniform overwound strings mounted on a rigid monochord. The measurements are in good agreement with the theoretical predictions taking account the nonuniformity of the winding.

1. INTRODUCTION

[1-8] The natural frequencies of a piano string depart somewhat from the harmonic series; the departure is called inharmonicity. In the late 19th century, **Lord Rayleigh** [2] described a theory for the vibration of strings, showing that in the piano, the stiffness of the strings affects the restoring force to a significant degree. He derived a formula to predict how the stiffness of a piano string can cause it to vibrate at frequencies somewhat greater than those of the ideal string. In 1964, **Fletcher** [8] conducted a more accurate treatment of Rayleigh's method, considering both clamped and hinged boundary conditions. He found that the equation was of the form $f_n = nF(1+Bn^2)^{1/2}$, where F and B are constants. B is described as the inharmonicity coefficient. Actually, all piano bass strings are characterised by a steel wire core wrapped with copper, or sometimes iron, used to increase the string's linear mass density. While the tight coiling of copper wire ensures close coupling to the core, the windings contribute considerably more to the increase in the string's linear mass density than to its bending stiffness. Most bass strings have a single winding of copper wire, and it is usually only within the lowest octave that double winding is used. A double-wound string consists of a bare steel core wrapped with a small diameter copper wire, which is then overspun with a second winding of larger diameter. A small part of the steel core is left exposed near the end of the string. The inharmonicity of the overwound piano strings does not only depend on the string stiffness; since the copper windings do not extend up to the string's supports, the resulting nonuniformity in the linear mass density must also be taken into account.

In a previous paper [10], an expression for the frequencies of vibration of a stepped stiff string was described. In the present paper this expression is used to calculate the inharmonicity of piano string with nonuniform winding. The theoretical results are compared with measurements carried out on a rigid monochord.

2. THEORETICAL CONSIDERATION AND NUMERICAL RESULTS

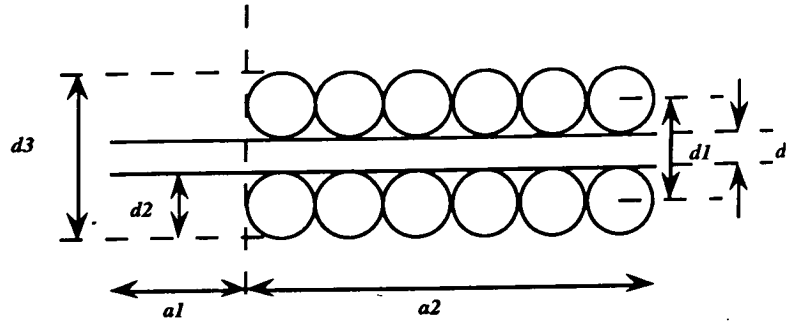

Fig. I The 2-segment overwound string.

Consider the frequency equation [10] in the case of the 2 segment stiff string (see Fig. I). Its frequency equation is

$$\left(\frac{\mu_{11}^2}{\mu_{22}^2}+1\right)\left(\frac{\mu_{12}^2}{\mu_{21}^2}+1\right)\left\{\frac{\mu_{11}}{\mu_{21}}\frac{\tanh(\mu_{21}a_2)}{\tanh(\mu_{11}a_1)}+1\right\}\left\{\frac{\mu_{12}}{\mu_{22}}\frac{\tan(\mu_{22}a_2)}{\tan(\mu_{12}a_1)}+1\right\}$$
$$-\left(\frac{\mu_{11}^2}{\mu_{21}^2}-1\right)\left(\frac{\mu_{12}^2}{\mu_{22}^2}-1\right)\left\{\frac{\mu_{11}}{\mu_{22}}\frac{\tan(\mu_{22}a_2)}{\tanh(\mu_{11}a_1)}+1\right\}\left\{\frac{\mu_{12}}{\mu_{21}}\frac{\tanh(\mu_{21}a_2)}{\tan(\mu_{12}a_1)}+1\right\}=0 \qquad (1)$$

$$\mu_{jk}=\left\{\sqrt{\left(\frac{T_j}{2(QS\kappa^2)_j}\right)^2+(2\pi f)^2\frac{\rho_j}{(Q\kappa^2)_j}}+(-1)^k\frac{T_j}{2(QS\kappa^2)_j}\right\}^{\frac{1}{2}} \qquad (2)$$

$$: j,k=1,2.$$

where T is the tension, S_j is the area of cross-section and κ_j the radius of gyration. ρ_j and Q_j are the density and modulus of elasticity of the material for the section j of the string.

The allowed frequencies, f_n: (n = 1, 2, 3, 4,...) can be found from equations (1) & (2). The values were found numerically by applying Newton's method; this was programmed on an Apple Macintosh computer using the Mathematica package. Numerical calculations have been undertaken to compute theoretical mode frequencies for several 2 segment overwound strings. Fig. I shows the notation used for defining the parameters of the overwound string. This was clamped at both ends and the linear density was calculated using the method of W T Goddard [9]. The first segment is the bare string (a_1) and the second segment has both the steel core and the wrapped copper wire (a_2). Graph I presents the relation between the square of the theoretical mode frequency per the square of mode number $(f_n/n)^2$ and the square of the mode number (n^2), for a uniform overwound string (length l = 80.0 cm.) and the 2 segment overwound string (a_1 = 5.0 cm. and a_2 = 75.0 cm.). It shows that the relation is linear in the case of the uniform overwound string. This is the case dealt with by Fletcher, and our results agree. In the case of the stepped overwound string, the inharmonicity is substantially increased, and the line is evidently curved. Graph II displays the residuals (the deviations from the best straight line fit to the data) for three 2-segment overwound strings. These have the same diameters (d_1 = 1.35 mm. and d_2 = 4.20 mm.), and the same lengths of bare steel string (a_1 = 5.0 cm.), but their overwound lengths are a_2 = 75.0 , 100.0 and 125.0 cm., respectively.

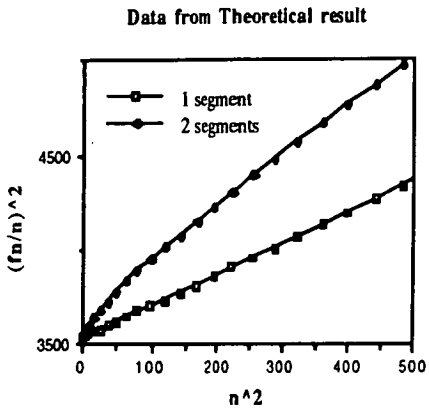

Graph I: The relation between the square of theoretical mode frequencies per the square of mode number $(f_n/n)^2$ and the square of mode number (n^2) for a uniform overwound string with l = 80.0 cm. and a 2 segment overwound string with a_1 = 5.0 cm. and a_2 = 75.0 cm.

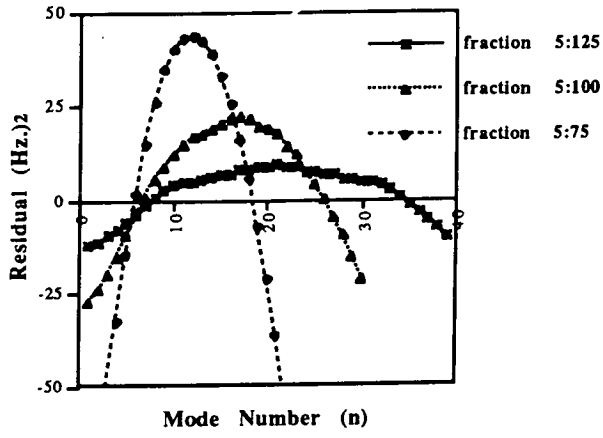

Graph II: The residuals from a straight line of the theoretical results for three 2-segment overwound strings with the same diameters (d_1 and d_2), and the same length of bare string (a_1 = 5.0 cm.), but with a_2 = 75.0, 100.0 and 125.0 cm.

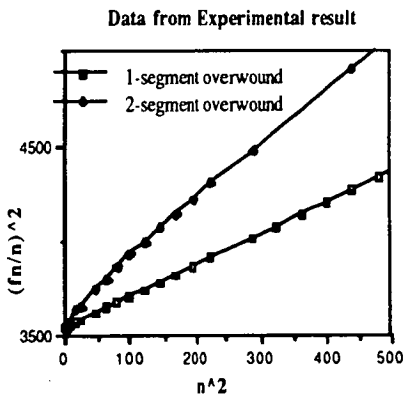

Graph III: The relation between the square of experimental mode frequencies per the square of mode number $(f_n/n)^2$ and the square of mode number (n^2) for a uniform overwound string with l = 80.0 cm. and a 2 segment overwound string with a_1 = 5.0 cm. and a_2 = 75.0 cm.

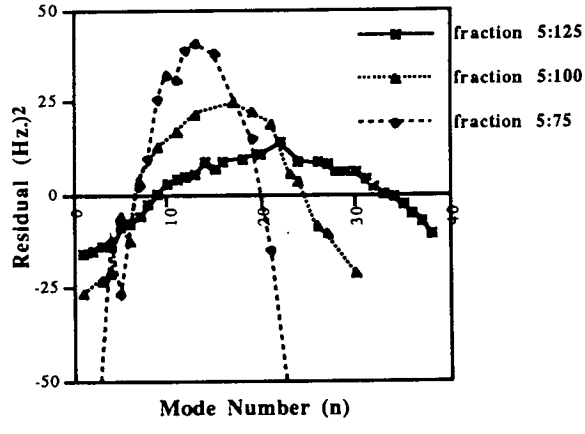

Graph IV The residuals from a straight line of the experimental results for three 2-segment overwound strings with the same diameters (d_1 and d_2), and the same length of bare string (a_1 = 5.0 cm.), but with a_2 = 75.0, 100.0 and 125.0 cm.

3. EXPERIMENTAL RESULTS

The experiment studied the vibration of 2 segment overwound strings (see Fig. I) on a purposed-designed monochord. The monochord is composed of a rigid steel bar, 2 pairs of specially designed rigid clamps, 2 tuner supports, and 2 tuners. Each pair of clamps stops each end of the string at 3 points in a plane perpendicular to the string length. The strings were plucked at a position close to the end and the sound was recorded at a point near to the centre of the string using a microphone mounted a short distance above. The acoustic signal was captured digitally using an A/D converter and was analysed using an FFT. A program developed in Edinburgh [11] locates the peaks in the spectrum with high accuracy.

The relation between the square of experimental mode frequencies per the square of mode number $(f_n/n)^2$ and the square of mode number (n^2) for a uniform overwound string (length l = 80.0 cm.) and for a 2 segment overwound string (a_1 = 5.0 cm. and a_2 = 75.0 cm.) are shown in Graph III. The relation is not linear in the case of the nonuniform overwound string, in agreement with the theoretical result. Experimental results for three 2 segment overwound strings are shown in Graph IV as residuals from a straight line. It is seen that the greater the fraction (a_1/a_2), the more curving is the trend. The theoretical result in Graph II gives a very good match.

4. CONCLUSION

The results from theory and experiment presented above show that the mode frequencies of nonuniform overwound strings depart from those predicted by Fletcher's equation. It is evident that this departure, graphed as the residual from a straight line fit to Fletcher's equation, gives a curving trend whose significance depends on the fraction a_1:a_2. The greater the fraction a_1:a_2, the more curving is the trend. For normal bass piano strings, the fraction of unwound string is usually considerably less than 1:25. Thus a straight line fit to Fletcher's equation is a resonable approximation. However, the inharmonicity coefficient will be considerably increased by the nonuniformity of the winding.

5. REFERENCES

[1] D.M. Campbell, C.A. Greated and R. Parks, *Proc. of the Inst. of Acoustics*, 12(1), 743-752 (1990).

[2] J.W. Strutt Lord Rayleigh, "The Theory of Sound", 2nd ed. Dover Publications, New-York, \ 1954.

[3] P.M. Morse, "Vibration and Sound", 2nd ed. McGraw-Hill, New York, 1948.

[4] R.S. Shankland and J.W. Coltman, *J. Acoust. Soc. Amer.*, 10(3), 161-1666 (1939).

[5] O.H. Shuck & R.W. Young, *J. Acoust. Soc. Amer.*, 15(1), 1-11 (1943).

[6] R.W. Young, *J. Acoust. Soc. Amer.*, 24(3), 267-273 (1952).

[7] R.W. Young, *Acustica*, 4, 259-262 (1954).

[8] H. Fletcher, *J. Acoust. Soc. Amer.*, 36(1), 203-210 (1964).

[9] W. Trow Goddard, "A handbook on the strings of the pianoforte and other keyboard instruments with design formulae", Billingham Press, Billingham, England, 1985.

[10] P Chumnantas, C A Greated and D M Campbell, *Proc. of the Inst. of Acoustics*, 15(3), 665-672 (1993).

[11] R Parks, *Proc. of the Inst. of Acoustics*, 15(3), 673-680, (1993).